Journal of the
OPTICAL SOCIETY
of AMERICA

VOLUME 40, NUMBER 7 JULY, 1950

An Integrating Photometer for Low Light Levels

HORACE W. BABCOCK
Mount Wilson and Palomar Observatories, Carnegie Institution of Washington, California Institute of Technology, Pasadena, California
(Received March 28, 1950)

Proper estimation of exposure times in astronomical spectroscopy is often difficult, largely because the quality of the stellar image is so dependent upon "seeing." The integrating photometer described here, while not new in principle, functions with satisfactory sensitivity and stability on only two percent of the light transmitted by the slit of the coudé spectrograph of the 100-inch telescope. When the meter indicates a predetermined number of counts, the finished spectrogram will have the proper density regardless of seeing, slit width, passing clouds, and efficiency of guiding.

THE photometer described here was developed as an integrating exposure meter for the coudé spectrograph of the 100-inch telescope. Several photoelectric exposure meters for laboratory use have been described previously,[1–3] but for most if not all of these, a much greater light-flux has been available than is encountered in astronomical spectroscopy. In the present application, a high degree of stability and sensitivity is required, but since accurate photoelectric photometry on stars and nebulae to the sixteenth magnitude or fainter is a routine matter with the 100-inch telescope, it is obvious that no fundamental difficulties need be overcome to develop a photometer for a spectrograph that is usually used on stars brighter than the ninth magnitude.

The principle of the coudé exposure meter is simple. A $\frac{3}{4}$-inch right-angle prism, placed behind the slit, near the collimator, where the light-beam is 6 inches in diameter, abstracts about 2 percent of the light and directs it through a simple lens into a phototube of the electron multiplier type. The output current of the phototube is collected by a small capacitor, which, whenever it becomes charged to a certain voltage, is abruptly discharged by the spontaneous ignition of a gas tube. The voltage pulses thus formed are amplified and applied to an electromagnetic counter with five digit-wheels. A predetermined number of counts indicates the proper exposure, and the developed spectrogram will then have the proper photographic density regardless of the magnitude of the star, seeing conditions,* passing clouds, efficiency of guiding, and slit width. Particularly for the coudé (250-foot) focus of the telescope, where slit widths in the range of 0.03 to 0.15 mm are customarily used, the seeing has a very important effect on exposure time. The standard exposure time for a star of given magnitude and color may have to be divided by 3 if the seeing is very good or multiplied by 5 or 10 if the seeing is very poor. This factor is sometimes difficult to estimate without instrumental aid; yet, especially if the plates are being made for spectrophotometric purposes, it is desirable that the density of the spectrum should fall within fairly narrow limits. With the exposure meter to take care of the main variable factors, the observer has the opportunity of altering the number of counts to allow for reciprocity failure of the emulsion on long exposures, and to allow for any deviation from the standard degree of widening the spectrum.

While the meter need not be highly precise for the purpose outlined here (an indication within 10 or 15 percent of the true value is probably sufficient), it should be stable in operation and should have a minimum of adjustments. The following requirements, laid down at the start of the design, have been met:

(1) There should be only a single control—an ON-OFF switch.

[1] H. C. Rentschler, J.A.I.E.E. **49**, 576 (1930).
[2] J. B. H. Kuper, F. S. Brackett, and M. Eicher, Rev. Sci. Inst. **12**, 87 (1941).
[3] H. F. Launer, Rev. Sci. Inst. **20**, 103 (1949).

* Astronomical "seeing" pertains to the amount of twinkling and blurring of a telescopic image due to atmospheric turbulence.

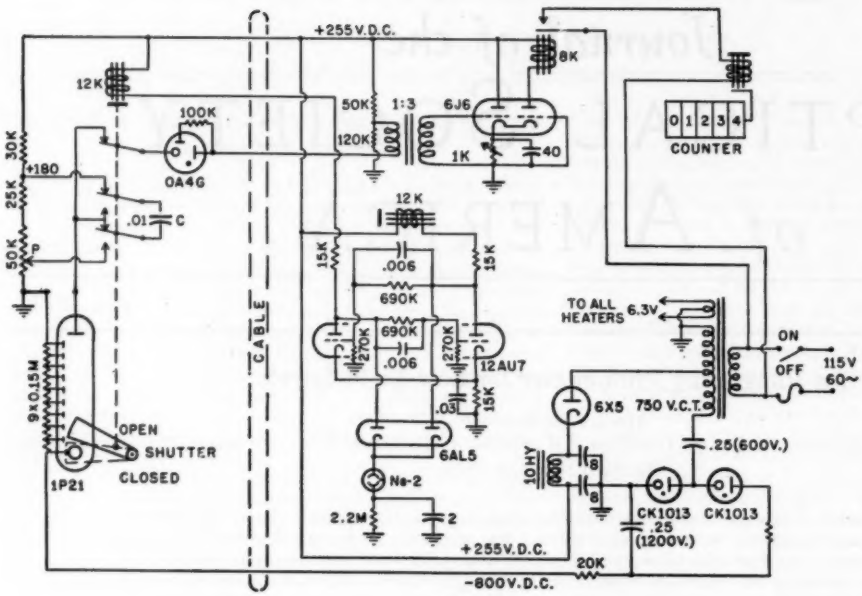

FIG. 1. Schematic diagram of the integrating exposure meter. The photo-tube unit at the left is placed inside the spectrograph near the collimator; it is connected by a cable to the indicator and power supply at the right.

(2) The meter should function without a change of scale or sensitivity on all stars from the first magnitude down to at least the eighth magnitude.

(3) Refrigeration of the phototube or other special attention should not be required.

(4) Introduction of the bright light of the Fe comparison arc into the slit should not adversely affect the phototube or the indication of the meter.

Since a one-inch aperture accepts 1.5×10^{-9} lumen from a second-magnitude star like Polaris[4] (spectral type F8), a similar star on the slit of the coudé spectrograph at the 100-inch telescope has an intensity of 1.5×10^{-5} lumens. We assume that with fairly good seeing 25 percent of the light passes through the slit, and of this, 2 percent, or 7.5×10^{-7} lumens, enters the phototube. If the sensitivity of the multiplier tube is 2 amperes/lumen (at reduced voltage), the anode photocurrent will be 1.5×10^{-6} ampere. As the dark current of the tube is not very much less than this (it may be as great as 10^{-7} ampere), it must be compensated or eliminated if the meter is to be useful on faint stars. The method of compensation devised was to interrupt the entering light-beam by a shutter that remains open and closed for equal intervals in a 3-second cycle; the terminals of the integrating capacitor, C (Fig. 1), are reversed by a relay synchonously with the shutter. The capacitor charges on photocurrent plus dark current for 1.5 seconds, then discharges for an equal time while receiving dark current alone.[5] After the capacitor C has been charged to a potential of 90 volts by the photocurrent, it is discharged abruptly to 70 volts by the firing of the cold-cathode gas tube (OA4-G); several discharges may occur during each "light-on" period of 1.5 seconds. Continuing our example with a second magnitude star, we find, with $C=0.01$ μf to be cycled over a range of 20 volts, that there will be one count every 0.13 seconds during the time the shutter is open, or averaged over several cycles there will be 4 counts per second. For a star of the seventh magnitude, there will be one count per 25 seconds.

The complete circuit of the photometer is given in Fig. 1. The instrument is made in two units connected by a multi-conductor cable, as indicated. The shutter is a small aluminum vane actuated directly by the armature of the 15,000-ohm telephone-type relay that switches the integrating capacitor. (A permalloy shield may be placed around the phototube to protect it from the stray magnetic field of the relay.) This shutter has the advantage over other possible types that it is exactly synchronous with the relay, and is quick-acting. When the comparison arc is operated, an inter-locking relay cuts off all power to the exposure meter; the shutter then falls by gravity and spring action to intercept the light beam, thereby protecting the sensitive cathode of the photo-multiplier from the bright light of the arc, which would have a deleterious effect on the phototube even with no applied voltage.

The potentiometer, P, is provided in order that the anode of the photo-multiplier may have the same potential, on the average, during the light and dark parts of the operating cycle; without this provision, the anode potential would change by 160 volts owing to the average potential of 80 volts on the reversing capacitor

[4] J. Strong (A. E. Whitford), *Procedures in Experimental Physics* (Prentice-Hall, Inc., New York, 1938), p. 397.

[5] After this device for compensation of dark current had been developed and used, it was found that it had already been described by Saunderson, Caldecourt, and Peterson, J. Opt. Soc. Am. 35, 681 (1945).

C. The anode current is almost, but not precisely, independent of anode voltage above a few volts; therefore, by adjusting P, the point of exact compensation for dark current and leakage may be found so that the rate of counting is zero when no light is admitted to the slit.

It is important that leakage currents be reduced to a minimum; therefore it is recommended that the phototube, its socket, the capacitor, the relay, and the glow-discharge tube be carefully mounted with short leads, dried, and the critical parts coated with ceresin wax. The capacitor C should be of a type having very high leakage resistance and low polarization; suitable capacitors for this type of integrating service are available under the trade name "Pasticon."

The power supply, pulse amplifier, counter, and relay circuit are contained in a small cabinet near the observer's position. The current pulses from the OA4-G gas discharge tube, stepped up by a small transformer, are applied to a 6J6 cathode-follower and amplifier. The plate current of the output stage actuates a small sensitive relay that in turn controls the 115v a.c. electromagnetic counter. The circuit for actuating the shutter relay is a stable double-triode flip-flop that is triggered, through a 6AL5 double diode, by a simple relaxation oscillator consisting of a resistor, a capacitor, and a miniature neon bulb. It is not necessary that the frequency of the oscillator be precisely constant, but only that successive pulses be equally spaced with high precision, so that over an extended period the sum of the "light-on" intervals will equal the sum of the "dark" intervals. The idle triode of the flip-flop has in its plate circuit a second 15,000-ohm relay to match the characteristics of the shutter relay, thus equalizing the charging of the oscillator capacitor in the two parts of the cycle.

The power supply employs a transformer having a center-tapped secondary rated at 750 volts. One end of the secondary is grounded; the other feeds a voltage-doubler using two cold-cathode miniature rectifiers. This, with an R-C filter, supplies a negative potential of 800 volts for the 1P21 phototube. The voltage divider for this tube consists of a series of $\frac{1}{2}$-watt, 150,000-ohm resistors soldered directly to the socket terminals. The center tap of the transformer secondary feeds a conventional half-wave rectifier and filter which provides a 255 v d.c. plate supply for the amplifier and relay circuit. For simplicity, no elaborate voltage regulator is used on the -800 volt supply for the phototube. Instead, the whole exposure meter receives its 115v a.c. supply through one of the ordinary constant-voltage transformers that maintain the voltage within one percent. This provides sufficient precision for the intended use of the meter; if, however, really high precision were required of such a photometer, more accurate regulation of the photo-tube supply voltage would be essential.

The 1P21 photo-tube fortunately has its maximum sensitivity near $\lambda 4200$, which is about the middle of the ordinary photographic region of the spectrum. Calibration shows that, when baked IIa-O plates are used in the spectrograph, the number of counts required for good density is approximately 60, 250, and 600 for the 32-inch, 73-inch, and 114-inch cameras, respectively. (The dispersions are 10.4, 4.5, and 2.9 A/mm in the third order.) When the yellow and orange regions of the spectrum are photographed, in the second order of the grating, a filter in front of the slit removes the shorter wave-lengths; the exposure meter has sufficient sensitivity between $\lambda 5400$ and $\lambda 6000$ to be useful, but requires a different calibration.

The integrating exposure meter has been in use for several months and has proved to be of real aid in obtaining properly exposed plates under varying conditions. The meter and the photoelectric guider,[6] for holding the image of the star on the slit, together form a pair of useful adjuncts to stellar spectroscopy.

[6] H. W. Babcock, Astrophys J. **739**, 107 (1948).

On the Design of Wide Angle Schmidt Optical Systems*†

ERIC M. WORMSER
Servo Corporation of America, New Hyde Park, New York
(Received April 13, 1950)

A method of balancing the optical aberrations over a wide angular field of a Schmidt optical system is described. This design method is demonstrated for a Schmidt optical system of focal ratio F:0.7 and covering an angular field of 40°. The reduction in off-axis secondary aberrations is obtained by computing a "wide angle" aspheric corrector plate through the use of "Lucy's Approximate Method" instead of using the conventional "exact equations."

INTRODUCTION

THE deviation error in the focal plane of any ray with respect to the corresponding chief ray is expressed by Schwarzschild[1] as a third-order equation as follows:

$$\Delta = Bh^3 - 3Fh^2\beta + (2C+D)h\beta^2 - E\beta^3.$$

In this equation:

h = distance of the ray from the axis in the plane of the entrance pupil,
β = the field angle,

and the five Seidel aberration coefficients are

B = coefficient of spherical aberration,
F = coefficient of coma,
C = coefficient of astigmatism,
D = coefficient of curvature of field,
E = coefficient of distortion.

For an optical system covering a wide angular field we desire the aberration function to be independent of the field angle β. This condition is ideally met if all Seidel coefficients are zero, except B, the coefficient of spherical aberration. Stroemgren has shown, again from third-order theory, that this condition is met uniquely by a spherical mirror system with an aperture at the center of curvature (see Fig. 1).

In this system, the amount of spherical aberration is independent of the field angle which is formed by the pencil of rays and the optical axis. The size of the geometrical image due to spherical aberration formed on the focal surface is, however, a cubic function of the focal ratio F of the optical system. Focal ratio is here defined as the ratio of focal length to the aperture diameter. The size of the circle of confusion on the focal surface as a function of focal ratio is shown in Fig. 2. As shown in this figure, the aberrations increase rapidly for focal ratios of less than $F=1.0$. It can be seen that for a focal ratio of 0.7 the size of the circle of least confusion amounts to 2.2°.

CLASSICAL SCHMIDT OPTICAL SYSTEM

In the classical Schmidt system spherical aberration is compensated through introduction of an aspheric corrector plate in the aperture at the center of curvature as shown in Fig. 3. For monochromatic light, complete correction can be achieved and stigmatic imagery obtained for one angular field position. For telescopic systems the contour of the Schmidt corrector plate is usually computed to produce stigmatic imagery for a pencil of light parallel to the optical axis. The optical axis is defined by the axis of symmetry of the corrector plate.

A number of equations for computing such a corrector plate are available. They are generally described as the "exact" equations. They are based on the hypothesis of equalizing the optical paths from a plane wave front tangential at the vertex of the corrector plate to the focal point.

Figure 4 gives equations for the optical paths from a plane wave front for a general ray and a paraxial ray. The radius of the spherical mirror is assumed to equal one (1). By setting these equations equal, the contour of the corrector plate can be computed.

Introducing a corrector plate of the type described above results in stigmatic imagery for a bundle of rays parallel to the axis. For pencils of rays inclined to the optical axis, secondary aberrations result. These second-

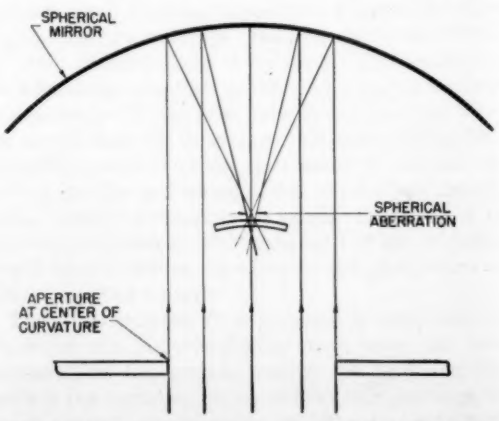

FIG. 1. Spherical mirror with aperture at center of curvature.

* Presented at the New York Meeting of the Optical Society of America (March, 1950).

† The work described in this abstract was carried out in part in connection with development work for the Bureau of Aeronautics of the Navy Department.

[1] V. B. Stroemgren, Vierteljahres. d. Astronom. Ges. **70**, 65 (1935).

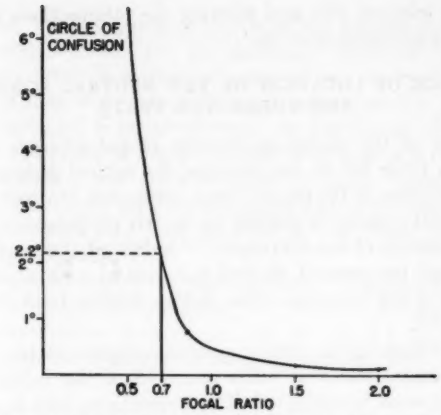

FIG. 2. Circle of confusion as a function of focal ratio for a spherical mirror with the aperture at the center of curvature.

ary aberrations increase with the angle of inclination to the optical axis and assume serious proportions for wide angular fields in optical systems of low focal ratio.

The increase in the geometrical image size on the focal surface as a function of field angle in a Schmidt optical system of focal ratio 0.7 is shown in Fig. 5 The focal surface is spherical and has a radius of curvature equal to the focal length. The size of the circle of confusion, as indicated in Fig. 5, increases from near 0° on axis to 0.32° at 15° off-axis and to 0.58° at 20° off-axis for monochromatic light.

For a color-minimized Schmidt corrector plate made of a low dispersion optical material, chromatic aberration in the particular system investigated amounted to 0.014° which is negligible compared to the off-axis monochromatic aberrations, and will hence not be further considered.

The size of the circle of confusion was obtained by ray tracing selected rays in the meridional plane and plotting intersections with their associated chief ray. It had been previously determined that ray tracing five

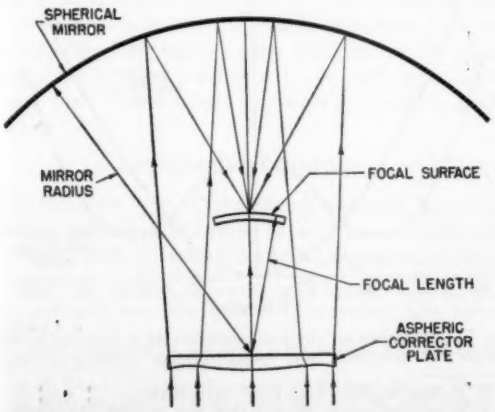

FIG. 3. Classical Schmidt optical system.

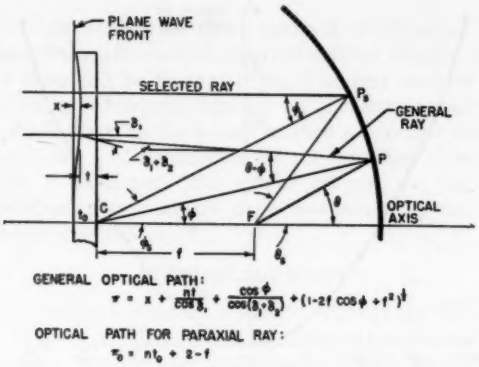

FIG. 4. "Exact" equations for computing a Schmidt corrector plate.

selected rays gives an adequate picture. The five selected rays used were the chief ray, the two marginal rays and two rays passing through the corrector plate near half the plate radius, which is the region of greatest slope for a corrector plate with neutral zone at 0.866 of the full plate radius.

"WIDE ANGLE" CORRECTOR PLATE CONTOUR

In order to obtain better uniformity of performance in wide angle Schmidt systems, it is desirable to reduce the amount of secondary monochromatic aberrations which occur at large field angles, possibly at the expense of imaging quality at the center of the angular field.

It was found in the design of the above Schmidt system of a focal ratio 0.7 and a total angular field of 40° that improved uniformity of performance can be achieved by changes in the contour of the corrector plate.

In the "wide angle" corrector plate design, the contour is determined by the so-called "approximate" equations developed by Frank A. Lucy.[2] The plate contour of any corrector plate can be expressed as a power series expansion of the form

$$x = ah^2 - \beta h^4 + \gamma h^6 - \cdots$$

In Lucy's "approximate method" the plate contour is expressed as

$$x = \alpha_1 h^2 - \beta_1 h^4.$$

Terms above the fourth power are eliminated, but the coefficients α_1 and β_1 are obtained by computing x_z, the plate excavation at the neutral zone, by exact optical path equations and then solving for α_1 and β_1 at this point.

This produces a Schmidt contour which differs in steepness of curvature from that computed by exact equations as shown to a greatly expanded scale in Fig. 6. The numerical values shown are for a spherical mirror of 60 mm radius.

[2] F. A. Lucy, J. Opt. Soc. Am. **30**, 251 (1940).

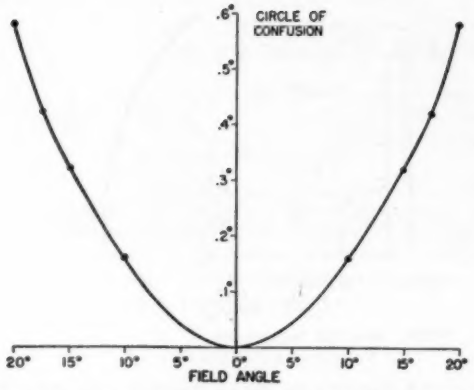

FIG. 5. Size of the circle of confusion as function of field angle for a Schmidt optical system F:0.7 with a corrector plate computed by "exact" methods.

The use of Lucy's approximate method results in residual spherical aberration on-axis. The variation of secondary aberration with field angle in a Schmidt system of focal ratio 0.7 designed according to Lucy's approximate method is shown in Fig. 7. A region of minimum aberration occurs for a field angle of about 12° and then increases slowly to equal the on-axis aberrations at approximately 17°. Beyond 17° the aberrations increase rapidly.

The aberration function for a similar system designed by the "exact method" is shown for comparison. These values were again obtained through ray tracing of the same selected rays and plotting the intersections with their associated chief ray.

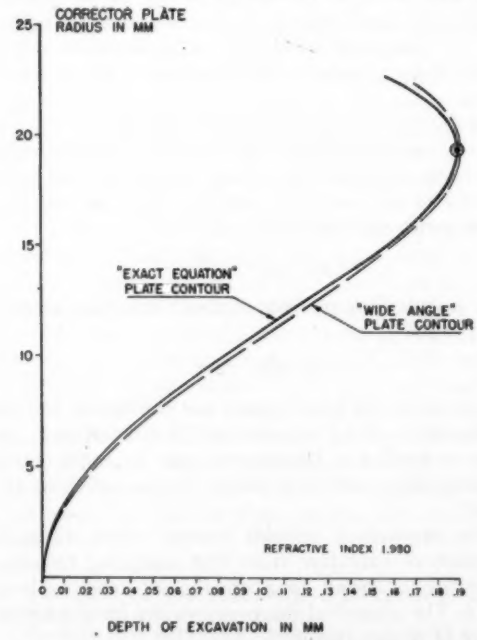
CORRECTOR PLATE RADIUS IN MM
25
20
15
10
5
"EXACT EQUATION" PLATE CONTOUR
"WIDE ANGLE" PLATE CONTOUR
REFRACTIVE INDEX 1.980
0 .01 .02 .03 .04 .05 .06 .07 .08 .09 .10 .11 .12 .13 .14 .15 .16 .17 .18 .19
DEPTH OF EXCAVATION IN MM

FIG. 6. Comparison of "exact equation" and "wide angle" corrector plate contours.

CHOICE OF LOCATION OF THE NEUTRAL ZONE IN THE CORRECTOR PLATE

One of the design parameters of the aspheric corrector plate left to the choice of the optical designer is the location of the neutral zone, the region at which the Schmidt contour is parallel to the flat plate face.

A survey of the literature[1,3–5] indicated that various authors recommend placing the neutral zone at fractions of the corrector plate radius ranging from 0.866 to 0.707.

In designing the present system, corrector plates with the neutral zones at 0.866 and 0.75 of the full plate radius were investigated. The aberrations, which consist principally of secondary off-axis monochromatic aberrations, did not significantly differ with a shift in the neutral zone.

The recently published recommendations of Linfoot and Wolf[4] on placing the neutral zone at the edge of the plate profile for wide field systems approaching F:1.0 have not as yet been investigated.

CONCLUSIONS

From the investigations reported, the following conclusions may be drawn.

The optical performance of wide-angle, low focal ratio classical Schmidt systems can be improved by reducing variation of secondary aberrations with field angle while allowing residual spherical aberration on axis.

This method has been described for a Schmidt optical system of focal ratio F:0.7 and covering an angular field of 40°. In this system the maximum amount of monochromatic geometrical aberration has been reduced from 0.58° for the conventional exact corrector plate to 0.34° for the "wide angle" corrector plate. It would

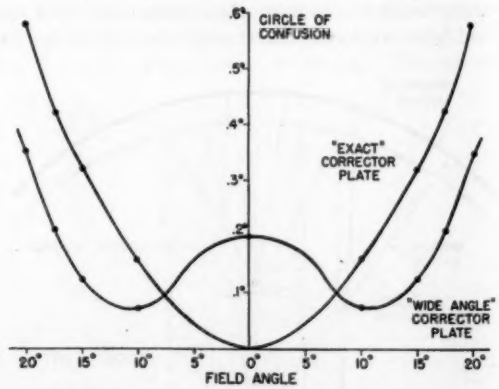

FIG. 7. Comparison of circle of confusion as a function of field angle for "wide angle" and "exact equation" corrector plates.

[3] F. B. Wright, Pub. A. S. P. **47**, 300 (1935).
[4] E. M. Linfoot and E. Wolf, J. Opt. Soc. Am. **39**, 752 (1949).
[5] E. M. Linfoot, M. N. R. A. S. **109**, 280 (1949).

appear advantageous to limit the full angular field of the system to 34°, i.e., 17° half-angle. For a 34° "wide angle" Schmidt system, the size of the circle of confusion does not exceed 0.2° as compared to 0.4° for a conventional Schmidt system. As previously shown, the aberrations of a spherical mirror system of 0.7 focal ratio without an aspheric corrector plate amount to 2.2°. Practically uniform imaging quality with variation in field angle has been achieved in the "wide angle" Schmidt system.

The reduction in off-axis secondary aberrations has been obtained by computing the "wide angle" aspheric corrector plate through the use of "Lucy's Approximate Method" instead of using the conventional "exact equations."

Two articles by Linfoot[5] and Linfoot and Wolf[4] have been published since the work described in this article was completed. Two other methods of balancing the monochromatic aberrations over a finite angular field are described in these articles. The first method involves an additional figuring on the mirror and the aspheric plate. In the second method a fictitious refractive index for computation of the modified corrector plate is developed. The author has not yet had an opportunity to compare these methods with the one described in this article.

ACKNOWLEDGMENTS

In closing, the author wishes to acknowledge the help of Walter A. Howland of the Servo Corporation of America who did the computational work for the example quoted and to thank R. E. Stephens of the National Bureau of Standards for reviewing the optical design work and making helpful suggestions.

JOURNAL OF THE OPTICAL SOCIETY OF AMERICA VOLUME 40, NUMBER 7 JULY, 1950

Infra-Red Transmitting Filters. II. The Region 1 to 6μ*†

ELKAN R. BLOUT, RICHARD S. CORLEY, AND PATRICIA L. SNOW
Research Laboratory, Polaroid Corporation, Cambridge, Massachusetts

(Received March 8, 1950)

A type of visible-absorbing, infra-red transmitting filter is described in which the absorbing units are produced from a plastic film that also serves as a supporting medium. Filters of this kind prepared from polyvinyl chloride and polyvinylidene chloride films are characterized by transmission bands between 1 and 3.3μ and between 3.5 and 5.8μ. Ways of isolating either of these bands are described. Such filters have obvious utility in connection with photoconductive cells.

INTRODUCTION

FILTERS have been described previously which absorb visible light and transmit near-infra-red radiation beyond approximately 0.9μ. For the most part the useful filters of this type have consisted of organic dyes dissolved in plastics or inorganic compounds in the form of glasses.[1,2] In this communication we describe a new type of visible-absorbing, infra-red transmitting filter made by the *conversion* of the plastic supporting medium itself to a light-absorbing structure rather than by the *addition* of extrinsic absorbing substances.

ABSORPTION FILTERS

In this new type of filter the chemically bound absorbing medium is produced *in situ* in an organic high polymer which is itself optically homogeneous and relatively transparent in the infra-red. Other desirable physical properties for the base medium are stability to heat and to thermal shock, as well as mechanical

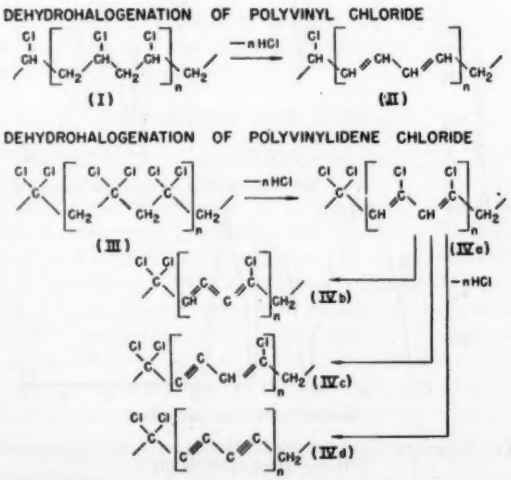

FIG. 1. Reactions of polyvinyl chloride and polyvinylidene chloride.

* This work has been performed under contract with the Engineer Research and Development Laboratories, Fort Belvoir, Virginia.

† Paper presented at the New York Meeting of the Optical Society of America, March, 1949.

[1] E. R. Blout, W. F. Amon, Jr., R. G. Shepherd, Jr., A. Thomas, C. D. West, and E. H. Land, J. Opt. Soc. Am. 36, 460 (1946).

[2] J. H. Shenk, E. S. Hodge, R. J. Morris, E. E. Pickett, and W. R. Brode, J. Opt. Soc. Am. 36, 569 (1946).

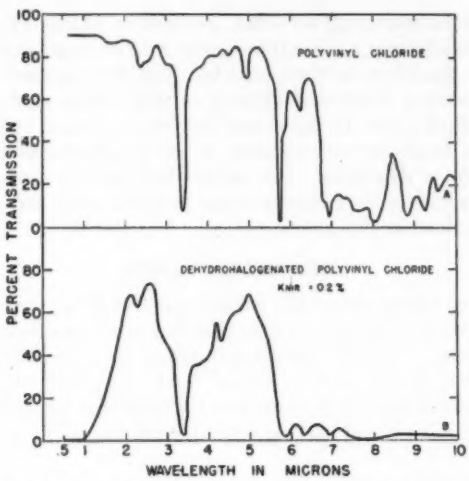

FIG. 2. Spectra of polyvinyl chloride and dehydrohalogenated polyvinyl chloride films.

strength. Certain polymers of the vinyl type fulfill these requirements and have the proper chemical structure to undergo the conversion reactions.

We have used films of polyvinyl chloride (I) and polyvinylidene chloride (III) for the preparation of visible-absorbing, infra-red transmitting filters.‡ The reactions (Fig. 1) used in the preparation of these filters involve dehydrohalogenation (the removal of the elements of hydrogen halide from successive groupings along the polymer chain), probably yielding in the case of polyvinyl chloride a polyene-type structure (II), that is, one containing alternate single and double carbon-carbon bonds. In the dehydrohalogenation reaction involving polyvinylidene chloride, the reaction may take several courses as indicated by four possible types of end products (IVa, IVb, IVc, IVd). It is not easy, and indeed we have not attempted, to determine the exact chemical structure of the end products of this reaction.

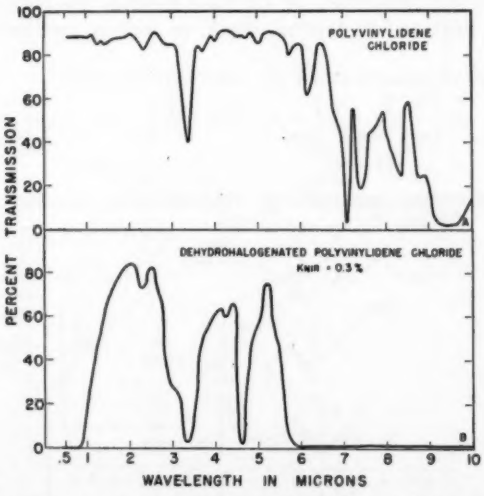

FIG. 3. Spectra of polyvinylidene chloride and dehydrohalogenated polyvinylidene chloride films.

‡ We are greatly indebted to J. E. Beaumont and R. S. Hallas of Bakelite Corporation for experimental samples of these films.

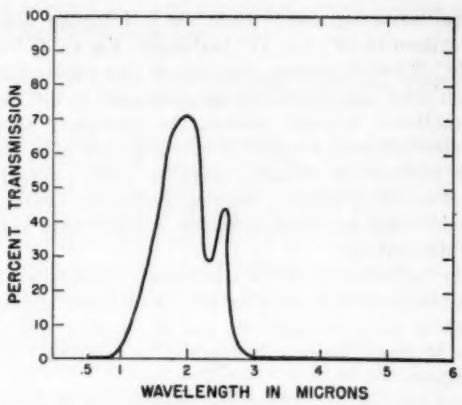

FIG. 4. Spectrum of glass-laminated dehydrohalogenated polyvinyl chloride filter.

When clear films of polyvinyl chloride or polyvinylidene chloride are immersed in mixtures of strong alkalies and swelling agents, and then heated for approximately five hours at 140°C, reactions occur similar to those shown in Fig. 1 concomitantly with the transformation of the transparent films to black films which are essentially opaque to ultraviolet and visible light. We assume that the absorption of radiation in the ultraviolet and visible by such films is due to electronic transitions possible in the polyene, polyine, and cumulene structures postulated. The position of the long wave-length cut-off (transmission < one percent) lies between 0.75 and 0.95μ and can be varied by controlling the extent and duration of the dehalogenation reaction.

Figure 2 shows the spectra over the region 0.5 to 10μ of the original polyvinyl chloride film (A) and the film after it has undergone the dehalogenation reaction (B). Besides the region of absorption in the visible, the region from 6 to 10μ also has lost transmittance as a result of the dehydrohalogenation. The dehydrohalogenated polyvinyl chloride film has essentially two broad transmission bands, one between 1 and 3.3μ

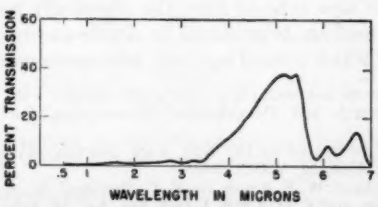

FIG. 5. Spectrum of dehydrohalogenated polyvinyl chloride with magnesium oxide fumed on surface.

and the second between 3.5 and 5.8μ. The absorption band at 3.3μ results from carbon-hydrogen stretching vibrations and the inflection point around 3μ is probably due to the presence in the sheet of a small amount of O-H groups formed during the reaction.

Analogous absorption spectra are shown in Fig. 3 for polyvinylidene chloride and its dehydrohalogenated product. In this case three transmission bands are seen after dehydrohalogenation. The long wave-length transmission region has been split into two regions by an absorption band lying at 4.6μ. This 4.6μ absorption can be attributed to the presence of $-C\equiv C-$ groupings in the material.

For some uses of such materials as filters it may be desirable to isolate one of the transmission bands of the dehydrohalogenated materials whose spectra are shown in Figs. 2 and 3. To obtain a filter having a broad transmission peak in the 1 to 2.8μ region, it is necessary only to laminate either of the dehydrohalogenated materials to or between glass plates of thickness greater than about 0.060 in., since such glass plates are an effective absorbing medium for wave-lengths greater than about 2.8μ (Fig. 4).

ABSORPTION-SCATTERING FILTERS

To obtain a filter showing transmission only in the 3.5 to 5.8μ region, we have employed scattering filters after the manner first described by Pfund[3] in combination with these visible-absorbing filters. Figure 5 shows the spectrum of a filter prepared by fuming magnesium oxide onto dehydrohalogenated polyvinyl chloride film. In order to obtain satisfactorily low transmission in the 1 to 3.4μ range, it is necessary to apply sufficient magnesium oxide so that the transmission in the 3.5 to 5.8μ range is also somewhat reduced (cf. Figs. 2B and 5). The effect of the particle size of the scattering medium upon the transmission characteristics of the filter may be seen in Fig. 6, where the spectra are shown of several filters prepared with zinc oxides of differing and known average particle sizes.§

These filters were prepared by dispersing the zinc oxide in linseed oil and coating this paste onto the dehydrohalogenated film in a layer approximately 50μ thick. It is evident that with increasing particle size the filters become less and less transparent to shorter wave-length radiation.

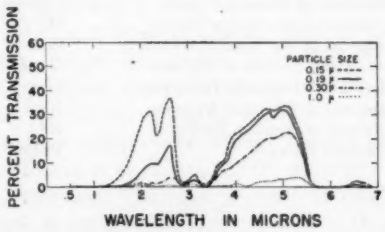

FIG. 6. Spectra of zinc oxides and dehydrohalogenated polyvinyl chloride showing effect of particle size.

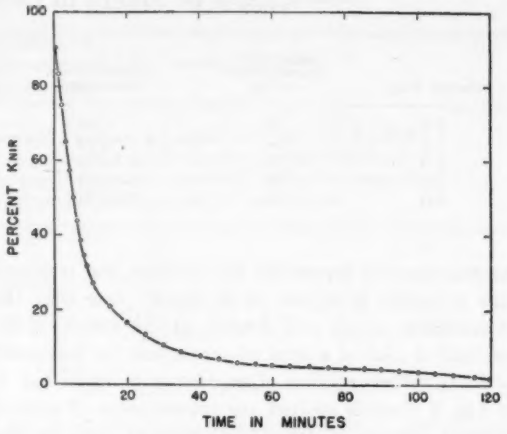

FIG. 7. Extent of dehydrohalogenation of polyvinyl chloride as measured by K_{NIR} shown as a function of time of heating. Circles indicate experimental points.

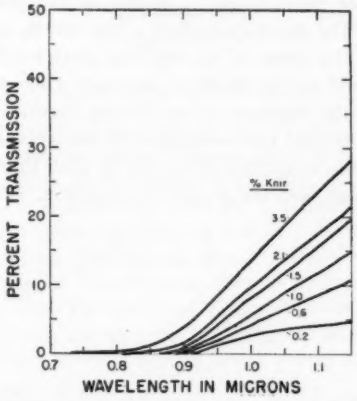

FIG. 8. Near-infra-red transmission of various samples of dehydrohalogenated polyvinyl chloride showing effect of variation of extent of reaction on transmission.

PREPARATION AND TESTING

Although filters have been prepared from both polyvinyl chloride and polyvinylidene chloride, the polyvinyl chloride film seems to be preferable since the resulting filters are less brittle. Polyvinyl chloride film (thickness ~0.005 in.) is immersed in a mixture of *100* parts methyl ethyl ketone, *25* parts Solox (as diluent), and *20* parts benzyl trimethyl ammonium hydroxide (MeOH solution)** at room temperature for about seven minutes. This film is then heated in an extended condition for five hours at 140°C, during which time it turns black as the reactions proceed. Obviously the extent of

[3] A. H. Pfund, Phys. Rev. **36**, 71 (1930).

§ We are indebted to C. E. Barnett of New Jersey Zinc Company for kindly supplying us with these samples of zinc oxide.

** Obtainable from Rohm and Haas Company, Philadelphia, Pennsylvania.

TABLE I.

Percent K_{NIR}	Maximum transmission at 2.2μ	Effective visual transmission
0.5	75	$<10^{-6}$
1.0	74	$<10^{-6}$
2.0	79	1.3×10^{-5}
3.0	80	2.4×10^{-5}
4.0	79	7.6×10^{-5}

the reaction will depend on the duration and temperature at which it occurs. It is equally true that the transmission cut-off will depend on the extent of the reaction. A plot of extent of conversion (as measured by K_{NIR} values) *vs.* time of reaction is shown in Fig. 7. In Fig. 8 there is plotted the transmission of several different samples of dehydrohalogenated films for the region 0.7 to 1.2μ.

The apparatus used for making and measuring small samples of these filters is shown in the photograph (Fig. 9). The apparatus offers a convenient means for following the extent of the reaction, since readings may be obtained as the reaction proceeds. One essentially measures the response of the filtered photo-tube. This response, termed the near-infra-red transmission or the K_{NIR} value, is roughly indicative of both the extent of the reaction and the visual transmission. In Table I there are given a few values of K_{NIR} and effective visual transmission of a series of filters.

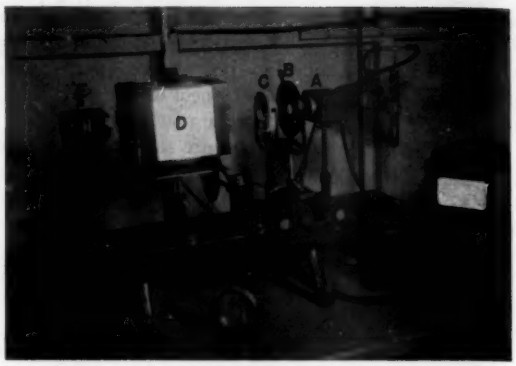

FIG. 9. Equipment used in preparation of filters and in measurement of K_{NIR}. (A) Closely coiled tungsten filament source. (B) Iris diaphragm (to adjust zero). (C) Condensing lens. (D) Temperature-controlled oven, with Pyrex glass end plates, in which reaction occurs. (E) RCA No. 922 photo-tube covered with Wratten No. 87 filter. (F) Sample holder. (G) Voltmeter which reads K_{NIR} directly.

The effective visual transmissions were measured using a Naval Research Laboratory high density filter photometer.[4]

[4] R. L. Tousey and D. E. Mitchell, J. Opt. Soc. Am. **36**, 362 (1946).

Announcement on Binding of Journals

From time to time, the Institute has received inquiries from subscribers for information as to where and how they may have their copies bound. After investigation the Institute has found that this may be best accomplished by selecting a capable bindery that will work to our specifications and produce a well-bound volume at as low a price as possible. The necessary arrangements have been completed with the Book Shop Bindery, 308 West Randolph Street, Chicago 6, Illinois.

The volumes will be bound in the best grade of washable buckram with facsimile gold stamping on the spine and the subscriber's name in gold on the front cover. A distinctive color for each of the Journals has been selected as listed below. Advertising matter and covers are removed before binding. The price of $3.00 per volume applies to any of these journals regardless of size. Issues, comprising complete volumes, should be sent by prepaid express or parcel post to the Book Shop Bindery. Bound volumes will be shipped approximately 30 days after receipt. Return transportation will be prepaid when remittance accompanies order.

No deviation in color or specification can be allowed in view of the favorable price.

Physical Review	Green
Reviews of Modern Physics	Orange
Journal of the Optical Society	Brown
Journal of the Acoustical Society	Orange
American Journal of Physics	Black
Review of Scientific Instruments	Grey
Journal of Chemical Physics	Blue
Journal of Applied Physics	Red
Physics Today	Purple

A Method for Calculating the Effect of Filters on Color Vision

HERMANN VON SCHELLING
Medical Research Laboratory, U. S. Naval Submarine Base, New London, Connecticut
(Received March 10, 1950)

The purpose of this paper is to calculate specimen curves which indicate in general how colors shift if a filter is applied. The first section contains the mathematical formulas. The method is used for studying the absorption by the macular pigment (Section II) and by the intraocular media (Section III). The last example (Section IV) refers to the change in illumination from illuminant C to illuminant A and inversely.

I.

THE appearances of object colors vary from individual to individual due to differences in macular and other ocular pigmentation and vary for each individual with the illumination. These are ever-present factors in color vision. They will be treated mathematically as negative and positive filters superposed upon the 1931 I.C.I. Coordinate and Standard Observer System.

The physical properties of a color stimulus are described completely by a spectral distribution curve of the radiant energy which reaches the eye. Regardless of the spectral composition of a color it may be represented on the I.C.I. diagram by a point which expresses the proportions of the three primaries in the system which will give a matching color for a standard observer and given illuminant. Every point in the I.C.I. diagram may be matched by an infinity of spectral distributions known as metamers. If a filter is introduced between a colored object and the eye, the spectral distribution from that object will naturally be modified and its I.C.I. match therefore altered, but metamers will not all be altered in the same way since the effect of the filter varies with the characteristics of the spectral distribution. The shifts of any point representing the full range of its metamers, when a particular filter is introduced, can be calculated and a representative direction and amount of shift determined, expressed as some equivalent point on a diagram.

Thus we can select any point P, which may be of any possible spectral composition, in the chromaticity diagram, Fig. 1, and find the area which includes all the points to which its metamers can shift as the result of the introduction of a specific filter. We will start with the simplest case in which the color is produced by a mixture of two wave-lengths opposite relatively to P. Let us draw straight lines through P which intersect the spectral locus in s_1, s_1'; s_2, s_2'; s_3', p_3; where p refers to the purple line. The color p could be produced by a mixture of the spectral lights s_1, and s_1', s_2 and s_2', s_3, and a mixture of s_{380} and s_{780} which equals p_3. For simplicity the unit of luminance is chosen so that the amounts a_1 and a_1'; a_2 and a_2', $\cdots$ of the combined spectral lights add to unity. Let us consider the mixtures

$$\left.\begin{array}{ll} a_1s_1+a_1's_1' & a_1+a_1'=1 \\ a_2s_2+a_2's_2' & a_2+a_2'=1 \\ \cdots\cdots\cdots & \cdots\cdots\cdots \\ b_3s_3+b_3's_{380}+b_3''s_{780} & b_3+b_3'+b_3''=1 \end{array}\right\}. \quad (1)$$

All these combinations of two or three spectral lights correspond to the one point P. If we insert a filter with the transmission curve $t(\lambda)$, we get the different points P'.

$$\left.\begin{array}{l} a_1t_1s_1+a_1't_1's_1' \\ a_2t_2s_2+a_2't_2's_2' \\ \cdots\cdots\cdots \\ b_3t_3s_3+b_3't_{380}s_{380}+b_3''t_{780}s_{780} \end{array}\right\}. \quad (2)$$

These points P' describe a closed curve. But it can happen that the curve intersects itself or is concave in some sections. If two couples of opposite lights in Fig. 2, produce the shifts PP_1' and PP_2', a mixture of these couples of lights can produce a shift PP_3' where P_3' is any point on the straight segment $P_1'P_2'$. Therefore, concavities of the P' curve have to be extended by a straight line. The corrected P' curve is the locus of all points which correspond to the original point P and to the set of reflection curves which reflect only two or three wave-lengths.

This set is an extreme. The selectivity of absorption of

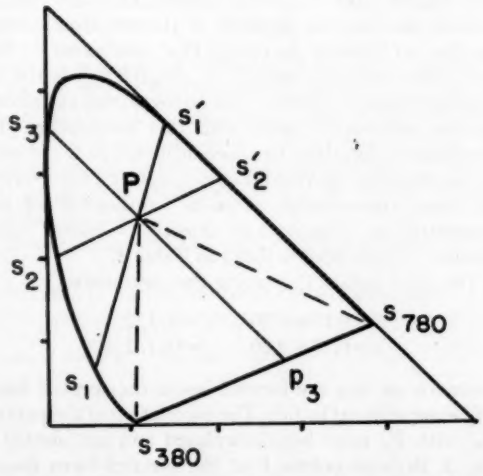

FIG. 1. The calculation of P from opposite spectral lights.

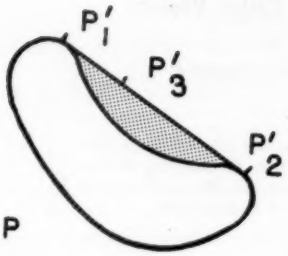

FIG. 2. The correction of the P' curve for limited sets of wave-lengths.

the filter must be strong for such conditions. The point P' corresponding to P will fall inside the convex area for all other reflection curves with a high probability. Only artificial examples can be constructed for which P' is located outside the convex area.

Let us cover the chromaticity diagram by a selected orthogonal lattice. We denote the points of intersection P_{ij} and calculate for every such point the convex area of points P_{ij}'. This patch contains all possible color shifts of the point P_{ij} which can occur, when we look through our filter.

If we calculate many patches, the graphical representation becomes confusing. But we can connect the geometric centers of these patches by smooth curves. These curves indicate how the original lattice is distorted on the average. The evidence of such a diagram is amazing. We survey instantaneously the average effect of the filter on color vision. The transmission curve of the filter describes the material physically, the new diagram pictures the typical color shifts when we look through the filter.

II.

Color perception reaches maximum sensitivity in the fovea centralis which is the region associated with, or surrounded by the macula. Therefore, we will consider that yellow filter as a first example. G. Wald[1] has extracted the macular pigment of the eye from a small number of human maculae. His conclusion is that crystalline leaf xanthophyll $[C_{40}H_{54}(OH)_2]$ is the absorbing substance. Wald's tests on foveal and extrafoveal spectral sensitivity agree with this assumption. The xanthophyll spectrum has been adjusted to the average of ten observers by Wald. Let us consider a filter having the same transmission curve as xanthophyll of unit concentration. The optical density $(=-\log^{10}$ transmission) of this filter is listed in Table I.

The eight points P_{ij} having the coordinates

$$x=0.15+0.20i, \quad i=0, 1, 2,$$
$$y=0.15+0.20j, \quad j=0, 1, 2, 3,$$

inasmuch as they are located inside the spectral locus, define our original lattice. The correlation of the patches P_{ij}' with P_{ij} have been calculated and are plotted in Fig. 3. Because points P at the spectral locus do not shift, the patches near the spectral locus are small. The scattering of the P_{ij}' depends significantly upon the faculty of the objects to reflect extreme violet rays.

If we form a simple average, those rare cases having a strong reflectance in the violet region would be overrated. It is convenient for practical purposes to represent the mean shift by the actual deviation of Munsell papers. The arrows in Fig. 3 for selected colors nearest the intersection points show such shifts if a xanthophyll filter of unit thickness is added to the filter assumed to be present in the standard observer eye. The length and direction of these arrows demonstrate that the most frequent position of shift will ordinarily be located in the upper right corner of the patches.

Average shifts as determined on the above principles have been drawn in Fig. 4. It indicates the changes which would occur in chromaticity for a man whose pigment is twice the normal. Since such variations of pigmentation have been observed by Wald[1] the example is of practical significance.

G. Wald observed almost unpigmented eyes too. Therefore, it would be interesting to get the set of curves for a xanthophyll filter of negative unit thickness. The positive filter may have shifted a point P to P'.

The straight line PP' in Fig. 5 may intersect the spectral locus in s and s'. Then, the negative filter pushes the point P the distance PP'' opposite to PP'. It is

$$P''P=sP/[1+(sP\times P's')/(PP'\times Ps')].$$

This equation holds for any point P' on the circumference of a patch. It should be correct for the most frequent shifts also. If applied to the points of intersections in Fig. 4 we get Fig. 6. This graph shows the chromaticity of an eye with zero macular pigment.

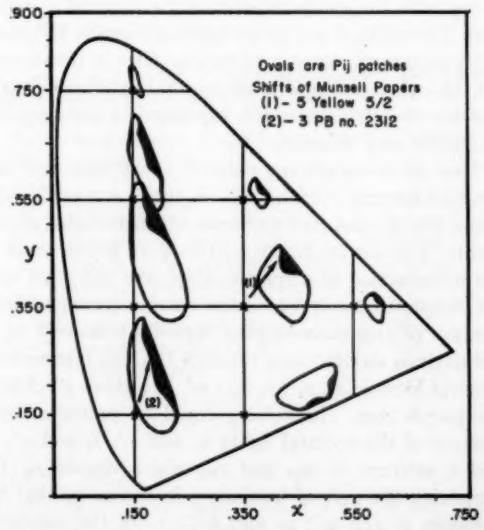

FIG. 3. Possible chromaticity shifts caused by xanthophyll filter of unit thickness.

[1] G. Wald, Science **101**, 653 (1945).

It may be noted that the white point of an unpigmented observer would be ($x=0.24$; $y=0.22$), if illuminant B (near to the lattice point $x=0.35$; $y=0.35$) is used. The white point of an almost unpigmented observer, mentioned in the following paragraph, is ($x=0.28$; $y=0.28$). He seems to have had traces of macular pigmentation.

We are indebted to W. D. Wright[2] for some numerical information which may be used for comparison. He determined the white point for 36 normal observers. Illuminant B was matched with a mixture of spectral lights of wave-lengths 460, 530, and 650 mμ. Illuminant B ($x=0.3485$; $y=0.3518$) is near to our lattice point ($x=0.35$; $y=0.35$). When we insert a xanthophyll filter of unit thickness, the mixture of Wright's spectral lights shifts to ($x=0.427$; $y=0.453$). This point is located at the circumference of the correlated patch. That was to be expected because the mixture had been formed by only three spectral lights.

Wright's data refer to a special coordinate system in which the primaries are the spectral lights of the wave-lengths 650, 530, and 460 mμ. The white point—using illuminant B—has the coordinates in the I.C.I. system:

	$x=0.3485$	$y=0.3518$.
Significant points are:		
Wright's white point age 22	$x=0.323$	$y=0.320$
Wright's white point age 38	0.367	0.373
White of a nearly unpigmented observer 0_1	0.28	0.28
White of a most pigmented observer 0_2	0.40	0.42.

The 36 white points of the normal observers are located in a narrow angle which is defined by connecting the point 0_1 with the points 570 and 578 mμ of the spectral locus by straight lines.

The wedge of Fig. 4 contains the white points (illuminant B) of Wright's 36 observers. The correlation between Wright's data and the calculated shift is excellent.

III.

Color vision may be influenced also by variations in the absorption of the intraocular media. Ludvigh and MacCarthy[3] have provided data on this absorption. They had the opportunity to test four human eyes immediately after their enucleation. The age of the four patients varied between 59 and 66 years. The authors cut the sclera and choroid near the posterior pole carefully with a use of a trephine 5 mm in diameter. The pigment epithelium and retina were painstakingly removed from the region of the aperture. The eye was placed in an appropriate container with the pupil facing down. The beam emerging from the exit slit of the spectrometer, when incident on the cornea, was never larger than 2 mm square. The authors measured the whole intraocular absorption except that of the macular pigment.

When these observations were finished, they determined separately the transmission of the lenses of each of the four eyes. They subtracted the absorption of the lens and added the absorption of an average of five normal lenses of a mean age of 21.5 years. By this method, they eliminated the dimming of the lens with age. Finally, they gave the transmission $t(\lambda)$ of the eye media. We get the corresponding optical density by the formula $D(\lambda)=-\log^{10}t(\lambda)$. The optical densities are listed in Table II for different wave-lengths.

These data are sufficient for constructing the color distortions which are an effect of the absorption in the intraocular media. But the calculation would not be worth while. If we look at an ideal white paper, using illuminant C ($x=0.310$; $y=0.316$), the point shifts to

x	y	
0.389	0.425	positive unit xanthophyll filter,
0.227	0.188	negative unit xanthophyll filter,
0.351	0.366	positive unit intraocular filter,[3]
0.264	0.246	negative unit intraocular filter.[3]

The directions of these shifts nearly coincide. The effects of the absorption by the macular pigment and by the intraocular media cannot be separated. It may be noted that color sensations of a young child having no intraocular absorption, would be represented by 50 percent of the distortions in Fig. 6, if the macular pigment is normal.

The fan-shaped scatter of Wright's observers (Fig. 4)

TABLE I. Xanthophyll of unit thickness.

λ in mμ	Optical density	λ in mμ	Optical density
360	0.182	465	0.487
70	0.193	70	0.429
80	0.228	75	0.426
90	0.246	80	0.465
400	0.311	85	0.479
05	0.350	90	0.431
10	0.360	500	0.228
20	0.410	10	0.083
30	0.504	20	0.031
35	0.484	30	0.014
40	0.472	40	0.008
45	0.509	60	0.003
50	0.572	80	0.001
55	0.598	600	0.0006
60	0.584		

TABLE II. Optical densities of the intraocular media.

in mμ	Optical density	in mμ	Optical density	in mμ	Optical density
400	1.066	70	0.359	80	0.226
10	0.975	80	0.339	600	0.215
20	0.796	90	0.318	20	0.200
30	0.606	500	0.305	40	0.188
40	0.498	20	0.280	60	0.178
50	0.411	40	0.253	80	0.161
60	0.371	60	0.243	700	0.152

[2] W. D. Wright, *Researches on Normal and Defective Color Vision* (C. V. Mosby Company, St. Louis, 1947).

[3] E. Ludvigh and E. F. MacCarthy, Archives of Ophthalmology **20**, 37 (1938).

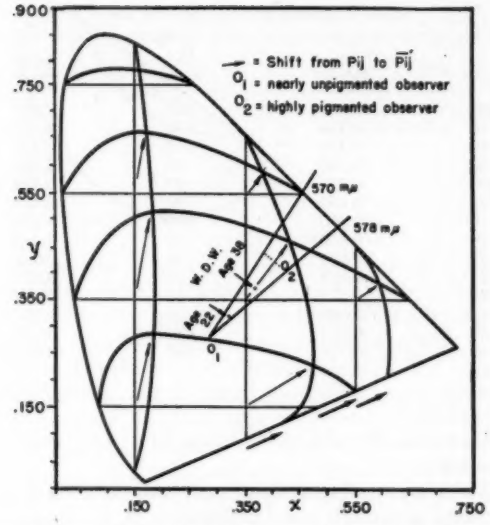

FIG. 4. Mean chromaticity shifts caused by xanthophyll filter of unit thickness weighted with Munsell papers.

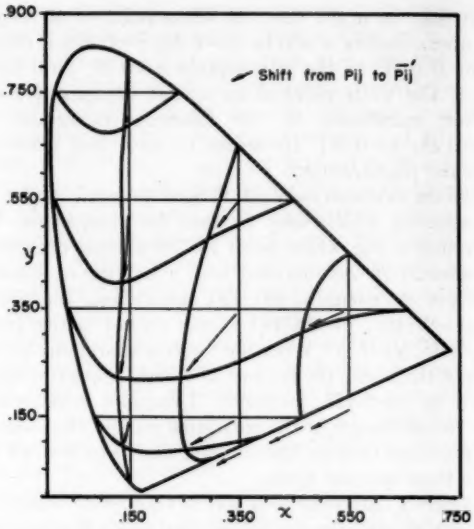

FIG. 6. Mean chromaticity shifts caused by xanthophyll filter of negative unit thickness (zero macular pigment).

is insufficiently explained by the combinations of ocular absorptions which have been examined. Additional dispersion would be introduced by considering eyes with neither macular nor ocular pigmentation. Some further scatter may be explained by the normal distribution of the red to green ratio of the retinal receptors.

IV.

Another application of Section I may be more frequently applicable. In the first example the filter was inserted between the illuminated object and the eyes. If it is put between the light source and the object, the illumination is changed. Therefore, our method can be applied to different light sources, for instance illuminants C and A. We can draw the possible and the average color shifts if we make use of illuminant A instead of C or if we go from daylight to a room illuminated by incandescent lamps.

The eight patches correlated to the former lattice are represented in Fig. 7. The narrow right lower ends of the patches depend upon rays of extreme long wave-lengths. Calculations were confined to lights between 380 and 700 mμ since brightness of illuminant C decreases rapidly above 700 mμ and the calculations become less reliable. The lengths of the tails of the patches are very sensitive to the upper limit of wave-length.

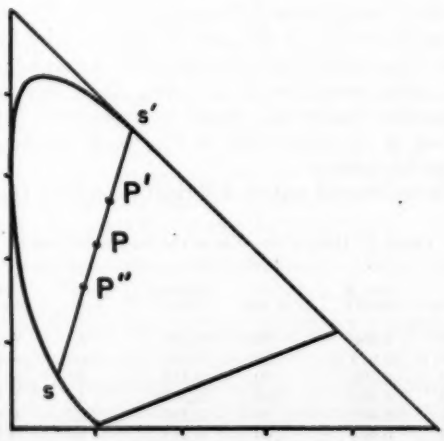

FIG. 5. Shift by a negative filter as compared with the shift by the corresponding positive filter.

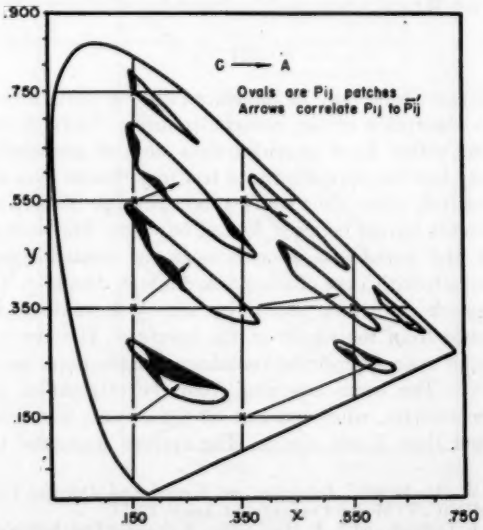

FIG. 7. Possible shifts in chromaticities from illuminant C to A.

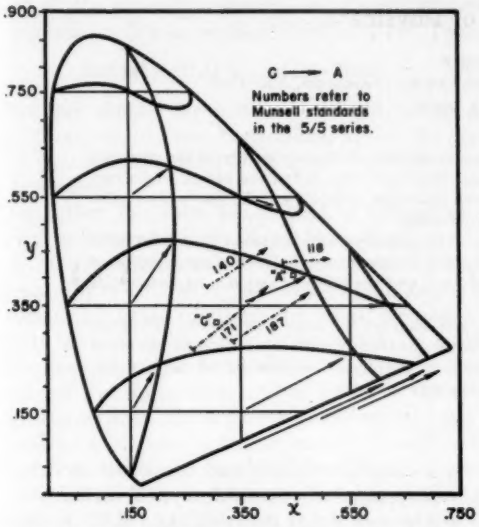

FIG. 8. Mean shifts in chromaticities weighted with Munsell papers.

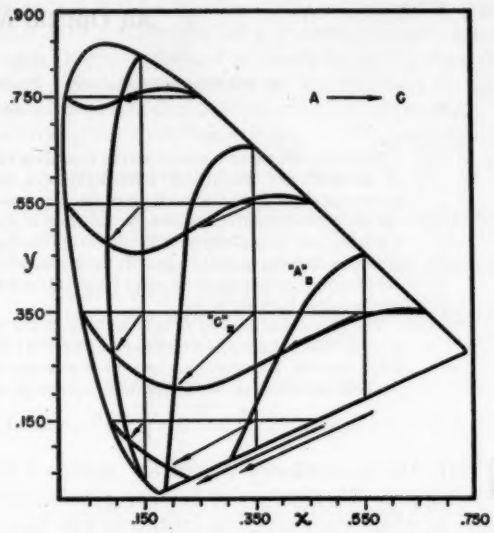

FIG. 9. Mean shifts in chromaticity from illuminant A to C.

Again Munsell papers may be used for weighting. Figure 8 shows the Munsell hues Nos. 118, 140, 171, and 187 for illuminants C and A. The arrows indicate that the correct mean divides the distance from the upper to the lower corner of the patches by the ratio of about 1 to 2. The mean shifts have been drawn as Fig. 8.

The most striking effect on chromaticity is the great change from a deep purple to a nearly pure red. Changes in chromaticity are always in the direction from short to long wave-lengths with the possible exception of violet since it can shift to the purple side. These results agree with our common experience and are useful because they fix our impressions numerically.

An attempt to invert the distortion curves $C \rightarrow A$ using the approximation in Section II yields erroneous results. It cannot be assumed that the shifts $A \rightarrow C$ are opposite to the shifts $C \rightarrow A$. Therefore, the x_C curves and the y_C curves have been determined for $C \rightarrow A$, using a spacing of only 0.025 unit of the I.C.I. chromaticity diagram. This chart has been inverted by interpolation. Figure 9 shows curves read from the exact diagram.

All figures have been given only as illustrations to supplement the test and the entire curves were not computed. More patches would be needed if exactness is necessary. If the method should be accepted generally, more exact distortion curves can be constructed for filters and for changes in illumination on the above principles.

Reprints of full-scale diagrams giving mean chromaticity shifts of pigments for illuminants C and A and for xanthophyll filter may be requested from the Naval Medical Research Laboratory, U. S. Submarine Base, New London, Connecticut.

ACKNOWLEDGMENT

I wish to thank Dean Farnsworth for directing my attention to the problems of color vision and for suggestions and assistance in this particular article.

An Optical Model of Physics*

MAX HERZBERGER
Kodak Research Laboratories, Eastman Kodak Company, Rochester, New York
(Received April 12, 1950)

Optics in the paper is considered as consisting of three layers: *geometrical optics*, which gives the geometry of the problem (straight lines equal light rays, spheres equal wave surfaces), *diffraction optics*, which considers a periodic disturbance of given frequency along selected light rays (a field), and the *theory of emission and absorption*, which considers the selection of discrete frequencies.

Physics can be built up parallel to it as optics in space-time. The *geometry* of physics based upon a variation principle contains general relativity as a special case; *diffraction physics* gives the laws of propagation of electromagnetic energy of all wave-lengths in a well-defined field; and the *theory of emission and absorption* selects suitable frequencies.

The paper describes in detail the laws of the first level and sketches the basic problems of diffraction physics. The problems of emission and absorption are only mentioned (Einstein effect) and will be treated in detail later on. Electricity and gravitation emerge in this theory as the physical equivalence of the fact that the field equations can be split into a symmetric and an antisymmetric part.

THE Michelson-Morley experiment shattered the hopes of the physicist of building a mechanical model in which every physical experience can be explained by the relative motion of particles with respect to each other.

It has been established beyond any doubt, because of the increased accuracy of the measurements, that the velocity of the propagation of radiant energy is a universal constant, the measure of which is independent of the motion of the observer. As a result, the development of physical theory has progressed rapidly in different directions. The theories of special and general relativity have aimed at a general field theory which covers at the same time gravitational and electrical fields and constitutes a continuum theory of physical phenomena in contrast to quantum-mechanics, the concepts of which have postulated a theory of matter and energy which not only considers matter as discontinuous, but assumes that energy transport also has a discontinuous structure. Both theories have remarkable successes to their credit, to which the most recent branch of physics, namely, nuclear physics, bears witness. Both models are in a certain way based on attempts to carry out and to modify the ideas which W. R. Hamilton introduced into physics. However, there are wide ranges of physical problems which only one of the two theories can explain simply, and the physicist vacillates in his explanation between a wave theory of radiation and an atomistic theory, without being able to combine both in a single model.

This paper will sketch a method in which physical experience is considered as a generalization of the laws of optics in an inhomogeneous, anisotropic space-time continuum. By superimposing on the field laws (corresponding in three dimensions to the laws of geometrical optics) a kind of diffraction theory, it is hoped that a basis will be found from which to attack the fundamental problems of quantum mechanics, and thus to obtain a relatively simple and consistent model with which to approach the facts of physical reality.

It will be shown that the basic ideas of W. R. Hamilton, if analyzed in detail, not only give a simple solution of the problem of a field theory combining gravitation and electromagnetism, but also contain general relativity as a special case. The superposition of diffraction theory in its simplest form as developed by Huygens and Fresnel gives a good working hypothesis for describing radiant energy in the field. The mathematical details will be described in another paper and will be applied to specific problems in different fields of physics. The present paper will give only the basic ideas of my theory and show that they are not more than the consistent continuation of the classical approach to similar problems in the field of physics. In spite of this restriction, the theory, if accepted, would have a great number of results which would be at variance with present ideas, though in my opinion not at variance with experimental evidence. Gravitational waves on the one hand and the existence of photons on the other will have no place in this theory. One of the results is that the theory predicts the existence of electromagnetic fields in certain mechanical experiments. The discovery of such fields would be a confirmation of the ideas developed here. This paper, for the greater part, will be restricted to considering the qualities of the field far away from its singular points.

1. THE OPTICAL MODEL IN THREE-SPACE

In 1929 the author published a paper under the title, "Ein allgemeines optisches Gesetz," in which he derived the laws of geometrical optics from a single theorem.[1]

Let $\mathbf{s}$, $\mathbf{s}^*$ be vectors in the direction of an object and its image ray, respectively; let $\mathbf{a}$ and $\mathbf{a}^*$ be the vectors from object and image origins to a point on the object and image ray, respectively; let n, n^* be the refractive indices in object and image space. It is assumed that $\mathbf{s}$ and $\mathbf{s}^*$ have lengths n and n^*, respectively.

* Communication No. 1337 from the Kodak Research Laboratories.

[1] M. Herzberger, Zeits. f. Physik 53, 237 (1929).

Consider, now, three neighboring rays, one given by $\mathbf{a}, \mathbf{s}, \mathbf{a}^*, \mathbf{s}^*$, the second by $\mathbf{a}+d\mathbf{a}, \mathbf{s}+d\mathbf{s}, \mathbf{a}^*+d\mathbf{a}^*, \mathbf{s}^*+d\mathbf{s}^*$, and the third by $\mathbf{a}+\delta\mathbf{a}, \mathbf{s}+\delta\mathbf{s}, \mathbf{a}^*+\delta\mathbf{a}^*, \mathbf{s}^*+\delta\mathbf{s}^*$. Then

$$(d\mathbf{s}^*\delta\mathbf{a}^*-\delta\mathbf{s}^*d\mathbf{a}^*)=(d\mathbf{s}\delta\mathbf{a}-\delta\mathbf{s}d\mathbf{a}). \tag{1.1}$$

This very general theorem can be taken, and in my book, *Strahlenoptik*, has been taken, to be the basic law of geometrical optics, since from it all other laws can be derived.

The author has since found that he cannot claim priority in discovering the above formula. It is to be found in the writings of W. R. Hamilton (1830), on optics and is even older, going back to J. L. Lagrange, who applied it to the problems of celestial mechanics in 1808. It has been rediscovered in many fields of mathematics and physics; it forms the basis of Lie's theory of contact transformations and of Cartan's theory of integral invariants, and is known as Helmholtz's law of vortices in aero- and hydromechanics, as well as the theorem of Liouville in statistical mechanics. In optics, R. Straubel first drew attention to some important special cases of it. In this paper it will be taken as the basic formula for a general field theory.

To return to optics, the author soon found that Eq. (1.1) can also be applied to geometrical optical problems in an inhomogeneous space (length n of $\mathbf{s}$ being variable), or to anisotropic media (crystals), if $\mathbf{s}$ is replaced by the momentum vector, $\mathbf{p}$, giving

$$d\mathbf{p}^*\delta\mathbf{a}^*-\delta\mathbf{p}^*d\mathbf{a}^*=d\mathbf{p}\delta\mathbf{a}-\delta\mathbf{p}d\mathbf{a}, \tag{1.2}$$

where $\mathbf{p}$ is given, if the refractive index is assumed as a function of the point, $\mathbf{a}(x_i)$, and direction cosines, $\mathbf{s}(\xi_i)$, by

$$\mathbf{p}=(\partial n/\partial\xi_i) \tag{1.3}$$

under the added condition that n is homogeneous of the first order in the ξ_i. This latter fact is equivalent to

$$\mathbf{pa}'=(\partial n/\partial\xi_i)\xi_i=n. \tag{1.4}$$

Equation (1.2) reveals that the expression on the right side is an invariant, if $\mathbf{a}$, $\mathbf{a}+\delta\mathbf{a}$, $\mathbf{a}+d\mathbf{a}$ are chosen arbitrarily on three neighboring light rays. Let $\mathbf{a}$ be a function of the curve parameter, τ. We then can write (1.2) in the form

$$(d/d\tau)(d\mathbf{p}\delta\mathbf{a}-\delta\mathbf{p}d\mathbf{a})=0. \tag{1.5}$$

Since Eq. (1.5) is independent of the curve parameter, it is assumed that the parameter is s, the arc length along the light rays.

The mathematician can interpret Eq. (1.5) in a different way. Let an arbitrary two-dimensional manifold of light rays be determined by a two-dimensional manifold of starting points, $\mathbf{a}(u, v)$, and starting momentum vectors, $\mathbf{p}(u, v)$. Let, in general, the points of the light rays be given by $\mathbf{a}(u, v; s)$ and $\mathbf{p}(u, v; s)$. Then, for the light rays,

$$\frac{d}{ds}\left(\frac{\partial\mathbf{p}}{\partial u}\frac{\partial\mathbf{a}}{\partial v}-\frac{\partial\mathbf{p}}{\partial v}\frac{\partial\mathbf{a}}{\partial u}\right)=0. \tag{1.6}$$

The reader, again, will notice that replacement of the parameters, u and v, by others will not change Eq. (1.6), i.e., it is the expression of a geometrical fact, which can be roughly expressed in words by saying that the flux of light is an invariant of the manifold of light rays, independent of the intersecting surface element.

Carrying out the differentiation in (1.5), we obtain

$$d\mathbf{p}'\delta\mathbf{a}+d\mathbf{p}\delta\mathbf{a}'-\partial\mathbf{p}'d\mathbf{a}-\partial\mathbf{p}d\mathbf{a}'=0, \tag{1.7}$$

if differentiation with respect to the curve parameter, $\mathbf{s}$, is designated by a prime.

Equation (1.7) can be considered as the integrability condition for a series of functions.

First, there is a function, $n(x_i, x_i')$, namely, the refractive index above, which is given by

$$dn=\mathbf{p}'d\mathbf{a}+\mathbf{p}d\mathbf{a}'=(d/ds)(\mathbf{p}d\mathbf{a}). \tag{1.8}$$

Second, there is a function, H, of $\mathbf{p}$ and $\mathbf{a}$ such that

$$dH=\mathbf{a}'d\mathbf{p}-\mathbf{p}'d\mathbf{a}. \tag{1.9}$$

The existence of both of these functions is equivalent to (1.5), which, in the language of mathematics, is the integrability condition of (1.6), because from (1.7) or (1.8) follows

$$\delta dn-d\delta n=d\delta H-\delta dH=\delta\mathbf{p}'da+\delta\mathbf{p}d\mathbf{a}'-d\mathbf{p}'\delta\mathbf{a}-d\mathbf{p}\delta\mathbf{a}', \tag{1.10}$$

d and δ meaning differentiation with respect to two independent parameters. Since H and n are only given in each case within an arbitrary constant, n can be assumed to be always positive and H to be given by

$$d(n+H)=d\mathbf{p}\cdot\mathbf{a}' \quad \text{or} \quad n+H=\mathbf{pa}'. \tag{1.11}$$

Because of the homogeneity relation, $n=pa$, the function, H, is identically zero in optics, i.e., at every point there exists a function,

$$H(\mathbf{p}, \mathbf{a})=0, \tag{1.12}$$

such that the end-points of $\mathbf{p}$ determine a surface, the *indicatrix*, which, in case the medium is isotropic, degenerates into a sphere.

Formula (1.7) shows that n is a function of $\mathbf{a}$ and $\mathbf{a}'$. If we consider a fixed object point (keeping $\mathbf{a}$ constant), n becomes a function of $\mathbf{a}$ alone. Therefore, $\mathbf{p}$ can be considered as a kind of gradient with respect to the vector field given by $\mathbf{a}$. Thus,

$$\begin{aligned}\mathbf{p}&=(\partial n/\partial u_i')\\ \mathbf{p}'&=(\partial n/\partial u_i),\end{aligned} \tag{1.13}$$

where u_i are arbitrary coordinates and $u_i'=du/ds$. Elimination of $\mathbf{p}$ from (1.13) leads to the Euler differential equations of variation-calculus,

$$(d/ds)(\partial n/\partial u_i')=(\partial n/\partial u_i), \tag{1.14}$$

which are of the same form as the Lagrange equations of the second kind in general mechanics. Carrying out the differentiation shows that the light rays are the

solutions of a simple system of linear differential equations of the second order:

$$\frac{\partial^2 n}{\partial u_i' \partial u_k'} u_k'' + \left(\frac{\partial^2 n}{\partial u_i' \partial u_k} - \frac{\partial^2 n}{\partial u_k' \partial u_i} \right) u_k' = 0. \quad (1.15)$$

As an example, let us compute the light rays for an inhomogeneous, isotropic medium, assuming Cartesian coordinates.

Since n must be homogeneous of the first order in x_i', the condition for isotropy is given by

$$n = n_0 (\mathbf{a}'^2)^{\frac{1}{2}} = n_0 (x_i'^2)^{\frac{1}{2}}, \quad (1.16)$$

with $\mathbf{a}'^2 = 1$.

This leads to

$$\frac{\partial^2 n}{\partial x_i' \partial x_k'} = \delta_{ik} n_0 \quad \text{with } \delta_{ik} = \begin{cases} 0 & i \neq k \\ 1 & i = k \end{cases}$$
$$\frac{\partial^2 n}{\partial x_i' \partial x_k} = \frac{\partial n_0}{\partial x_k} x_i'. \quad (1.17)$$

The Euler-Lagrange equations then become

$$n_0 \mathbf{a}'' + \left(\frac{\partial n_0}{\partial x_i^2} x_i' \right) \mathbf{a}' = \frac{\partial n_0}{\partial x_i} (\mathbf{a}'^2), \quad (1.18)$$

or simply

$$\mathbf{a}'' = \mathbf{g}(\mathbf{a}')^2 - (\mathbf{g}\mathbf{a}')\mathbf{a}',$$
$$\mathbf{g} = \frac{1}{n_0} \left(\frac{\partial n_0}{\partial x_i} \right), \quad (1.19)$$

where $\mathbf{g}$ is the logarithmic gradient of the surfaces, $n_0 =$ constant.

Using the Andreas cross ($\times$) for vector multiplication, we obtain

$$\mathbf{a}'' = (\mathbf{a}^* \times \mathbf{g}^*) \times \mathbf{a}' \quad (1.20)$$

as the equation of the light rays. This shows that for homogeneous media ($\mathbf{g} = 0$) the light rays are straight lines. For inhomogeneous media, torsion and curvature can be calculated from (1.20) as

$$\frac{1}{\rho^2} = \frac{(\mathbf{a}' \times \mathbf{a}'')^2}{(\mathbf{a}'^2)^3} = (\mathbf{g} \times \mathbf{a}')^2$$
$$\frac{1}{\tau} = \frac{[\mathbf{a}'\mathbf{a}''\mathbf{a}''']}{(\mathbf{a}' \times \mathbf{a}'')^2} = \frac{[\mathbf{a}'\mathbf{g}\mathbf{g}']}{(\mathbf{g} \times \mathbf{a}')^2}, \quad (1.21)$$

the bracket indicating the determinant product defined by

$$[\mathbf{abc}] = (\mathbf{a} \times \mathbf{b}) \cdot \mathbf{c} = \mathbf{b} \cdot (\mathbf{c} \times \mathbf{a}) = \mathbf{c} \cdot (\mathbf{a} \times \mathbf{b}). \quad (1.22)$$

Going back to the basic formulas, we form

$$E = \int n ds \quad (1.23)$$

along the light rays, E being the *light path* between two points. Since n is homogeneous of the first order in the u_i, then

$$E = \int n ds = \int \mathbf{p} d\mathbf{a}, \quad (1.24)$$

which shows that the integral is independent of the parameter chosen.

Consider, now, a one-parameter manifold of light rays with points, $\mathbf{a}(u, l)$, and on each beginning- and end-points, $\mathbf{a}(u)$, and $\mathbf{a}^*(u)$. The light path between $\mathbf{a}(u)$ and $\mathbf{a}^*(u)$ is then also a function of u, and from (1.8) it is seen that

$$dE = \mathbf{p}^* d\mathbf{a}^* - \mathbf{p} d\mathbf{a}, \quad (1.25)$$

where $\mathbf{p}^*$ is the normal vector along the extremal at the end-points. Since Eq. (1.25) is valid for an arbitrary one-dimensional manifold of light rays, it is equally valid for a two-, three- or four-dimensional manifold, which means that the expression on the right side is a total differential in all its parameters.

Formula (1.25) goes back to W. R. Hamilton and is used in the Hamilton-Jacobi theory of differential equations and in Lie's theory of contact transformations. The formula has been called the "Bible" by my assistant, E. Marchand, since, on account of the freedom which it affords in choosing the manifold of rays and the manifold of beginning- and end-points, all laws of optics can easily be obtained by specializing, as Hamilton has shown in many cases and the author has in many others.

A few examples follow. Consider the rays from a fixed object point and choose this point as the starting manifold. Then $d\mathbf{a} = 0$. Consider the points, $\mathbf{a}^*$, which have the constant optical distance, E_0, from $\mathbf{a}$ on the light rays. This leads to a surface $\mathbf{a}^*$ such that

$$\mathbf{p}^* d\mathbf{a}^* = 0. \quad (1.26)$$

Such a surface is called a *normal surface*, and rays which have normal surfaces are called *normal systems*.

It is seen that the momentum vector, $\mathbf{p}$, for a normal system is normal to the wave surfaces.

Another application is the law of refraction. Let $\mathbf{a}(u, v)$ be the vector from the (arbitrary) origin to the refracting surface, i.e., a surface of discontinuity for n, such that on both sides n is continuous as a function of point and direction.

By a simple limiting process, we reach the case where $\mathbf{a}$ and $\mathbf{a}^*$ coincide at the refracting surface, and E is equal to zero. Then formula (1.25) gives

$$(\mathbf{p}^* - \mathbf{p}) d\mathbf{a} = 0, \quad (1.27)$$

or the vector, $\mathbf{p}^* - \mathbf{p}$, has the direction of the surface normal, $\mathbf{o}$, at the point of incidence. This is equivalent to

$$\mathbf{p}^* \times \mathbf{o} = \mathbf{p} \times \mathbf{o}, \quad (1.28)$$

which is the expression of the law of refraction in inhomogeneous isotropic media.

Another result can be obtained by this theory. Since $\mathbf{p}$ is uniquely given along any extremal, there exists at each point of space a linear transformation,

$$\delta\mathbf{p}=\alpha_{ik}\delta\mathbf{a}=\frac{\partial^2 n}{\partial x_i'\partial x_k}\delta x_k. \tag{1.29}$$

This transformation is called the *basic optical field*. It can be split up into a symmetric and an antisymmetric transformation. The antisymmetric transformation is given by the vector,

$$\left(\frac{\partial^2 n}{\partial x_i'\partial x_k}-\frac{\partial^2 n}{\partial x_i\partial x_k'}\right)=\text{curl}\mathbf{p}=\left(\frac{\partial p_i}{\partial x_k}-\frac{\partial p_k}{\partial x_i}\right), \tag{1.30}$$

if the p_i's are the components of $\mathbf{p}$.

Our basic equation means that

$$\frac{d}{ds}\left(\frac{\partial\mathbf{a}d\mathbf{p}}{\partial'}-d\mathbf{a}\partial\mathbf{p}\right)=\frac{d}{ds}\left(\frac{\partial^2 n}{\partial x_i'\partial x_k}-\frac{\partial^2 n}{\partial x_k'\partial x_i}\right)$$
$$\times(\partial x_i\delta x_k-\partial x_k\delta x_i)=0, \tag{1.31}$$

i.e., that the antisymmetric part of the field is invariant along the extremals.†

Later this antisymmetric part of the field will be considered as the carrier of the diffraction theory.

2. PHYSICS AS THE OPTICAL MODEL IN FOUR-SPACE

In the first section of this paper, the laws of geometrical optics were described as a kind of field theory in three-dimensional space. Here it will be shown how a similar field theory in four-dimensional Euclidean space can account for the elements of physical experience in the same sense as the geometrical optical theory accounts for the bulk of optical experience.

Assume in four-space a function, $L(x_i, \xi_i=dx_i/ds)$ (L stands for Lagrange), given for every directed line element.

Assume L to be positive in space and finite and also homogeneous of the first order with respect to the ξ_i, i.e., if

$$(\partial L/\partial\xi_i)=\mathbf{p} \tag{2.1}$$

then

$$\mathbf{p}\cdot\mathbf{a}'=(\partial L/\partial\xi_i)\xi_i=L. \tag{2.2}$$

Consider as world lines the lines for which,

$$d/ds[\delta\mathbf{a}d\mathbf{p}-d\mathbf{a}\delta\mathbf{p}]=0, \tag{2.3}$$

or

$$dL=\mathbf{p}'d\mathbf{a}+\mathbf{p}d\mathbf{a}', \tag{2.4}$$

i.e., the curves given by the Euler-Lagrange differential equations:

$$(d/ds)\mathbf{p}=(\partial L/\partial x_i)=\text{grad}L; \tag{2.5}$$

or, if the field parameters are introduced,

$$\partial^2 L/\partial x_i\partial x_k=\alpha_{ik} \tag{2.6}$$

$$(\partial^2 L/\partial x_i'\partial x_k')\mathbf{a}''+(\alpha_{ik}-\alpha_{ki})\mathbf{a}'=0. \tag{2.7}$$

Equation (2.3) shows that the bivector with the six components,

$$(d/ds)[(\alpha_{ik}-\alpha_{ki})/2](\delta x_i dx_k-\delta x_k dx_i)=0, \tag{2.8}$$

remains invariant along the curves. It is well known that the existence of an antisymmetric bivector, which remains invariant along the world lines, is equivalent to the existence of an electromagnetic field. One way of coordinating, for instance, is that given by Van Dantzig, who considers the α_{ik} as the components of the so-called vector potential.

The symmetric part of the transformation on the other hand leads to a potential field. The fact that the differential equations of the field are linear makes it possible to separate at every point the gravitational and electromagnetic fields, to investigate each separately, and to consider the real field as the superposition of both.

The geometrical facts in four-space are the same as in three-space. The extremals from a point are orthogonal to a set of wave surfaces, which in four-space are equidistant.

The equations of the extremals lead to a characteristic function,

$$E=\int Lds=\int\mathbf{p}d\mathbf{a}, \tag{2.9}$$

where ds is the line element in space, with

$$dE=\mathbf{p}^*d\mathbf{a}^*-\mathbf{p}d\mathbf{a}, \tag{2.10}$$

for any one- to six-dimensional manifold of extremals which are here called world lines.

It is obvious that all problems in physics, whether in mechanics, in optics, or in statistical mechanics, can be brought into this form.

It is of interest to see that general relativity, with all its consequences, forms a special case of this field theory. If there is a function,

$$L^2=g_{ik}\xi_i\xi_k, \tag{2.11}$$

where the g_{ik}'s are functions of position alone, we obtain the most general Riemannian geometry in four-space, where the world lines are the geodesic lines of the Riemannian manifold and the Euler equations go over into the Christoffel equations of the geodesics. The author thinks that the use of the linear Euler equations offers great advantages in comparison to the computation of Christoffel's quadratic equations leading to the same geodesics.

To conform with the ideas of Einstein's gravitation theory, it must be assumed that the g_{ik}'s have the signature three, i.e. that the quadratic form, $(g_{ik}\xi_i\xi_k=c)$,

† If a field of extremals is considered and coordinates u_i be chosen such that to each choice of the u_i there corresponds one and only one extremal, we find that for any choice of i and kappa,

$$\frac{d}{ds}\left(\frac{\partial^2 n}{\partial u_i'\partial u_k}-\frac{\partial^2 n}{\partial u_i\partial u_k'}\right)=0. \tag{1.31a}$$

The same remark holds with respect to Eq. (2.8).

is the equation of a surface with three positive curvatures and one negative. This idea of Einstein's seems to suggest that in the general problem also the quadratic form,

$$\frac{\partial'(L^2)}{\partial\xi_i\partial\xi_k}=g_{ik}, \tag{2.12}$$

should have the signature three. In different parts of physics, sometimes L, and sometimes L^2, is considered a basic form. The interrelation of these two forms and of the corresponding differential equations gives a parallel treatment of the same subject.

3. DIFFRACTION PHYSICS

The author believes that the general field theory, as developed here, or any other field theory will only be able to give the equivalent of geometrical optics. If the phenomena which quantum-mechanics purports to describe should be embodied in the theory, something must be added, which is equivalent to the wave theory of optics. Since quantum-mechanics has not done a very good job in explaining the simple facts of interference and diffraction, which optics explains easily, it might not be considered too far out of order if a diffraction theory of physics is outlined which is built in analogy to the optical diffraction theory, and in which, though willing to use statistical methods for statistical problems, I should like to avoid using probability theory, where no probability is involved. The intention of this theory is to explain in a more direct way the phenomena of radiation in all wave-lengths.

It may or may not be essential that a certain other type of basic physical experience be analyzed, namely, the problems derived from the interaction between matter and energy. At this stage, this problem will be dealt with rather sketchily, assuming that the Einstein effect contains the basic answer.

To understand this diffraction theory, we shall again deal with the basic problem in optics.

Assume a point of disturbance (light source) which is fixed in three-space. This point of disturbance sends out waves, which we can consider as superpositions of single sine waves of different wave-lengths. Consider radiation of a fixed frequency, ν. Assume an optical system and in the image space a diaphragm of fixed aperture, beyond which there is total absorption.

The problem of finding the luminous energy at a point in image space can now be solved in the following way, which gives correct results as long as the point is far away from the diaphragm:

Assume along the light ray a transverse vibration, which is given by a bivector in the wave surface, with component periodic functions of $c/n\nu$, where n is the refractive index and c is the velocity of light in a vacuum.

The value of this vector can be computed at every point of the diaphragm plane, assuming it to be zero at the points of total absorption.

This computation will give this vector function at every point of a closed surface. Since its components obey the wave equation, its value can be calculated at every point in image space, with the help of Green's theorem.

This procedure is, in principle, equivalent to the method of Huygens-Fresnel-Kirchhoff, the points of the plane being considered origins of new waves with a well-known phase difference and the disturbances coming from every point of the aperture integrated at the point to be investigated.

This simplest diffraction experiment shows that, because of diffraction, a point source cannot be distinguished from a source of small extension. The conclusion to be drawn from this is that, for the experiment in question, an apparently small object can be called a point, and *vice versa*. Since they cannot be distinguished, we offer as a definition of *coherent light*, light that comes from an object that cannot be distinguished from a point.

This definition is tacitly adopted by all experimental physicists who use star light as a source for interference experiments, but it seems advisable to point this out explicitly. Coherence has nothing to do with the object, only with the diffracted image.

The fact of diffraction brings with it the experience that in using a fixed instrument only a finite number of object points can be recognized. Thus, in any case, the light field can be described by superimposing the fields coming from the finite points of disturbance. Owing to the linearity of the differential equations, these fields can simply be added, and it is then seen that the disturbances can be assumed to be independent of each other. The simple assumption that there is total absorption outside the working aperture does not cover all the facts. It will be assumed that it is a partial absorption, i.e., the bivector describing the disturbance will, in general, have at every point an amplitude factor which may vary from zero to one.

It cannot be assumed that the fiction of a point light source holds true in the neighborhood of the light source itself. If the light source can be approached, it will be found that it has a structure, since a point source would have infinite energy, and is therefore physically impossible. It can be considered again as an assembly of a finite number of singular points. However, the position of these points can be determined with only limited accuracy. Ultimately, a limit of accuracy is reached, not an indivisible element.

The difference between this viewpoint and that of quantum-mechanics is a philosophical difference, which can be clearly perceived if the simplest diffraction experiment is analyzed. If a light source is observed through a small circular pinhole, there is seen at the plane of the light source a diffraction image, the intensity of which is given as a function of the radial center distance in the form of a Bessel function.

The interpretation of quantum theory would be that

there is a point light source, the probability of whose position is given by the Bessel function, so that there exists a probability that the light point might be somewhere in the rings surrounding the Airy disk.

The interpretation of diffraction theory is quite different. It is assumed that there exist centers of disturbance emitting light, these being situated near the point corresponding to the center of the Airy disk. This phenomenon can be replaced mathematically by assuming a point disturbance at the center of the disk, to simplify computation, since no added experiment can resolve the image.

4. DIFFRACTION PHYSICS IN FOUR-SPACE

The problem of diffraction physics in four-space is complicated by the fact that the disturbing point source moves, i.e., forms a line in four-space.

As long as a single disturbing point is considered, this would not matter, since this moving point could be chosen as origin, the laws of physics being independent of the motion of the origin. However, since a second moving event would disturb this picture, it is preferable to consider a single disturbance as consisting of the points of a world line in space-time. Each point of this world line now sends out waves of all wave-lengths with a velocity, c, which is independent of the velocity of the moving particle. These waves are determined by the electromagnetic (antisymmetric) part of the field alone, i.e., only radiant energy is considered.

Replace the antisymmetric bivector, F, by a bivector whose direction is that of F and whose length is a periodic function, i.e., with wave-length, $c/L\nu$. Again, we can assume an absorption factor and have as carrier of the energy flux the electromagnetic field generated by the vector,

$$\mathbf{F}=x\sin\left[\frac{\partial^2 L}{\partial x_i'\delta x_k'}-\frac{\partial^2 L}{\partial x_k'\partial x_i}\right](\delta x_i dx_k-\delta x_k dx_i). \quad (4.1)$$

Again this vector can be calculated, if a finite number of disturbance lines is assumed and the effects coming from a surface which divides space in two parts are added, one containing all the disturbances, the other the point where we want to compute the energy flux.

This method, which is in agreement with relativistic electrodynamics, must be carried out in detail.

In this theory, mass and charge are conceived not as intrinsic physical quantities but as quantities which are connected with the approximations with which physical realities are approached. Any physical field can be approximated by assuming a finite number of points (or lines) as singularities. These approximations can be carried out for the symmetric and antisymmetric parts independently. Assuming an inverse square law, the field can be calculated by superimposing gravitational fields (resulting from mass points), and electrical fields resulting from dipoles, certain residuals being assumed for the $\oint \mathbf{p}d\mathbf{a}$ around these points. The residuals will be called the "charges" or the "masses," respectively.

5. THREE BASIC PROBLEMS OF PHYSICS

There are three basic problems of physics. The first is the measurement of distances in space-time. Since, in general, light rays are used to measure these distances, the critical methods of the relativity theory must be applied to interpret the results of these measurements.

The second problem is the basic experiment in which a test body is brought into a field. The field determines, according to the laws of mechanics, the motion of the test body. This is one of the methods of determining the field.

The third problem arises if a human eye, a photo-cell, a photographic plate, or any instrument which can detect or record the energy flux through a small surface element is brought into the field. Here the integral,

$$\int\int \mathbf{F}^2 d\sigma d\lambda,$$

will be made visible, but, according to the Einstein effect, this is only registered in finite multiples of $h\nu$, ν designating the frequency of the energy flux. Here and at the emission seem to be the only places for a quantum effect and the only possible point where such an effect can be experienced.

6. CONCLUSION

In this paper, an attempt has been made to bring together some ideas which may lead to a unified picture of physics. It has been shown that relativity, gravitation, and electricity can be explained as special cases of a single field theory. This theory offers a unifying connection between formerly unconnected fields.

A diffraction theory of physics has been sketched, with the intention of replacing parts of quantum-mechanics with it. This idea is separate from the field theory and additional to it. Special examples should be worked out in detail to see how the results of the diffraction theory check with experience and whether or not the methods employed are simpler than those in quantum-mechanics. I hope that physicists will be able to carry out such detailed investigations. One of the basic ideas of Einstein's theory is preserved in this paper, namely, physics is transformed into a part of geometry where only intrinsically geometric laws have value.

I do not claim that the basic ideas developed solve all physical problems, since the problems of emission and absorption may or may not have laws of their own.

However, I believe I have succeeded in showing that classical methods can be used to describe most of the results of contemporary physics.

ACKNOWLEDGMENT

I wish to acknowledge the valuable advice and assistance of D. L. MacAdam, T. H. Auerbach, and E. W. Marchand, in connection with the preparation of this paper.

Observations on Exceptional Duration of Mineral Phosphorescence

HENRY E. MILLSON AND HENRY E. MILLSON, JR.
American Cyanamid Company, Calco Chemical Division, Bound Brook, New Jersey
(Received March 2, 1950)

The purpose of the present investigation was to obtain data concerning the duration of phosphorescence of minerals. Some minerals with protracted emissions have been discovered and the features of their phosphorescence determined with dark-adapted eyes, and in some cases, with photographic film.

Studies have shown that the phosphorescence caused by a short exposure to 2437A ultraviolet rays will continue for a long period of time. Dark-adapted eyes were used to determine the duration of colored and colorless phosphorescence and photographic film was used to obtain phosphorographs and thereby record the emission of light long after it became imperceptible to the eye. Protracted phosphorescence has been discovered in calcite, fluorite, spodumene, wernerite, willemite, and synthetic phosphors. After an initial exposure of one minute, Texas calcite emitted an afterglow which was distinguishable to dark-adapted eyes for 4600 hours and was capable of producing a photographic image after more than 5½ years. Fluorite from Trumbull, Connecticut, similarly exposed, continued to emit a phosphorescence perceptible to the eye for more than four years. The Texas calcite, fluorite, and spodumene are still phosphorescing.

Data on color and duration of visible phosphorescence of natural minerals are tabulated.

GENERAL BEHAVIOR

THOUSANDS of mineral specimens were examined and those that showed protracted phosphorescence were selected for further study. Some of the minerals which were found to exhibit visual phosphorescence for more than 24 hours are listed in Tables I and II. Two general types of phosphorescent behavior were observed. With most of the minerals having long duration phosphorescence, there was a short period of time immediately after the removal of the exciting ultraviolet light when the phosphorescence had a distinct color which was apparent to the eye. Following this short interval there was a longer period of time when phosphorescence was detectable to the dark-adapted eye but color determination was impossible. After the mineral no longer emitted phosphorescent energy of a high enough intensity to be detected by the human eye, the presence of this energy was recorded by photographic means.

Table I lists seven illustrative minerals and gives the time of duration of phosphorescent color determined visually to illustrate the first, or colored stage of this type of phosphorescent behavior. The total duration of visible phosphorescence of the first (colored) and second (colorless) phases, is also listed.

A chlorophane variety of fluorite from Trumbull, Connecticut, gave phosphorescent emission which was visible to dark-adapted eyes for a longer period than any other mineral examined. The specimen used for these observations consisted of pieces about one-half inch in length, which were placed in a small bottle to provide a larger area for study. This mineral was visible to dark-adapted eyes by its phosphorescence for more than 36,350 hours.

The colorless type of phosphorescence is exemplified by those minerals listed in Table II for which the initial phosphorescence is described as white. In these cases, there was no indication of an initial color. The phosphorescence appeared white immediately after removal of the ultraviolet excitation and continued to appear white to the dark-adapted eye until it was no longer visible. Certain specimens, such as aragonite, goshenite beryl, and rhaetizite cyanite gave an intermediate shade exhibiting a yellowish-white, bluish-white, and a greenish-white, respectively.

Following the period of visible discernibility, photographic evidence of emission was obtained from some of these specimens. The mineral scheelite always showed a white phosphorescence immediately after excitation. However, when this mineral was placed in contact with a Kodachrome film, the resulting picture was blue.

Care was taken to avoid observations on surface alterations such as weathered areas because these alterations may radically modify the phosphorescence of the original mineral. It was also noted that transparent and translucent crystal coatings sometimes gave an apparent phosphorescence while in reality the underlying rock was glowing.

The presence of foreign substances in concentrations as low as 1 p.p.m. has been known to change the properties of some phosphors very noticeably. Maintaining identical chemical composition but changing crystal structure by polymorphic transition also produces pronounced changes in phosphorescent properties. Because of these factors, mineral specimens in other collections which are otherwise identical to those listed in Tables I and II may show lesser or greater phosphorescence than those examined by the authors.

Several synthetic phosphors were studied for comparison with natural minerals. One of these, a zinc sulfide phosphor incorporated in plastic, excited for one minute by irradiation of ultraviolet rays of 2537A, gave photographic proof of light emission between 6,283 and 6,811 hours later.

SOURCE OF IRRADIATION USED

The source of excitation energy was a Skidmore Quartzlite, a low pressure mercury vapor lamp, de-

TABLE I. Duration of visible phosphorescence color.

Mineral	Locality	Color of phosphorescence	Duration of phosphorescent color	Approximate duration of visible phosphorescence (hrs.)
Willemite-white radiated	Franklin, New Jersey	Green	1 hr. 30 minutes	360
Clinohedrite-polished	Franklin, New Jersey	Orange	11 minutes	288
Wernerite	Grenville, Quebec, Canada	Reddish-Orange	3 min. 30 seconds	750
Willemite-polished	Franklin, New Jersey	Green	1 min. 35 seconds	125
Fluorite-phantom	Weardale, England	Violet	1 min. 5 seconds	310
Fluorite-grey	Weardale, England	Violet	30 seconds	600
Fluorite-brown	Clay Center, Ohio	Yellow	20 seconds	2¼

veloped by Mr. Edwin Skidmore of Mountainside, New Jersey. The radiation from this cold-quartz lamp is peaked sharply at 2537A. For phosphorescent excitation the unfiltered radiation of the lamp was allowed to fall upon the specimen for one minute at a distance of 2.5 cm. The high emission of 2537A radiation by the Skidmore lamp is responsible for the prolonged observation of phosphorescence in many minerals.

VISUAL EXAMINATION

For those minerals which showed an initial visual color, a switch which turned off the ultraviolet lamp and started the timer simultaneously, was used. Specimens were observed continuously in total darkness with dark-adapted eyes until they were no longer visible or until the mineral showed indications of continuing to phosphoresce for 24 hours or longer. The specimens were examined in total darkness twice each day or more often if necessary, and timed until phosphorescence was no longer detected. Between observations, the specimens were kept wrapped in heavy, dark, wool cloth and placed in lightproof containers to prevent exposure to light of any kind.

In order to facilitate determination of visibility of phosphorescence, one side of the mineral was generally covered during excitation to prevent absorption of ultraviolet rays. This unexposed side was used for comparison with the phosphorescing side by rotating the mineral in the hand. If the emission disappeared and reappeared as the mineral was rotated, it was concluded that the phosphorescence of the mineral was still visible. Check determinations were made by both authors.

It was found that large areas were visible longer than very small areas of equal intensity. Therefore, it is believed that some of the durations recorded for the small crystals and particles in specimens would have been longer if larger crystals and areas had been available for the tests.

BLACK AND WHITE PHOSPHOROGRAPHS

When the intensity of phosphorescence fell below the threshold of human vision, a photographic film (Kodak sheet contrast process panchromatic) was used to detect continued light emission. The photographs produced in this manner have been termed phosphorographs. Specimens used for taking phosphorographs must have a smooth or polished surface so that the glowing areas come in direct contact with the photographic film. If the specimen has a rough surface, the negative will be blurred by the emitted light and the outline of the phosphorescing areas will not be clearly defined. The phosphorographs of the glowing areas were obtained by

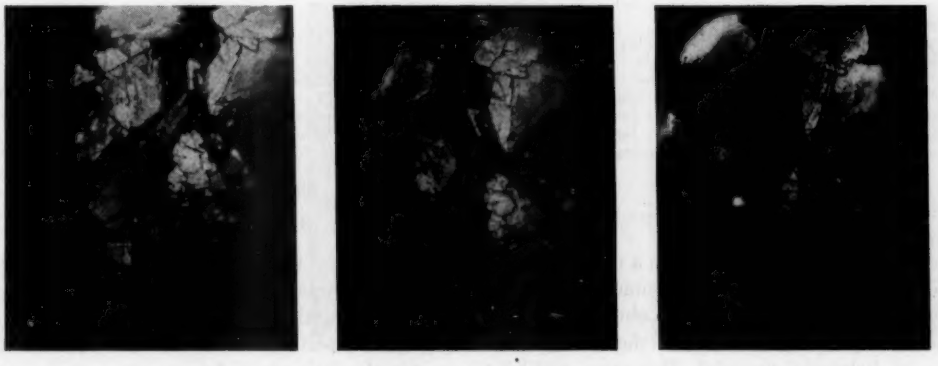

(a) (b) (c)

FIG. 1. Phosphorographs. Phosphorescence of calcite, Chisos Mountains, Texas. Specimen exposed to ultraviolet rays for 1 minute. (a) Specimen on film during the 410½ to 419 hour interval. Temperature range 68°–72°F. Total exposure 8½ hours. (b) Specimen on film during the 24672 to 26712 hour interval. Temperature range 67°–78°F. Total exposure 2040 hours. (c) Specimen on film during the 49757 to 55016 hour interval. Temperature range 62°–78°F. Total exposure 5259 hours.

TABLE II. Color and duration of visible phosphorescence of natural minerals.

Name	Locality	Color of phosphorescence	Approximate duration visible phosphorescence hours
Albite	Gillette Quarry, Haddam Neck, Connecticut	Yellowish-orange	275 hours
Apatite	Brinton's Quarry, Delaware County, Pennsylvania	Orange	124 hours
Aragonite	Alston Moor, England	Yellowish-white	80 hours
Beryl—goshenite	San Puro in Campo, Island of Elba	Bluish-white	152 hours
Beryl—morganite	Gillette Quarry, Haddam Neck, Connecticut	Pink	296 hours
Bustamite	Franklin, New Jersey	Orange	29 hours
Calcite	Bisbee, Arizona	Scarlet flash then orange	113 hours
Calcite	Joplin, Missouri	Orange	24 hours
Calcite	Picher, Oklahoma	White changing to dull orange	41 hours
Calcite	Terlingua, Brewster County, Chisos Mountains, Texas	Brilliant blue-violet then colorless	4600 hours
Calcite	Frizington, Cumberland, England	Scarlet flash then pinkish-white	82 hours
Calcium—larsenite	Franklin, New Jersey	Yellow	33 hours
Clinohedrite	Franklin, New Jersey	Yellowish-orange	175 hours
Cyanite—rhaetizite	Pfitsch, Tyrol	Greenish white	51 hours
Fluorite	Gillette Quarry, Haddam Neck, Connecticut	Green	4900 hours
Fluorite	Rosiclare, Illinois	Violet	102 hours
Fluorite	Rosiclare, Illinois	Light violet	130 hours
Fluorite	Rosiclare, Illinois	Greenish-yellow phantom surrounded with violet	380 hours
Fluorite	Rosiclare, Illinois	Bright violet	1500 hours
Fluorite	Franklin, New Jersey	Green	200 hours
Fluorite	Westmoreland, New Hampshire	Violet	680 hours
Fluorite	Grimmel Stallen, Berner, Oberland Switzerland	Orange and violet	135 hours
Fluorite	England	Bright violet	370 hours
Fluorite	Durham, Weardale County, England	Violet	140 hours
Fluorite	Durham, Weardale County, England	Light blue	72 hours
Fluorite	Durham, Weardale County, England	Bright violet	600 hours
Fluorite	Cumberland, England	Bright violet	2960 hours
Fluorite	Weardale County, England	Bright violet	820 hours
Fluorite	Trumbull, Connecticut	Bluish-white	510 hours
Fluorite—chlorophane	Trumbull, Connecticut	Green	36,347+hours
Lazurite	Andes of Ovalle, Chile	Blue	50 hours
Phenacite	San Miguel de Piracicaba, Minas Geraes, Brazil	Blue	120 hours
Phosgenite	Monti Poni, Sardinia	Orange	58 hours
Scapolite—wernerite	Grenville, Quebec, Canada	Golden Orange	1050 hours
Scapolite—wernerite	New locality at Grenville, Quebec, Canada	Yellow	4500 hours
Scheelite	Greenhorn Mountains, Kernville, Kern County, California	White	31 hours
Scheelite	Mill City, Pershing County, Nevada	White	25 hours
Scheelite	Lucin, Utah	White	44 hours
Sodalite	Hastings County, Ontario, Canada	White	70 hours
Spodumene	Pala, California	Orange	3800 hours
Spodumene—kunzite	Pala, California	Bright orange	69 hours
Tarbutite	Northern Rhodesia, Africa	Orange	57 hours
Willemite	Franklin, New Jersey	Brilliant yellow-green	340 hours
Willemite	Franklin, New Jersey	Bright green	27 hours
Wollastonite	Crestmore, Riverside County, California	Orange	590 hours
Zircon	Siam	Bluish-white	720 hours

placing the phosphorescing mineral on a negative in the dark and allowing it to remain in the same position for a definite length of time. In order to obtain a distinct outline of the specimen, the sides of the mineral were covered with lightproof material. This prevented light emitted from the portion of the mineral immediately above the film from fogging the negative at the sides with consequent loss of definition of the image. When the negative was developed and printed, all of the glowing areas were plainly evident. By using this technique, it was possible to demonstrate that irradiated substances continued to emit light long after the intensity of the afterglow was too weak to be discerned by completely dark-adapted eyes.

Figures 1a, b, and c are typical phosphorographs of Texas calcite which were obtained in this manner. Figures 2a, b, and c are photographs of Texas calcite in daylight, fluorescing in 2537A ultraviolet light, and

phosphorescing after excitation. Figures 3a, b, and c are phosphorographs produced by the phosphorescent emission of this same specimen.

KODACHROME PHOSPHOROGRAPHS

The phosphorescence of a specimen of Texas calcite from the Chisos Mountains, Texas, remained visible to the dark-adapted eye for 4,600 hours and could still be detected by the photographic film more than six years after excitation. After the 4,600 hours, during which time 103 visual observations were made, 52 phosphorographs were made. The temperature of the specimen was allowed to follow seasonal changes between 7°C and 35°C, and while the intensity of the phosphorescence may have varied, the phosphorographs demonstrated the continuity of the emission.

Some excited specimens, which produced well-defined phosphorographs, were then boiled in water in the dark for 60 minutes, and were not exposed to any light prior to placing them on a second film. In these cases, images were not obtained despite the fact that the time, weight and pressure of the mineral was the same in both experiments. These experiments deny the occurrence of a pressure effect, i.e., the striking of a photographic emulsion as a consequence of pressure only. They also suggest that the images often ascribed to the Russell effect by investigators working with minerals[1] actually may have been phosphorographs.

Beautifully colored phosphorographs were obtained by using Kodachrome film, Type B. Colored film has an advantage over black and white film in that it allows an identification and a permanent record of the colors emitted by phosphorescing minerals. Although phosphorescence of very low intensity appears colorless to

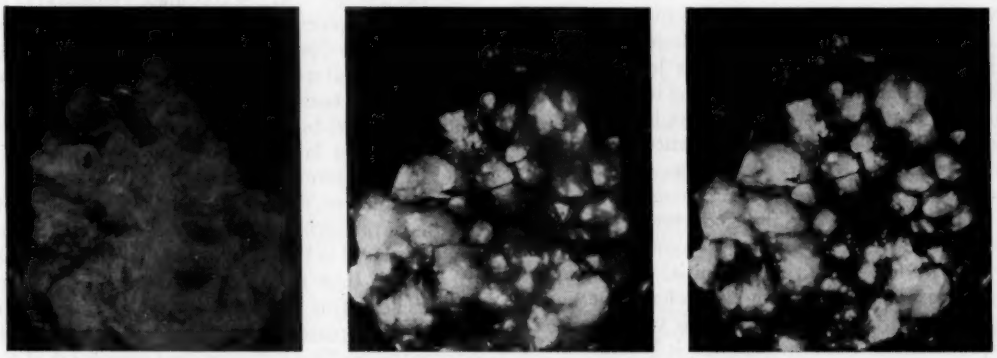

(a) (b) (c)

FIG. 2. Photographs. Phosphorescence of calcite, Chisos Mountains, Texas. Specimen exposed to ultraviolet rays for 1 minute. (a) Photograph of specimen in daylight. (b) Photograph of specimen fluorescing in 2537A ultraviolet. (c) Photograph of specimen phosphorescing after excitation by 2537A ultraviolet.

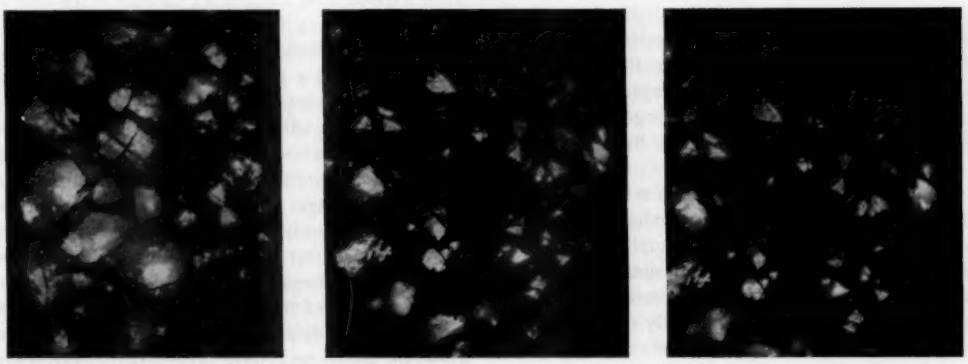

(a) (b) (c)

FIG. 3. Phosphorographs. Phosphorescence of calcite, Chisos Mountains, Texas. Specimen exposed to ultraviolet rays for 1 minute. (a) Specimen on film during the 7176 to 7696 hour interval. Temperature range 69°–78°F. Total exposure 520 hours. (b) Specimen on film during the 24190 to 26230 hour interval. Temperature range 66°–72°F. Total exposure 2040 hours. (c) Specimen on film during the 49275 to 54534 hour interval. Temperature range 62°–78°F. Total exposure 5259 hours.

[1] E. N. Harvey, *Living Light* (Princeton University Press, Princeton, 1940).

TABLE III. Filters used for radiometry.[a]

Name	Identification	Range in A
1—Clear	Filter 0	3000–7000
2—Dark Red	Filter 70	6500–7000
3—Red	Filter 25	5700–7000
4—Orange	Filter 21	5400–7000
5—Yellow	Filter 12	5000–7000
6—Yellow-Green	Filter 3	4500–7000

[a] Eastman Kodak Company, Wratten Light Filters, sixteenth edition, revised 1940, Rochester, New York.

the eye, minerals nevertheless record various colors on Kodachrome film.

Specimens of scheelite although visually colorless produced a blue Kodachrome phosphorograph. In this particular case there may be a combined effect of the emission of ultraviolet light together with blue light in the phosphorescence. Scheelite is known to emit ultraviolet as well as visible light during fluorescence, and this may also be true for the phosphorescent process.[2] Calcite specimens from Franklin, New Jersey, produced Kodachrome phosphorographs varying in color from an orange-scarlet to a yellow-orange. Pink beryl morganite variety from Haddam Neck, Connecticut, produced a bright cerise pink, and willemite from Franklin, New Jersey, gave a brilliant green. In general, it was found that the color produced on the Kodachrome film by the visually colorless phosphorescence coincided with the color seen by the eye during the initial stages of phosphorescence when the emission was colored. Because of this color similarity and because of the variety of colors observed with the Kodachrome film, it is believed that the ultraviolet emission was not a major factor contributing to the development of an image on the film.

SPECTRAL DISTRIBUTION OF PHOSPHORESCENT LIGHT

An approximate analysis of the light emitted by several specimens was obtained by preparing black and white phosphorographs with Wratten filter strips between the mineral and the photographic film, these strips were not sensitive to radiation longer than 7000A. The filters used for these tests are listed below in Table III.

Three sets of pictures were obtained for each of several specimens. The first was taken immediately after excitation while the emitted light was visually colored; the second an hour after the light emission had become apparently colorless; and the third, months or years later after the specimen had apparently ceased to emit visual light. These three sets all showed some darkening of the photographic film through certain of the Wratten filters, and no darkening through others. Densitometer measurements were made on the developed negative to determine the relative amounts of light energy which fell upon each film after passing through the various Wratten filters. By comparing these values it was found that the spectral composition of the phosphorescence of each mineral remained constant during the phosphorescing life of the specimen after exposure to excitation, confirming the fact that the apparent transition to "colorless" is a visual function of intensity.[3]

These Wratten filter tests indicate the dependability of the Kodachrome method for recording the true color of the phosphorescent emission. A comparison of three Kodachrome phosphorographs of Chisos Mountain calcite taken immediately after excitation, 571 days later, and 2007 days later showed all to be approximately the same shade of blue. This again suggests the reliability of the Kodachrome method of determining the "color" of the "colorless" radiation.

PROOF THAT RADIOACTIVITY WAS NOT PRESENT

It was thought that the continuous emission of radiation, photographically recorded over so long a period of time, might be due to the presence of some radioactive element. Several specimens were tested for radioactivity by means of both the electroscope and the Geiger-Müller counter, but yielded negative results. Spectroscopic analyses failed to reveal the presence of any known radioactive elements.

A specimen of Texas calcite which was known to be capable of producing a phosphorograph in less than one day was placed in boiling water in the dark for one hour, after which time it gave no visual evidence of phosphorescence. This specimen placed in contact with a photographic plate for 40 days produced no photographic image. This indicated that the absorbed energy had been very largely, if not entirely, released from the specimen by thermal means, and hence that the source of radiation was phosphorescence and not radioactivity.

In another experiment, a specimen of Texas calcite, after exposure to ultraviolet radiation for one minute, was placed upon a double thickness of photographic film. The top film which was in direct contact with the mineral showed a photographic image, but the second film, which was separated from the first only by a piece of black paper, showed no image. In a further experiment the calcite was placed in contact with the reverse side of the photographic film after excitation, but again showed no image. In another experiment, a polished specimen of dendritic uraninite, known to be radioactive, was placed in contact with four thicknesses of film. All four negatives upon development showed a definite outline of the uraninite. This demonstrated that under the conditions of the experiment, radioactive minerals would produce images upon covered layers in the film, whereas the phosphorescent minerals would not. A further distinction between radioactivity and phosphorescent emissions was shown by the Kodachrome phosphorographs. Texas calcite gave a phosphorograph predominantly blue in color, whereas uraninite and

[2] J. DeMent, *Fluorochemistry* (Chemical Publishing Company, New York, 1945).

[3] E. L. Nickols *et al.*, Carnegie Inst. Rept. No. 284 (1938).

other radioactive minerals gave gray or colorless negatives.

SUMMARY

Studies have shown that the phosphorescence caused by a short exposure to 2537A ultraviolet rays will continue for a long period of time. Dark-adapted eyes were used to determine the duration of colored and colorless phosphorescence and photographic film was used to obtain phosphorographs and thereby record the emission of light long after it became imperceptible to the eye. Protracted phosphorescence has been discovered in calcite, fluorite, spodumene, wernerite, willemite, and synthetic phosphors. After an initial exposure of one minute, Texas calcite emitted an afterglow which was distinguishable to dark-adapted eyes for 4600 hours and was capable of producing a photographic image after more than six years. Fluorite from Trumbull, Connecticut, similarly exposed, continued to emit a phosphorescence perceptible to the eye for more than four years. The Texas calcite, fluorite and spodumene are still phosphorescing.

Data on color and duration of visible phosphorescence of natural minerals are tabulated.

The authors are indebted to Edwin Skidmore for his gifts of specimens and for cutting and polishing many of the specimens used during this investigation; to Joseph D'Agostino of Plainfield, New Jersey, and Harold Arndt of Ardmore, Pennsylvania, for the use of specimens from their private collections. They are also indebted to May E. Dunn of Clay Center, Ohio, for her gift of many unusual and interesting specimens from the Clay Center locality.

They are indebted to C. Maresh for developing and printing the phosphorographs.

Sincere thanks are due Jack DeMent of the Fluorescence Laboratories, Portland, Oregon, L. H. Turl, and E. I. Stearns for reading and correcting the manuscript.

JOURNAL OF THE OPTICAL SOCIETY OF AMERICA VOLUME 40, NUMBER 7 JULY, 1950

The Permanence of Glass Standards of Spectral Transmittance*

KASSON S. GIBSON AND MARION A. BELKNAP
National Bureau of Standards, Washington, D. C.

(Received March 31, 1950)

Shortly after the introduction of commercially available photoelectric spectrophotometers, the National Bureau of Standards began issuing calibrated disks for checking the photometric scale of spectrophotometers. At the time these standards were selected no precise information was available regarding their permanence. Recent measurements show that the glass standards kept in the files for 16 years with only occasional use have not changed. Data have also been obtained showing the nature of the changes occurring in glasses similar to the standards when exposed under glass to south skylight (including sunlight) for periods up to nearly three years.

I. INTRODUCTION

ONE of the essential parts of a spectrophotometer is the photometric equipment, and the accuracy of the photometric scale is one of the major items with which both the manufacturer and the user of the spectrophotometer should be concerned. This photometric scale may be based on optical principles and devices, as in all visual spectrophotometers and the Hardy or General Electric recording spectrophotometer, or it may be based on electrical principles and devices, as in many of the other photoelectric spectrophotometers. Whatever the method, the user of the spectrophotometer should have some means available to insure that the instrument is giving reliable results or to warn him that something is wrong.

On a visual spectrophotometer this can be done by means of rapidly rotating sectored disks, whose apertures can be mechanically calibrated with high accuracy. On photoelectric spectrophotometers, however, for one reason or another, such a procedure is not generally feasible. An acceptable alternative, and one that is in general much more convenient, is the use of solutions or glass disks whose spectral transmissive properties are accurately known over the desired spectral range.

At first thought one might wish for a series of filters whose respective transmittances do not vary with wavelength, which will not displace the beam, which do not reflect strongly, and for which the transmittances can be independently determined with high accuracy. Such filters would enable a test of the photometric scale to be made that would be independent of all other sources of error, and if available they would probably be useful. They are not available, however, and in fact would probably not be as useful as the series of moderately selective filters that are discussed in the present paper. This is because the non-selective filters would not enable the detection of wave-length errors no matter how great; they would give no information regarding the effects of wide slits; nor would they detect the

* A more complete treatment of this work will be described in J. Research Nat. Bur. Stand. 44, 463 (1950), RP2093.

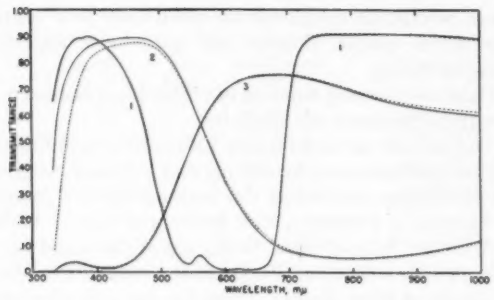

FIG. 1. Continuous lines show typical spectral transmittance curves of (1) cobalt blue, (2) copper green, and (3) carbon yellow glass standards issued by the National Bureau of Standards. Dotted lines show the spectral transmittances of the same glasses after outdoor exposure for 2 years and 8 months. Similar standards kept in the files for 16 years with only occasional use show no change.

presence of stray spectral energy. The selective filters, on the other hand, will often yield valuable information about these things in addition to affording the desired check of the photometric scale over most of its range.

II. THE STANDARDS

Shortly after the appearance of commercially available photoelectric spectrophotometers in 1930 the National Bureau of Standards began the preparation and issuance of glass standards of spectral transmittance. These were described at a meeting of the Optical Society of America in 1933.[1] They have been noted in various Bureau publications since that date[2–4] and they have been listed in past and present Bureau test fee schedules. To date about 170 of these filters have been issued.†

At the time that decision was made on the types of filters to use, little quantitative information was available as to the permanence of colored glasses. Manganese glasses were known to be unstable, and the spectral transmittances of many glasses were known to vary in the ultraviolet upon exposure to strong ultraviolet radiant flux. On the other hand it can be assumed that many kinds of colored glass have high stability in the visible spectrum, else cathedral windows would have paled or otherwise deteriorated to a notable degree through the centuries of exposure.

Since no evidence was available that the common types of colored glass other than manganese would change, the selection of the filters was made wholly from the standpoint of suitable spectral transmittances in suitable thicknesses. Of necessity it was assumed that these glasses would remain constant until sufficient time had elapsed that changes could be ascertained even though small. For each type two glasses were selected for initial measurement and these have been kept in the Bureau files, unused except for occasional measurement. These remeasurements were not systematic but were sufficient to show that no important changes were taking place.

Naturally there were often differences in the third decimal between the original and the repeat values of transmittance but these were usually slight and always within the combined experimental uncertainties. Nevertheless, consideration of these small differences made it seem desirable to carry out some kind of accelerated exposure test in order to find out the nature of any real changes that might be expected. This was accordingly done over a three-year period.

These standards are of the type designated respectively as "cobalt blue," "copper green," "carbon yellow," and "selenium orange." Typical spectral transmittance curves of the first three are shown by the continuous lines of Fig. 1. The standards are normally issued for use only over the range from 390 to 750 mμ. In addition to the references noted above, these standards are described in detail in the more complete Bureau publication, including data on temperature effects.

Regarding selection of these standards by those who wish to check the photometric scale of their spectrophotometers, it is generally found that two are sufficient, (1) the carbon yellow and (2) either the cobalt blue or the copper green, depending on the desires of the user. The selenium orange has not proved very useful for this purpose and its purchase is not recommended. Only a few have been issued.

III. PERMANENCE OF UNEXPOSED SAMPLES

The pairs of glasses originally selected for retention as Bureau standards have been kept mostly in the files, with only occasional use and with no excessive exposure to radiant flux. In 1933 these glasses had been carefully measured at various selected wave-lengths from 390 to 750 mμ and values of spectral transmittance adopted at that time. After the intervening 16 years, one of each of these pairs of glasses was remeasured in 1949.

Details of this comparison are given in the Bureau publication. The net result of the work was to show that the spectral transmittances of these standards had not changed over this 16-year period.

IV. ACCELERATED EXPOSURE TESTS

It was desired that the accelerated exposures should be made under conditions not too widely different from ordinary indoor conditions. The samples were accordingly placed in a small box with a plate glass cover, which was kept outside of a south window on the fourth floor. The samples were thus exposed to daylight, including sunlight, from the south half of the sky, in all kinds of weather. However, the plate glass and box

[1] K. S. Gibson, G. K. Walker, and M. E. Brown, J. Opt. Soc. Am. **24**, 58 (1934).
[2] K. S. Gibson and M. M. Balcom, J. Research Nat. Bur. Stand. **38**, 601 (1947), RP1798; J. Opt. Soc. Am. **37**, 593 (1947).
[3] Standards for checking the calibration of spectrophotometers, NBS Letter Circular, LC929 (1948).
[4] K. S. Gibson, Spectrophotometry (200 to 1000 millimicrons), NBS Circular, C484 (1949).
† Solution standards of spectral transmittancy are described, with data, in NBS letter circular LC929 (see reference 3) and in NBS circular C484 (see reference 4).

kept the samples dry at all times. The plate glass further served to keep the solar ultraviolet radiant flux of the shortest wave-lengths from the glasses, since conditions would otherwise not have been comparable in this respect with those indoors. Small holes in the box permitted circulation of air and helped to prevent condensation of moisture on the plate glass cover.

These exposure tests were made with carbon yellow, copper green, and cobalt blue glasses similar to the respective standards. No corresponding tests have been made of the selenium orange glass. Measurements on the three glasses were made prior to the start of the exposures and further measurements have been made after various periods up to 2 years and 8 months.

In most cases definite changes in the spectral transmittances of the glasses were obtained by this long exposure. In the Bureau publication the ratios of the transmittances of the exposed to the unexposed samples are plotted as a function of wave-length for various exposure periods, and the reader should refer to that paper for this detailed analysis. It seems sufficient here to show the actual transmittance curves for the original unexposed samples and for the same samples after 2 years and 8 months of exposure. These curves are shown in Fig. 1, the dotted lines representing the exposed samples.

Definite changes may be noted for the copper green glass, the large changes in the ultraviolet being the typical solarization effect shown by many glasses.

The cobalt blue glass shows no very certain changes over the wave-length range from 300 to 1000 mμ. In this range the ratio of transmittances of exposed (2 years, 8 months) to unexposed sample deviate from unity nowhere by more than ± 1 percent.

In Fig. 1 the carbon yellow glass likewise appears to have changed but little. Actually, however, the ratios of exposed to unexposed deviate considerably from unity below 500 mμ, reaching approximately 1.07 at 420 mμ and 0.93 at 334 mμ. Furthermore, these changes begin to occur immediately on exposure and reach half of the total change within a week's time.

In general the changes illustrated in Fig. 1 confirm the stability of the standards issued by the National Bureau of Standards. Since these changes occurred only after 2 years, 8 months of outdoor exposure, one would not expect any significant changes to occur when the glasses are subject to normal indoor use over the range from 390 to 750 mμ, the region for which the standards are issued. The only exception is the carbon yellow standard, which can show a measurable change at certain wave-lengths if left in sunlight for only 1 day. The reader is again referred to the Bureau publication for additional details.

Acknowledgment is made to various individuals who have cooperated in this work. Most of the original measurements were made by Geraldine Walker Haupt and Mabel E. Brown.[1] Recordings of the spectral transmittances of the standards were made at various times by Harry J. Keegan. Recent calibrations of new standards of the same type of glass were made by Margaret M. Balcom and Lois Peterson Gloster.[2] Miss Peterson also made new and more precise determinations of the change of transmittance with temperature than had been possible with the previous instruments, and made the initial measurements on the exposure tests.

Raman Spectrum of 1,3-Butadiene in the Gaseous and Liquid States*

CHARLES M. RICHARDS† AND J. RUD NIELSEN
Department of Physics, University of Oklahoma, Norman, Oklahoma
(Received March 31, 1950)

The Raman spectrum of gaseous 1,3-butadiene has been photographed with a three-prism glass spectrograph of linear dispersion 15 A/mm near 4358A. Polarization data have been obtained for the liquid. The observed Raman spectrum has been interpreted in some detail in terms of a planar *trans*-configuration of the molecule. Two fundamentals have been added to previous assignments, and several assignments have been made more specific. It is concluded that at room temperature a small fraction of the molecules have a *cis*-configuration.

INTRODUCTION

An understanding of the structure of 1,3-butadiene and a knowledge of the relative abundance of the possible isomers should aid in the study of conjugation and of isomeric structural variations about a carbon single bond. Moreover, the configuration of this molecule is of considerable interest to the synthetic rubber chemist.

Aston, Szasz, Woolley, and Brickwedde[1] have reviewed the numerous investigations on the structure of 1,3-butadiene. The results have frequently been inconclusive and sometimes mutually contradictory. Aston and his co-workers[1] concluded that molecules of a planar *trans*-form predominate and are more stable than those of a planar *cis*-form by about 2000 calories per mole. Their calculations, based on thermodynamic data, indicate that about four percent of the molecules have the *cis*-form at 298°K and 46 percent at 1500°K.

In the present paper the Raman spectrum of gaseous 1,3-butadiene is reported, together with polarization data obtained for this compound in the liquid state, and an effort is made to interpret these data as completely as possible.

EXPERIMENTAL

The 1,3-butadiene sample was a Phillips Petroleum Company Research Grade Hydrocarbon having a stated purity of 99.87 mole percent, with 2-butene as the most likely impurity. The sample contained 0.02 weight percent of tertiary butyl catechol to inhibit polymerization.

The spectrograph and the irradiation apparatus used have been briefly described elsewhere.[2] The gaseous 1,3-butadiene sample polymerized when exposed to unfiltered mercury light, and the inhibitor fluoresced strongly. These difficulties were overcome with the use of an ultraviolet-absorbing, 4047 A-transmitting dope filter.‡ During the exposures of the gas with this filter, the Raman tube had a temperature of about 55°C, compared to 32°C for the other exposures.

RESULTS

The observed frequency shifts for gaseous and liquid 1,3-butadiene are listed in the first and third columns of Table I, the exciting lines being designated by the conventional symbols[3] in the second and fourth columns. Qualitative descriptions of the Raman bands are given in the fifth column, together with the measured depolarization ratios. The approximate intensities are indicated by the initials *s* (strong), *m* (medium), *w* (weak), and *v* (very), and unusual band contours by *sh* (sharp) or *d* (diffuse). The interpretation of the Raman bands is given in the last column.

In Fig. 1 are shown the Raman spectra of gaseous and liquid 1,3-butadiene. The Raman bands of the gas are somewhat less strongly exposed than those of the liquid and therefore appear sharper. For several bands a frequency change with change of state of aggregation may be seen. Of particular interest, in the spectrum of the gas, is the appearance of rotational branches of several bands and of a weak band at 1659 cm^{-1} not found in the spectrum of the liquid.

DISCUSSION OF RESULTS

The band observed near 1678 cm^{-1} in the spectrum of liquid 1,3-butadiene may have been caused by *trans*-2-butene. This would seem unlikely in view of its intensity and the stated purity of the sample; however, the coincidence of this band and a weak mercury line may account for its appearance even with a very small concentration of the impurity.

The bands identified as 1659 *e* and 2256 *k* were observed only in the spectrum of the gas. Failure to distinguish the former band in the liquid may result from its being shifted so much towards lower wave numbers as to be masked by the very intense band at 1638. The band designated as 2256 *k* was observed in only one exposure with the 4047 A-transmitting dope filter. Its

* This paper is based upon a thesis presented by Charles M. Richards to the faculty of the Graduate College of the University of Oklahoma in partial fulfillment of the requirements for the degree of Doctor of Philosophy.

† Present address: Universal Oil Products Company, Research and Development Laboratories, Riverside, Illinois.

[1] J. G. Aston, G. Szasz, H. W. Woolley, and F. G. Brickwedde, J. Chem. Phys. 14, 67 (1946).

[2] D. C. Smith, J. Rud Nielsen and H. H. Claassen, J. Chem. Phys. 18, 326 (1950).

‡ General Aniline and Film Company, Sample 1809-146-1.

[3] K. W. F. Kohlrausch, *Der Smekal-Raman Effekt* (Julius Springer, Berlin, 1931).

TABLE I. Raman spectrum of 1,3-butadiene.

Gas Wave number	Exciting lines	Liquid Wave number	Exciting lines	Description and polarization			Interpretation
		320 cm^{-1}	*e*	*vw*	*vd*		B_u skeletal deformation
513.4 cm^{-1}	*e*, *i*, *k*	514.0	*e*, *f*, *g*, *i*, *k*	*s*	*sh*	0.1	A_g skeletal deformation
		618 ?	*e*	*vvw*			
686	*e*	686	*e*	*vw*	*vd*		B_g CH_2 torsion
		752 ?	*k*	*vvw*			
		890	*e*, *k*	*w*			B_g CH wagging
910	*e*	911	*e*, *f*, *i*, *k*	*m*	*d*	0.7	B_g CH_2 wagging
		967	*e*, *k*	*w*	*d*	0.8	
		1130	*e*	*vvw*			
1204.8	*e*, *i*, *k*	1202	*e*, *f*, *g*, *i*, *k*, *l*	*vs*	*sh*	0.3	A_g C−C stretching
1279.3	*e*, *k*	1278.8	*e*, *i*, *k*, *l*	*vs*	*sh*	0.2	A_g CH_2 rocking
1302	*e*, *k*	1303	*e*, *i*, *k*	*s*		0.2	A_g CH rocking
		1401	*e*	*vvw*			513+890=1403 B_g
1442	*e*, *k*	1438.6	*e*, *f*, *k*, *l*	*vs*	*sh*	0.3	A_g CH_2 deformation
1643	*e*, *f*, *g*, *l*	1638	*e*, *f*, *g*, *h*, *l*, *m*	*vvs*		0.1	A_g C=C stretching
1659	*e*			*vvw*			
		1678	*e*	*vw*			
1780	*e*	1779	*e*	*w*		0.2	2×890=1780 A_g
2092	*e*	2089	*e*, *k*	*vw*			890+1205=2095 B_g
2256	*k*			*vvw*			
		2327	*e*, *i*, *k*	*vvw*			890+1442=2332 B_g; 686+1643=2329 B_g
		2400.7	*e*, *k*	*vvw*			2×1205=2410 A_g
		2523	*e*, *k*	*vw*	*vd*		890+1643=2533 B_g
2842	*k*	2838.4	*e*, *k*	*vw*			1205+1643=2848 A_g
2879	*k*	2874 ?	*e*, *i*, *k*	*vvw*			2×1442=2884 A_g
3014	*e*, *i*, *k*	3004	*e*, *f*, *g*, *i*, *k*, *l*	*vs*	*sh*	0.1	A_g CH stretching
3101	*e*, *i*, *k*	3093	*e*, *i*, *k*	*m*		0.6	A_g CH stretching
		3187	*e*, *i*, *k*	*vw*			2×1599*=3198 A_g
		3267	*e*, *k*	*vw*			2×1643=3286 A_g

* Infra-red frequency.

assignment to the mercury line *k* is not altogether satisfactory, but any alternative seems less plausible. These two bands cannot readily be attributed to a light impurity having a large concentration in the first samples taken from the cylinder.

A very weak Raman band at 1025 cm^{-1} reported by Bradacs and Kahovec[4] in the spectrum of liquid 1,3-butadiene has not been found in the present work. All other frequencies observed by them and by Dadieu and Kohlrausch[5] have been found in the spectrum of the liquid, and all but two in the gas. Fifteen new frequencies have been observed for the liquid.

The bands found by Bradacs and Kahovec[4] at 338 and 899 cm^{-1} have been observed at 320 and 890 cm^{-1}. However, most of the present frequencies are from one to five cm^{-1} higher than those reported earlier. The depolarization ratios measured in the present investigation are generally somewhat lower than those reported by the previous workers.[4] The diffuse band at 911 cm^{-1} is surely depolarized, despite the low depolarization ratio observed.

Most of the frequencies below 1400 cm^{-1} for gaseous 1,3-butadiene are about the same as for the liquid. However, the shift from 1202 cm^{-1} in the liquid to 1204.8 cm^{-1} in the gas seems to be real. The higher frequencies generally increase as much as 10 cm^{-1} on passing to the gaseous state.

The Raman frequency 513.4 cm^{-1} in the gas is not very different from the infra-red frequency 520 cm^{-1} reported by Bartholomé and Karweil.[6] The frequencies 686, 910, 1279.3, 1302, and 1442 cm^{-1} in the gas and the doubtful frequencies 618 and 752 cm^{-1} observed only in the liquid coincide almost exactly with infra-red frequencies given by Rasmussen and Brattain.[7] Whether these coincidences are real or only apparent must be considered carefully in designating the predominant configuration of the 1,3-butadiene molecules as *cis* or *trans*.

INTERPRETATION

Most of the experimental evidence, as summarized by Aston, Szasz, Wooley, and Brickwedde,[1] favors the assumption that the molecules of 1,3-butadiene have predominantly a planar *trans*-form. The symmetry of this form is that of the point group C_{2h}, and the fundamentals are divided into $9A_g+4A_u+3B_g+8B_u$. The vibrations of species A_g and B_g are Raman-active, those of species A_u and B_u infra-red-active. The relatively small number of frequencies observed in the Raman and infra-red spectra and the small number of coincidences

[4] K. Bradacs and L. Kahovec, Zeits. f. physik. Chemie **48**, 63 (1940).

[5] A. Dadieu and K. W. F. Kohlrausch, Ber. d. d. chem. Ges. **63**, 1657 (1930).

[6] E. Bartholomé and J. Karweil, Zeits. f. physik. Chemie **35**, 442 (1937).

[7] R. S. Rasmussen and R. R. Brattain, J. Chem. Phys. **15**, 131 (1947).

between Raman and infra-red frequencies seem to justify the assumption of a *trans*-configuration at the outset.

Bradacs and Kahovec[4] assigned their Raman frequencies and the infra-red frequencies reported by Bartholomé and Karweil[6] to the fundamentals of a planar *trans*-molecule. Aston and his co-workers[1] have supplemented this assignment with some estimated and calculated frequencies. In the present work, these assignments have been examined critically and found essentially correct. One observed frequency has been added to the Raman-active fundamentals and one to those active in the infra-red. Several fundamentals have been given more accurate frequency values and the corresponding vibrations have been characterized in greater detail. The revised assignment of fundamentals is given in Table II. The Raman frequencies observed for gaseous 1,3-butadiene are followed by R, one observed only for the liquid by R'. Infra-red frequencies are indicated by IR, and a previously calculated value by a.

The Raman frequencies 3014 and 3101 cm^{-1} of gaseous 1,3-butadiene are clearly C—H bond-stretching fundamentals. The lower frequency has been assigned to two of the fundamentals of this type because of its much greater intensity. The infra-red spectrum for this region provides further evidence in support of this distinction.

Creitz and Smith[8] have recently recorded the infra-red spectra of gaseous and liquid 1,3-butadiene, using a lithium fluoride prism between 2400 and 10,000 cm^{-1}. They have not reported the measured frequencies, but it seems clear that there are three bands of species B_u with centers near 3000, 3060, and 3100 cm^{-1}. These frequencies have been assigned to the three B_u C—H bond stretching vibrations.

The Raman frequency 1442 cm^{-1} has been assigned to the A_g deformation mode of the CH_2 groups of 1,3-butadiene. This is in agreement with the results of a correlation study recently published by Sheppard.[9] The infra-red frequency 1484 cm^{-1} has been assigned to the corresponding B_u mode, which should have the higher frequency.

The Raman frequency 1279 cm^{-1} has been assigned to the totally symmetric rocking motion of the CH_2 groups of 1,3-butadiene. A band near this frequency occurs in 2-methyl-1,3-butadiene,[5] 1,4-pentadiene, and 1,5-hexadiene,[10] although not in 2,3-dimethyl-1,3-butadiene.[5] In this spectral region only this totally symmetric vibration would be expected to have about the same frequency in all of these molecules. The frequency 1302 cm^{-1} must then be assigned to the remaining A_g fundamental in this region, the in-plane rocking of the single hydrogen atoms attached to the singly-bonded carbons. This is in agreement with the assignment of the analogous mode in *trans*-2-butene.[11] The infra-red frequencies 1290 and 1379 cm^{-1} have been assigned to the B_u rocking modes of the CH_2 and CH groups respectively.

Aston, Szasz, Woolley, and Brickwedde[1] calculated a frequency of 667 cm^{-1} for the B_g twisting motions of the CH_2 groups in 1,3-butadiene. The Raman frequency 686 cm^{-1}, first observed in the present work, is in good agreement with their value and has been assigned to this mode.

Aston and his co-workers interpreted the Raman frequencies 914 and 899 cm^{-1} as the remaining B_g fundamentals. The Raman band found at 911 in the present work is undoubtedly depolarized, and hence must belong to B_g. It has been identified as the even out-of-plane wagging vibration of the CH_2 groups. The infra-red band at 909 cm^{-1} has been assigned to the corresponding A_u fundamental. The lower Raman frequency, found at 890 cm^{-1} in the present work, appears to be polarized, although the evidence is not conclusive, while the band at 967 cm^{-1} is definitely depolarized. At first, the latter band was interpreted as a B_g fundamental. However, this assumption was not useful in the interpretation of the Raman spectrum, whereas the assignment of 890 cm^{-1} as a B_g fundamental led to a satisfactory interpretation of five weaker bands. The latter assignment has therefore been made. As indicated in Table II, this vibration is largely an out-of-plane wagging of the single hydrogen atoms attached to the single-bonded carbons. The abnormality in the depolarization ratio, if real, may be a result of a distortion of the molecules in the liquid

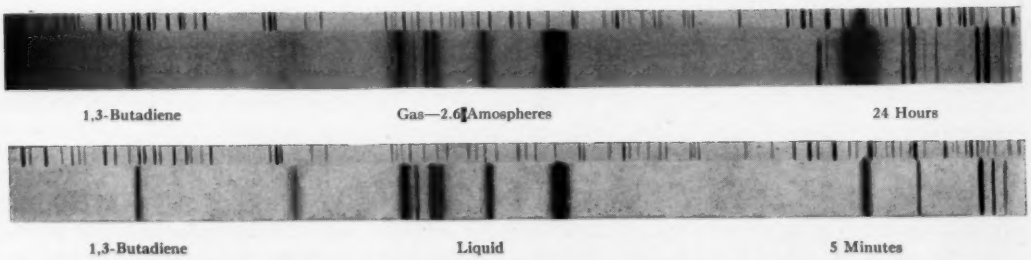

FIG. 1. Raman spectra of 1,3-butadiene in the gaseous and liquid states. Exposure times: for gas (2.6 atmos.) 24 hours; for liquid 5 minutes.

[8] E. C. Creitz and F. A. Smith, J. Research Nat. Bur. Stand. **43**, 365 (1949).
[9] N. Sheppard, J. Chem. Phys. **17**, 74 (1949).
[10] K. W. F. Kohlrausch, *Ramanspektren* (Akademische Verlag Becker and Erler, Leipzig, 1943).
[11] C. M. Richards and J. Rud Nielsen, J. Opt. Soc. Am. **40**, 442 (1950).

state. The only remaining strong infra-red band in this region, at 1014 cm^{-1}, has been identified with the CH wagging fundamental of species A_u.

The Raman band at 320 cm^{-1}, found only in the spectrum of liquid butadiene, is presumably the same band as that interpreted by Aston and co-workers[1] as the overtone of the A_u skeletal deformation frequency, which they assumed to be at 170 cm^{-1}. However, the band at 320 cm^{-1} is so diffuse that it can hardly belong to species A_g. It lies close to the value 326 cm^{-1} for the B_u skeletal deformation frequency used by Aston and co-workers[1] to fit the observed thermodynamic data. In view of these facts, it has been assumed that the selection rules are violated in the liquid state, and the Raman band at 320 cm^{-1} has been assigned tentatively to the B_u skeletal deformation.

With the assignment of fundamentals given in Table II seven Raman bands cannot be satisfactorily interpreted as overtones or combination bands. Four weak infra-red bands below 1700 cm^{-1} are also difficult to interpret. Thus, it seems reasonable to assume that a small fraction of the *cis*-isomer is present. It appears likely that the very faint Raman band observed at 1659 cm^{-1} in the spectrum of the gas represents the C=C stretching fundamental of the *cis*-form. The presence of a weak maximum at 1660 cm^{-1} in the infra-red spectrum supports this conclusion. The approximative coincidence of the faint Raman and infra-red bands near 750 cm^{-1} may be explained by regarding them as a fundamental of the *cis*-isomer. Only the negative evidence that the weak Raman bands at 618, 967, and 1130 cm^{-1} have not been interpreted otherwise suggests that they too belong to the *cis*-isomer. The band identified as 2256 *k* in the gas is probably the first overtone of 1130 cm^{-1}.

The concentration of 1,3-butadiene molecules having the *cis*-form seems to be less than four percent at room temperature, as estimated by Aston and co-workers.[1]

TABLE II. Fundamental frequencies of 1,3-butadiene (C_{2h}).*

Type of vibration	A_g	B_g	A_u	B_u
CH stretching	3101 *R*			3100 *IR*
	3014 *R*			3060 *IR*
	3014 *R*			3000 *IR*
CH_2 deformation	1442 *R*			1484 *IR*
CH rocking	1302 *R*			1379 *IR*
CH_2 rocking	1279 *R*			1290 *IR*
CH_2 wagging		911 *R*	909 *IR*	
CH wagging		890 *R*	1014 *IR*	
CH_2 torsion		686 *R*	520 *IR*	
C=C stretching	1643 *R*			1599 *IR*
C−C stretching	1205 *R*			
Skeletal deformation	513 *R*		170[a]	320 *R'*

* *R*: Raman (gas); *R'* = Raman (liquid); *IR* = Infra-red (gas).
[a] Calculated by Aston, Szasz, Woolley and Brickwedde (see reference 1).

This is indicated by the weakness of the band at 1659 cm^{-1} as compared to that at 1643 cm^{-1}, and also by the small number of bands that can be attributed to the *cis*-isomer. Conclusive proof of the existence of the *cis*-isomer would require intensity measurements at widely different temperatures. It seems doubtful that low temperature measurements alone would identify the unassigned bands as belonging to the *cis*-isomer; for in view of the experimental difficulties at low temperatures, the disappearance of so weak bands would hardly be accepted as conclusive. Spectra of the gas at higher temperatures would probably furnish more reliable information. They could be obtained only with adequate precautions to avoid polymerization.

ACKNOWLEDGMENT

One of the writers (C.M.R.) wishes to express his appreciation to the Phillips Petroleum Company for the grant of a fellowship.

Deane B. Judd Receives Commerce Department Medal

On February 14, 1950 the Department of Commerce awarded Deane B. Judd of the National Bureau of Standards the "Exceptional Service Award, Gold Medal, for Outstanding Contribution to the Public Service, the Nation, or Humanity." Charles Sawyer, Secretary of Commerce, presented the award to Dr. Judd and the citation read in connection with the award detailed his technical accomplishments from which the following is quoted:

"The Commerce Department awards its gold medal to Dr. Judd for outstanding scientific accomplishment in colorimetry and color vision and for his highly distinguished authorship in these fields. Dr. Judd has been with the Bureau of Standards for over twenty years. Since 1933 he has been in charge of the Bureau's colorimetric work, carrying on a program of research, developing test methods and instruments, initiating programs, and otherwise representing the Bureau in that field. It is in the field of color vision, however, that he has made his most outstanding contributions. He has more than fifty publications to his credit dealing with such subjects as color measurement, color systems, and camouflage. Many of these papers have received national and international recognition. In 1937 he received the Journal Award from the Society of Motion Picture Engineers for a paper entitled "Color Blindness and Anomalies of Color Vision." The mathematical treatment of color blindness, combining theory and experiment, has afforded an understanding of the relations between normal and color-blind vision never before possible. . . . He has participated in international conferences in England, France, and Holland; is president of the Board of Trustees of the Munsell Color Foundation; and has been chairman of the Inter-Society Color Council."

Dr. Judd, in addition to serving as an active member of the Colorimetry Committee of the Optical Society of America, has served this Society as an Associate Editor of the Journal of the Optical Society, a member of its Board of Directors, and representative of the Society on the Physical Division of the National Research Council.

Raman Spectra of *Cis*- and *Trans*-2-Butene in the Gaseous and Liquid States*

CHARLES M. RICHARDS† AND J. RUD NIELSEN
Department of Physics, University of Oklahoma, Norman, Oklahoma
(Received March 29, 1950)

The Raman spectra of gaseous and liquid *cis*- and *trans*-2-butene have been obtained with a three-prism glass spectrograph of linear dispersion 15A/mm at 4358A, together with polarization data for these compounds in the liquid state. For each compound six or seven fundamentals have been added to previous assignments, and one change has been made in the latter. The observed spectra have been interpreted in detail.

INTRODUCTION

RAMAN data have been reported for a large number of hydrocarbons in the liquid state but for only about a dozen in the gaseous state. Data for gases are generally of greater value than those for liquids, since the present theory of scattering applies strictly only to free molecules. A vibration that is Raman-inactive for the free molecules may be observed in the Raman spectrum of the liquid when the closely packed molecules suffer a reduction of symmetry. The shape of a Raman band, as well as its frequency shift, may be different in the liquid and the gaseous states because of the distortion of the molecules in the liquid and their lack of free rotation. Nevertheless, because of the experimental difficulties involved in the study of gases, most workers have obtained data only for compounds in the liquid state but have treated such data as representative of free molecules.

In the present paper the Raman spectra of gaseous *cis*- and *trans*-2-butene are reported, together with polarization data obtained for these compounds in the liquid state. Assignments of fundamentals are made, and the spectra are interpreted in detail.

EXPERIMENTAL

The *cis*- and *trans*-2-butene samples were Phillips Petroleum Company Research Grade Hydrocarbons having stated purities of not less than 96.18 and 98.92 mole percent, respectively. In each compound the most probable impurity was the isomeric 2-butene. The Raman spectrum of the *cis*-2-butene indicated that it contained between one and three mole percent of *trans*-2-butene but no appreciable amount of any other impurity. No *cis*-2-butene could be detected in the *trans*-2-butene.

The spectra were photographed with a Lane-Wells spectrograph. This instrument, and the irradiation apparatus used, have been described briefly in a recent paper by Smith, Nielsen, and Claassen.[1] Either a solution of sodium nitrite in distilled water or tap water was circulated through the filter jacket. The temperature of the Raman tube was about 32°C during all exposures. The gases were exposed at their saturated vapor pressures, about 2.6 atmos., for as long as 40 hr. The liquids were exposed in the same apparatus in Raman tubes about eight mm in inside diameter and fifteen cm in length. Rather complete spectra were obtained with 45-min. exposures. Longer exposures were necessary for accurate measurement of the weakest Raman bands. The frequency shifts were determined by interpolation between the lines of an iron arc spectrum photographed adjacent to each Raman spectrum.

Polarization measurements were made for the liquids with the apparatus described by Nielsen, Claassen, and Smith.[2] A filter made by coating a Pyrex tube with a 4047A-absorbing dope‡ was used in addition to the sodium nitrite filter. Such dope filters have been discussed by Glockler and Haskin.[3]

RESULTS

The Raman spectra of *cis*- and *trans*-2-butene are presented in Tables I and II. In the first and third columns are listed the wave number shifts observed in the gaseous and liquid states, respectively. These values are weighted averages of measurements, on several films, for the bands excited by the mercury lines indicated by the conventional symbols[4] in the second and fourth columns. The underscoring of a symbol indicates that anti-Stokes excitation was also observed. In the fifth column the relative band intensities are indicated by the initials *s* (strong), *m* (medium), *w* (weak), and *v* (very); unusually sharp or diffuse bands are further denoted by *sh* or *d*. The measured depolarization ratios are also given in this column.

DISCUSSION OF RESULTS

Gershinowitz and Wilson[5] obtained Raman data for liquid *cis*- and *trans*-2-butene, using samples estimated to be at least 99.5 mole percent pure. More recently, the

* This paper is based upon a thesis presented by Charles M. Richards to the faculty of the Graduate College of the University of Oklahoma in partial fulfillment of the requirements for the degree of Doctor of Philosophy.

† Present address: Universal Oil Products Company, Research and Development Laboratories, Riverside, Illinois.

[1] Smith, Nielsen, and Claassen, J. Chem. Phys. **18**, 326 (1950).

[2] Nielsen, Claassen, and Smith, J. Chem. Phys. **18**, 485 (1950).

‡ General Aniline and Film Company, Sample 1809-146-2.

[3] G. Glockler and J. F. Haskin, J. Chem. Phys. **15**, 759 (1947).

[4] K. W. F. Kohlrausch, *Der Smekal-Raman-Effekt* (Verlag Julius Springer, Berlin, Germany, 1931).

[5] H. Gershinowitz and E. B. Wilson, Jr., J. Chem. Phys. **6**, 247 (1938).

TABLE I. Raman spectrum of *cis*-2-butene.*

Gas Wave number	Gas Exciting lines	Liquid Wave number	Liquid Exciting lines	Description and polarization			Interpretation
		258 cm^{-1}	*e*	*vvw*			A_1 skeletal deformation
		290	*e, k*	*vw*	*vd*		A_2, B_1 CH_3 torsion
		396	*e, i, k*	*m*	*d*	0.8	A_2 skeletal deformation
		575	*e, k*	*vw*	*d*		B_2 skeletal deformation
		673	*e, k*	*vw*	*d*		B_1 C−H wagging
		786	*e, k*	*vw*	*d*		$2\times396=792(A_1)$
873 cm^{-1}	*e, i, k*	873.2	*e, f, i, k*	*s*	*sh*	0.0	A_1 C−C stretching
		970	*e, k*	*w*	*d*	0.7[a]	B_2 C−C stretching
1009	*e, k*	1008	*e, i, k*	*m*		0.1	A_1 CH_3 rocking
(1045)	(*e*)	1037	*e, k*	*w*	*d*		B_1 CH_3 wagging
(1142)	(*e*)	1134	*e, k*	*vvvw*			B_2 CH_3 rocking
1261	*e, i, k, (l)*	1255	*e, i, k*	*m*		0.4	A_1 C−H rocking
1387	*e, k*	1380.8	*e, k*	*m*	*sh*	0.2	A_1 CH_3 deformation (symmetrical)
1464	*e, k*	1455	*e, k*	*m*	*d*	0.6[b]	A_1, A_2, B_1, B_2 CH_3 deformation (unsymmetrical)
		1636	*e*	*vvw*			$258+1387=1645(A_1)$; $970+673=1643(A_2)$
1670	*e*	1660.0	*e, f, g*	*vs*	*sh*	0.0	A_1 C=C stretching
		1709	*e*	*vw*			$1134+575=1709(A_1)$
		2538[c]	*k*	*vvvw*			$1660.0+873.2=2533.2(A_1)$; $2\times1255=2510(A_1)$
2715	*i, k*	2705.0	*e, k*	*vw*	*sh*		$1660.0+1037=2697(B_1)$
2757	*k*	2746	*e, k*	*vw*			$2\times1380.8=2761.6(A_1)$
2813	*k*	2803	*e, k*	*w*			$1660.0+1134=2794(B_2)$
2878	*e, i, k*	2868	*e, k, o*	*s*		0.0	A_1 C−H stretching (methyl)
2935	*e, i, k*	2923	*e, i, k, o, p, q*	*vs*		0.2	A_1 C−H stretching (methyl)
(2988)	(*k*)	2977	*e, k, o, q*	*w*			A_2, B_1, B_2 C−H stretching (methyl)
3036	*e, i, k, o, q*	3023	*e, i, k, o, q*	*s*	*sh*	0.1	A_1 C−H stretching (ethylenic)
		3312	*e, k*	*vvw*			$2\times1660.0=3320.0(A_1)$

* Doubtful frequencies and the corresponding symbols are placed in parenthesis. The superscripts refer to uncertainties as follow: [a] Depolarization ratio probably too low because of 2746 *k*. [b] Depolarization ratio may be too low because of 3023 *i*. [c] This band may be 2923 *l*.

Illinois Institute of Technology Spectroscopy Laboratory has contributed Raman spectra of these compounds in the liquid state to the catalog of the American Petroleum Institute Research Project 44.[6]

Cis-2-Butene

Except for three intense bands of *trans*-2-butene, none of the bands in the spectrum of liquid *cis*-2-butene seem to have been caused by an impurity. Gershinowitz and Wilson[5] reported a very weak band at 2671 cm^{-1}, excited only by the 4358A line. The A.P.I. spectrum[6] does not include this band but contains one at 1422 cm^{-1} not observed by the previous workers. Neither of these bands has been found in the present work, and their reality is questioned. All of the other frequencies reported previously have been observed and, in addition, the frequencies 258, 786, 1134, 1636, 1709, 2538, and 3312 cm^{-1}. Of these, only 2538 cm^{-1} is in doubt; it may possibly be 2923 cm^{-1} excited by the 3984A mercury line. Despite the low depolarization ratio measured for the weak band at 970 cm^{-1}, it seems fairly certain that it is depolarized.

Trans-2-Butene

None of the bands of *cis*-2-butene were found in the Raman spectrum of *trans*-2-butene. All of the frequencies reported previously have been observed in the present work. The band at 210 cm^{-1} was reported only by Gershinowitz and Wilson[5]; those at 1146 and 2887 cm^{-1} were included only in the A.P.I. spectrum[6]. The frequencies 1650, 1733, 2000, 2115, 2346, 2407, 2476, 2558, 2764, 2887, and 3343 cm^{-1} have not been reported previously. Of these, 2346, 2476, and 2558 cm^{-1} may possibly be 2734.9, 2862, and 2948 cm^{-1}, respectively, excited by the 3984A line. Gershinowitz and Wilson[5] regarded the bands at 1382, 1450, and 2919 cm^{-1} in liquid *trans*-2-butene as depolarized. However, the present depolarization ratio of 0.6 for both 1382 and 1450 seems to be correct or even slightly too large. There appears to be no doubt that the band at 2919 cm^{-1} is strongly polarized. The frequencies obtained in the present work, both for *cis*- and *trans*-2-butene, are generally somewhat lower than those given by Gershinowitz and Wilson.[5] The agreement with the values listed in the A.P.I. catalog[6] is much better.

Most frequencies lower than 1037 cm^{-1} for *cis*-2-butene and 1382 cm^{-1} for *trans*-2-butene have about the same values in the liquid and gaseous states. The other frequencies are somewhat higher in the spectra of the gases. No appreciable differences have been noted in the relative intensities or in the shapes of the Raman bands as observed in the liquid and the gaseous states.

It is of interest that most of the observed Raman frequencies of gaseous *cis*-2-butene coincide, within fairly small limits, with infra-red frequencies reported by

[6] American Petroleum Institute Research Project 44 at the National Bureau of Standards. Catalog of Raman Spectral Data. Serial Nos. 25 and 26.

TABLE II. Raman spectrum of *trans*-2-butene.*

Gas Wave number	Exciting lines	Liquid Wave number	Exciting lines	Description and polarization			Interpretation
		210 cm^{-1}	*e*	*vw*	*d*		B_g CH_3 torsion
500.9 cm^{-1}	*g, k*	502.5	*g, f, i, k*	*m*		0.2	A_g skeletal deformation
750	*e*	742	*e, k*	*w*	*d*	0.9	B_g C−H wagging
866.3	*e, k*	867.2	*e, f, i, k*	*m*	*sh*	0.0	A_g C−H stretching
		1039	*e, k*	*w*	*d*		B_g CH_3 wagging
		1146	*e, k*	*vw*			A_g CH_3 rocking
1308.7	*e, i, k*	1307.8	*e, i, k*	*s*	*sh*	0.2	A_g C−H rocking
1385	*e, k*	1382	*e, k*	*m*		0.6	A_g CH_3 deformation (symmetrical)
1457	*e, k*	1450	*e, k*	*m*		0.6	A_g CH_3 deformation (unsymmetrical)
		1650	*e*	*vvw*			1146+502=1648(A_g)
1680.1	*e*	1675.5	*e, f, g*	*s*	*sh*	0.1	A_g C=C stretching
		1733	*e*	*vvw*			2×867.2=1734.4(A_g)
		2000	*e*	*vvvw*			1146+867.2=2013(A_g); 1039+964*=2003(B_u)*
		2115	*e, k*	*vvvw*			1382+742=2124(B_g); 2×1065*=2130(A_g)
		2346[b]	*k*	*vvvw*			1307.8+1039=2347(B_g)
		2407	*e, i, k*	*vvw*			1449*+964*=2413(A_g)
		2476[c]	*k*	*vvvw*			1449*+1030*=2479(A_g)
		2558[d]	*k*	*vvvw*			1675.5+867.2=2542.7(A_g)
2743	*i, k*	2734.9	*e, i, k*	*m*		0.0	
		2764	*k*	*vw*			1450+1308=2758(A_g)
2874	*e, i, k*	2862	*e, i, k, o*	*m*		0.1	2×1382=2764(A_g)
2904	*k*	2887	*e, i, k, o, p*	*m*		0.2	2×1450=2900(A_g); 2×1449*=2898(A_g)
2930	*e, i, k*	2919	*e, i, k, o, p, q*	*s*		0.2	A_g C−H stretching (methyl)
2954	*e, i, k*	2948	*e, i, k, o*	*s*		0.4	A_g C−H stretching (methyl)
3011	*e, i, k*	3007	*e, i, k, m, o, p, q*	*m*		0.2	A_g C−H stretching (ethylenic)
		3343	*k*	*vvvw*			2×1675.5=3351.0(A_g)

* Frequencies taken from the infra-red data (see reference 7) are marked with an asterisk in the last column. The superscripts refer to uncertainties as follows: [a] This transition is forbidden in the Raman effect but may be active in the liquid state. [b] This band may be 2734.9 *l*. [c] This band may be 2862 *l*. [d] This band may be 2948 *l*.

Rasmussen and Brattain.[7] However, the Raman frequencies 1308.7, 1457, and 2954 cm^{-1} of gaseous *trans*-2-butene are also nearly equal to infra-red frequencies reported by these workers. In this case coincidences are forbidden by the selection rules, since this molecule possesses a center of symmetry. Hence, the nearly equal frequencies must belong to different species.

ASSIGNMENT OF FUNDAMENTALS AND INTERPRETATION OF SPECTRA

Kilpatrick and Pitzer[8] have carried out a normal coordinate analysis of the vibrations of *cis*- and *trans*-2-butene and have assigned previously observed Raman and infra-red frequencies to most of the fundamentals of these molecules. The present assignments have been guided largely by their work. With the more complete Raman spectra obtained, some additional assignments have been possible and some changes have been made. These are discussed briefly in the following sections.

Cis-2-Butene

This molecule belongs to the symmetry group C_{2v}, and its normal vibrations divide into $10A_1+6A_2+5B_1+9B_2$,§ all of which are Raman-active. Observed Raman frequencies have been assigned to all of the totally symmetric vibrations. Bands of the other species are more difficult to distinguish, and the assignments of the non-totally symmetric vibrations are less complete.

The assignments of fundamentals for *cis*-2-butene are summarized in Table III. Raman frequencies observed in the gaseous state are given where possible and are followed by the symbol *R*. Those observed only in the liquid state are indicated by *R'*, infra-red frequencies by *IR*, and calculated and conventional frequencies taken from the work of Kilpatrick and Pitzer[8] by *a* and *c*, respectively.

Kilpatrick and Pitzer[8] assigned the Raman frequency 304 cm^{-1} (290 in the present work) to the A_1 skeletal deformation mode. The frequency 258 cm^{-1}, first observed in the present work, is closer to their calculated value of 238 cm^{-1}. Moreover, this band is fairly sharp, while that at 290 cm^{-1} has the diffuse appearance characteristic of a depolarized band. Hence, 258 cm^{-1} has been interpreted as the A_1 skeletal deformation fundamental and 290 cm^{-1} as a superposition of the A_2 and B_1 torsional frequencies of the methyl groups. The latter fundamentals are usually assumed to lie somewhat lower.

[7] R. S. Rasmussen and R. R. Brattain, J. Chem. Phys. 15, 120 (1947).

[8] J. E. Kilpatrick and K. S. Pitzer, J. Research Nat. Bur. Stand. 38, 191 (1947).

§ The convention adopted by Kilpatrick and Pitzer has been followed in the present work, that vibrations of species A_1 and B_2 are symmetric, those of species A_2 and B_1 anti-symmetric, with respect to the plane of the carbon atoms.

TABLE III. Fundamental frequencies of *cis*-2-butene.

Type of vibration	A_1	A_2	B_1	B_2
CH stretching (ethylenic)	3036 *R*			3050 *c*
CH stretching (methyl)	2935 *R*	2988 *R*	2988 *R*	2988 *R*
	2878 *R*			2950 *c*
CH_3 deformation (unsymmetrical)	1464 *R*	1464 *R*	1464 *R*	1464 *R*
CH_3 deformation (symmetrical)	1387 *R*			1380 *c*
CH_3 rocking (wagging)	1009 *R*, *IR*	950 *a*	1037 *R'*	1134 *R'*
CH rocking (wagging)	1261 *R*	1050 *a*	673 *R'*, *IR*	1408 *IR*
C=C stretching	1670 *R*, *IR*			
C−C stretching	873 *R*, *IR*			970 *R'*, *IR*
Skeletal deformation	258 *R'*	396 *R'*		575 *R'*
CH_3 torsion		290 *R'*	290 *R'*	

TABLE IV. Fundamental frequencies of *trans*-2-butene.

Type of vibration	A_g	A_u	B_g	B_u
CH stretching (ethylenic)	3011 *R*			3050 *c*
CH stretching (methyl)	2954 *R*	2950 *c*	2950 *c*	2950 *c*
	2930 *R*			2950 *c*
CH_3 deformation (unsymmetrical)	1457 *R*	1449 *IR*	1457 *R*	1449 *IR*
CH_3 deformation (symmetrical)	1385 *R*			1380 *c*
CH_3 rocking	1146 *R'*	1030 *a*	1039 *R'*	973 *IR*
CH rocking	1309 *R*	964 *IR*	750 *R*	1302 *IR*
C=C stretching	1680 *R*			
C−C stretching	866 *R*			1065 *IR*
Skeletal deformation	501 *R*	240 *a*		290 *a*
CH_3 torsion		210 *R'*	210 *R'*	

The frequencies 1037 and 1134 cm^{-1}, assigned to the B_1 and B_2 rocking modes, respectively, of the methyl groups, agree fairly well with the values calculated by Kilpatrick and Pitzer.[8] Their complete table of assignments seems to contain erroneous values for these frequencies. The higher frequency was not included in the data of Gershinowitz and Wilson[6] used by them.

The previous workers[8] assigned both the Raman and the infra-red frequencies near 1390 cm^{-1} to the B_2 rocking mode of the ethylenic hydrogens of *cis*-2-butene. Since the Raman band is strongly polarized, its present assignment to the A_1 symmetrical deformation mode of the methyl groups must be correct. The center of the strong absorption in this region seems to be at a considerably higher frequency than that of the Raman band in the spectrum of the gas. The previous assignment of this infra-red frequency is therefore probably correct.

The Raman band at 1464 cm^{-1} in gaseous *cis*-2-butene appears to be complex and depolarized. It can hardly be attributed to any one of the unsymmetrical deformation vibrations of the methyl groups but must be a superposition of two or more of these fundamentals. The assignment of the three strongest Raman bands near 2900 cm^{-1} to the particular vibration modes is in accord with conventional values and seems fully justified. The assignment of the weakest band in this region, 2988 cm^{-1}, as a superposition of three fundamentals, on the other hand, is rather arbitrary.

The interpretation of the overtone and combination frequencies has been difficult because these bands are too weak to permit polarization measurements. Most of the assignments given are therefore subject to some uncertainty. In particular, the interpretation of the band at 786 cm^{-1} as a first overtone is not entirely satisfactory.

Trans-2-Butene

This molecule belongs to the symmetry group C_{2h}, and the normal vibrations divide into $10A_g+6A_u+5B_g+9B_u$. The vibrations of species A_g and B_g are Raman-active. As for *cis*-2-butene, observed Raman frequencies have been assigned to all of the totally symmetric vibrations, but the assignment of the remaining Raman-active fundamentals is not quite complete. The assignments of fundamentals are summarized in Table IV. The symbols are the same as in Table III.

The Raman frequency 210 cm^{-1} for liquid *trans*-2-butene was assigned to the B_g twisting of the methyl groups by Kilpatrick and Pitzer;[8] the assignment of the same frequency to the corresponding A_u mode as well is somewhat arbitrary but probably not very wrong. The Raman frequency 1146 cm^{-1} has been assigned to the A_g rocking mode of the methyl groups despite its low intensity. This frequency was not available to the previous workers and is somewhat higher than their calculated value of 1080 cm^{-1}.

The assignment of the Raman frequency 1385 cm^{-1} for gaseous *trans*-2-butene to the A_g symmetrical deformation of the methyl groups seems unequivocal and is in accord with the work of Sheppard and Sutherland.[9,10] The assignment of 1457 cm^{-1} to the A_g unsymmetric methyl deformation is also in accord with their work. The assignment of this frequency to the corresponding B_g mode as well and the assignment of the infra-red frequency 1449 cm^{-1} to the corresponding A_u and B_u modes are somewhat arbitrary. As in the case of *cis*-2-butene, the assignment of the three strongest bands in the 2900 cm^{-1} region to particular C−H stretching modes seems fully justified.

The interpretation of overtone and combination frequencies of *trans*-2-butene has generally been simpler than for *cis*-2-butene. However, in two important instances considerable uncertainty remains. The frequencies 2734.9 and 2874 cm^{-1} in the Raman spectrum of the gas are almost certainly first overtones, either of $1358(A_g)$ and $1457(A_g)$ or the infra-red-active $1449(A_u)$, or of unobserved fundamentals near 1370 and 1435 cm^{-1}.

ACKNOWLEDGMENT

One of the writers (C.M.R.) wishes to express his appreciation to the Phillips Petroleum Company for the grant of a fellowship.

[9] N. Sheppard and G. B. B. M. Sutherland, Proc. Roy. Soc. **A196**, 195 (1949).
[10] N. Sheppard, J. Chem. Phys. **17**, 74 (1949).

New Automatic Colorimeter for Cotton

DOROTHY NICKERSON
Production and Marketing Administration, U. S. Department of Agriculture, Washington, D. C.

AND

RICHARD S. HUNTER, AND MARSHALL G. POWELL
Henry A. Gardner Laboratory, Bethesda, Maryland

(Received March 20, 1950)

This new instrument for measuring the color of cotton is based on a satisfactory application of the Hunter Color and Color-Difference Meter to problems of raw cotton measurement. It is designed to be fully automatic and self-standardizing, and graphically to show values for reflectance (R_d) and yellowness ($+b$) on a two-dimensional chart. It is self-contained in a movable cabinet, with a minimum of exposed parts. Although this particular model is limited to measurements in the range of cotton color, the principles on which it is designed are adaptable to other limited ranges of color, in either two or three dimensions, thus providing an automatic, self-standardizing small-difference colorimeter for other limited ranges of color.

COLOR measurements have been made on raw cotton as part of the preparation of cotton grade standards for many years.[1,2] In fact, as early as 1931 a disk colorimeter for such use was described before this society, with a companion discussion of color measurements in psychological terms.[3,4]

The desirability of expressing color measurements in terms related to the psychological attributes of color has been increasingly recognized by color workers in the years since 1931. Extensive work published by a subcommittee of the OSA Colorimetry Committee[5] now allows one to use the smoothed scales of the Munsell renotation space as a guide for understanding results of color measurements no matter what instrument or color space is used for their expression, providing only that it is possible to convert them either to I.C.I. or to Munsell space.[6,7]

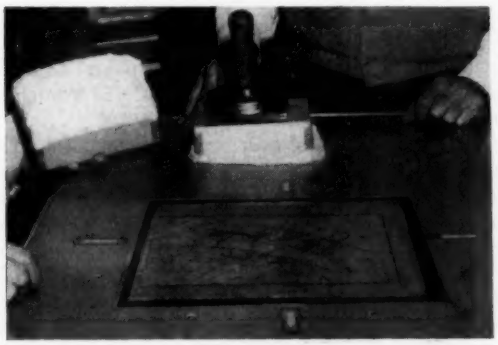

FIG. 1. Top of automatic cotton colorimeter.

Although the expression of results in color-meaningful terms has progressed in a fairly direct manner during these past years, the method of disk colorimetry, while as sound as ever in providing a direct and simple method of additive colorimetry, has a disadvantage for routine testing work in that it is visual and therefore depends somewhat upon the skill and judgment of the operator. In this modern age, measurements made by turning a few dials on a suitable photoelectric device have much more appeal for routine laboratory tests than the painstaking and tedious work of making careful visual judgments. The operation of the instrument to be described is very simple; the operator steps on a foot switch to start operation of an appropriate set of balancing motors which do the work.

The new instrument is based on a satisfactory application of the Hunter Color and Color-Difference Meter, described in 1948 before the Optical Society,[8,9] to problems of raw cotton measurement. It was found that for the limited range of cotton colors a plot of Hunter's coordinates "R_d" and "b" provided, without conversion, a chart very close to that of long-established cotton measurements plotted in terms of Munsell value and chroma.

Since the Color-Difference Meter worked so well, specifications were written for a fully automatic instrument to embody the photo-cell and filter combinations of the present instrument. The requirements were that the instrument maintain itself in standardization, and be direct reading on a two-dimensional scale, that it measure automatically, and show values graphically and simultaneously for reflectance and yellowness in a range of 40 to 90 percent R_d, and 0 to 20 units of $+b$. In this limited range it was required that the precision and accuracy of the R_d and b scale readings approximate 0.4 step or less of Munsell value and chroma scales. It was further required that the instrument be self-contained in a movable cabinet about table height,

[1] D. Nickerson, Am. Dyestuff Reporter **21**, 4 (1932); Fiber and Fabric **85**, 11 (1932).
[2] D. Nickerson, Textile Research J. **16**, 441 (1946).
[3] D. Nickerson, J. Opt. Soc. Am. **21**, 640 (1931).
[4] D. Nickerson, J. Opt. Soc. Am. **21**, 643 (1931).
[5] S. M. Newhall, D. Nickerson, and D. B. Judd, J. Opt. Soc. Am. **33**, 385 (1943).
[6] R. W. Burnham, J. Opt. Soc. Am. **39**, 387 (1949).
[7] D. Nickerson, J. Opt. Soc. Am. **40**, 85 (1950).
[8] R. S. Hunter, J. Opt. Soc. Am. **38**, 661(A) (1948).
[9] R. S. Hunter, J. Opt. Soc. Am. **38**, 1094(A) (1948).

that it have a minimum of exposed parts, that working parts be in the horizontal plane of the table top, and since it is intended for use in lint-filled classing rooms, that dust-absorbing gaskets be used to seal all enclosures for working parts.

Such an instrument was delivered for use in the early part of 1950. To date it has been in almost constant operation, having already measured several thousand samples of cotton in preparation for an international grade standards conference held in May. It satisfies the requirements for which it was designed.

To operate the instrument, the operator places a sample of cotton over the sample window, and steps on a foot switch. Two indicators under the chart diagram automatically move to a position of balance. Since a chart of the color of the grade standards appears on the glass panel on which the (R_d, b) scale is indicated, the operator can check against a particular position within each grade and can pass or fail a test sample by a comparison of results for that sample to the standard position indicated on the instrument chart.

Although this particular model of the instrument is limited to the range of cotton colors and measures in only two color dimensions, the principles upon which it is designed are completely adaptable to use for any other limited range of colors, in either two or all three color dimensions. For cotton a plot of R_d against $+b$ is required. For some other product a plot of $\pm a$ against $\pm b$ might be preferable, with R_d indicated on a separate scale. There are many possibilities for application of such an instrument in color inspection and grading work where a limited range of color is to be determined.

DESCRIPTION OF INSTRUMENT

The instrument was in operation when the photograph shown in Fig. 1 was taken. The sample is in position over the exposure window. Beside it is the translucent chart from which color is read by the position of the intersection of two straight-line shadows. This chart is marked with the colors of the cotton grade standards. For much of the work no record is needed since a glance at the indicator positions will tell the cotton man how the color of his sample compares to the color of the cotton grade standards which are diagrammed on the translucent screen. When records are needed, the results may be recorded in chart form as on a dot chart, with many samples for any single test plotted on one sheet. When needed, the R_d and b values may be read from the scales.

Figure 2 shows an interior view of the instrument in which the separate components are indicated by number.* The instrument consists of two parts, an exposure head, labeled 2, and a detection unit, with indicators labeled 4 and 5. These parts will be described in detail; the instrument circuit will be discussed separately.

Exposure Head

The exposure head, diagrammed in Fig. 3, is contained in a light-and-dust-tight housing, with a window

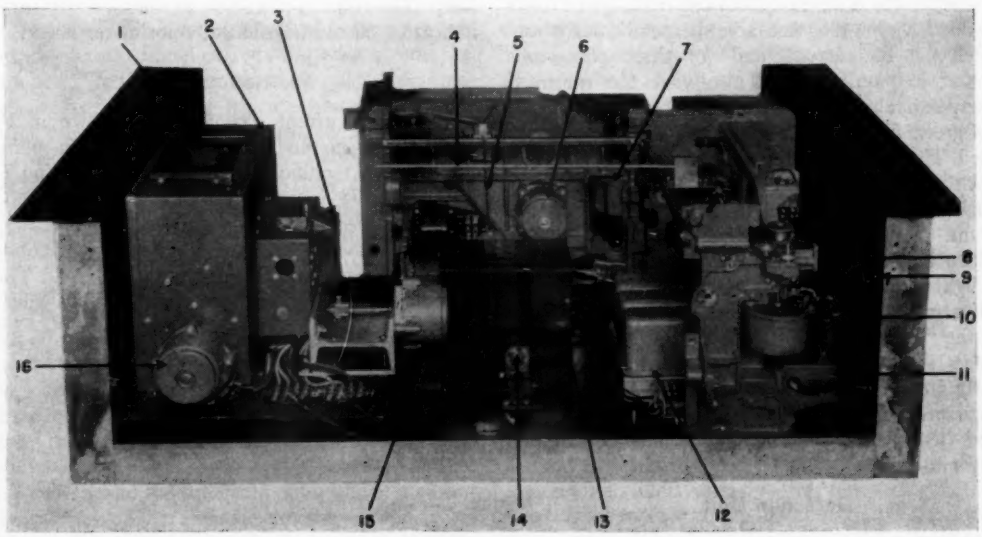

FIG. 2. Interior view of instrument, with numbers identifying components. 1, Sample area; 2, exposure head; 3, lamp guard; 4, R_d indicator; 5, b indicator; 6, R_d balancing motor; 7, R_d slide wire; 8, amplifier off-on switch; 9, lamps off-on switch; 10, b slide wire; 11, b amplifier; 12, relays; 13, CV transformer; 14, lamp for indicating scale; 15, comparison balancing motor; 16, b balancing motor.

* The labeling numbers used in Figs. 2–4 refer to identical components of the instrument.

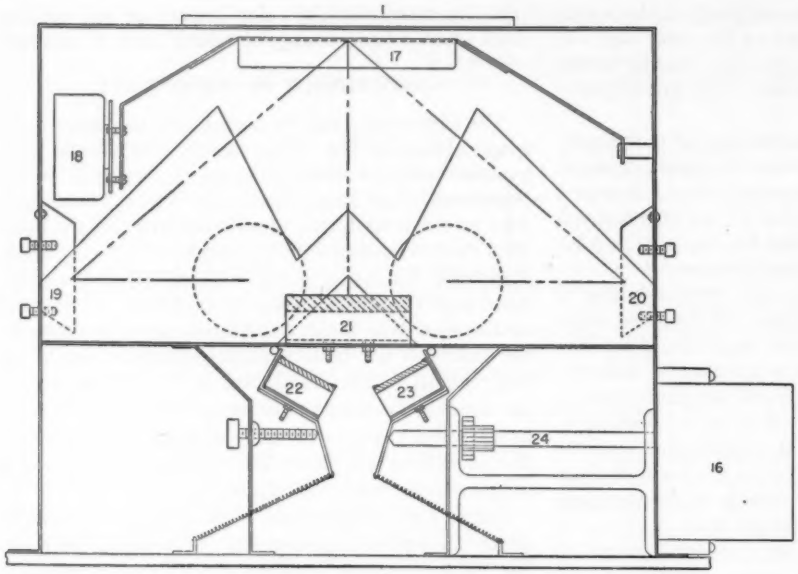

FIG. 3. Diagram of interior of exposure head, with numbers identifying components. 1, Sample area; 16, *b* balancing motor; 17, standard; 18, rotary solenoid; 19, mirror; 20, mirror; 21, photo-cells (one back, one front) blue filter; 22, photo-cell green filter; 23, photo-cell green filter; 24, micrometer adj. screw.

at the top where specimens are exposed. In this exposure head are the following:

1. A six-volt, 32 CP automobile spotlight lamp, lenses, aluminum mirrors (19, 20), and adjusting screws for directing, at 45° from opposite sides, two beams of light onto the exposure area.

2. Five barrier-layer photo-cells: (a) One comparison photo-cell with a heat-absorbing filter which views the light source, (b) a single photo-cell with green filter (22) which views the test area perpendicularly and provides the R_d current, and (c) three photo-cells connected in parallel which also view the specimen area perpendicularly, two with blue filters and one (23) with a green filter that is connected with its polarity reversed. These three photo-cells provide a residual "*b*" current that is proportional to the reflectance difference between the blue and yellow-green regions of the spectrum.

3. Two balancing motors, one (15) for adjustment of the light signal to the comparison cell, the other (16) for adjustment of the light signal to the green filter cell of the "*b*" group.

4. One internally mounted standard (17) which normally faces the R_d and "*b*" photo-cells from inside the exposure window. This standard is moved by a solenoid (18) when a specimen (at 1) is to be exposed to the photo-cells.

Detection Unit

The detection unit contains:

1. Two sensitive electronic amplifiers (one shown at 11) each with a converter for changing small d.c. signals to a.c. before amplification.

2. Two motors (one shown at 6) similar to those in the exposure head but connected in this case to slide-wire assemblies (7, 10) with moving scale indicators (4, 5). The indicators lie under a translucent sheet on which the color values are indicated.

3. Frames to hold the several assemblies.

4. Two manually operated potentiometer rheostats (at rear of instrument, not shown).

5. Constant voltage transformer (13) for the exposure head light source (under 3), relay (12), and a lamp (14) which is placed so as to cast a shadow of the indicators on the translucent colorimeter screen.

Instrument Circuit

The photo-current d.c. circuit is shown in Fig. 4. The balance method of measuring relative photo-cell currents is a modification of the Campbell and Freeth method and is similar to the circuit used in the Color-Difference Meter. When brightly illuminated the comparison photo-cell generates a constant current which is passed through two potentiometer rheostats. The two currents from the photo-cell combinations which ob-

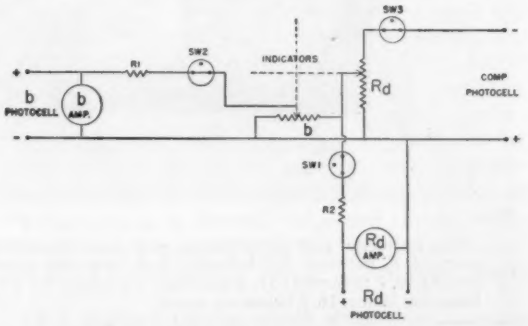

FIG. 4. Simplified d.c. measuring circuit.

serve the sample area are much smaller than this comparison current, so that each can be balanced with a small fraction of the comparison photo-cell current. The exact fraction required to balance any current from the R_d or b photo-cells is determined, respectively, by fixed resistances R_1 and R_2, and the positions of the contacts on the corresponding potentiometer rheostats b and R_d.

Any unbalance between current from the sample-viewing photo-cells and the fractional amount from the comparison photo-cell produces a potential unbalance in the corresponding amplifier input. After amplification, this current unbalance is fed to one of the balancing motors which then acts to restore balance, either by adjustment of a photo-cell position during standardization, or by adjustment of a potentiometer contact during sample measurement.

The comparison current passed through the "b" potentiometer varies with the R_d setting. This is deliberately done, as in the Color-Difference Meter, so that values of "b" measure degrees of yellowness more uniformly at all reflectance levels. The current passing through the remainder of the R_d potentiometer is also a function of the R_d setting. This causes the R_d scale of the instrument to be non-uniform in spacing, unit increments of R_d having a greater spacing at the top of the scale than at the bottom.

One performance requirement for the instrument was that it automatically maintain adjustment of the indicating scales in terms of signal outputs of the photo-cells. Since current outputs of these barrier-layer photo-cells are sensitive to temperature, and in this instrument may also vary with accumulation of dust or other extraneous factors, these current variations must be counteracted. This is done by having duplicate potentiometer circuits, only one of which is shown in Fig. 4. One is for use during standardization, the other during sample measurement. These circuits are alike in resistance values and are interchanged by simultaneous action of switches *Sw* 1, *Sw* 2, and *Sw* 3. In the normally connected circuit for standardization, contacts are set manually to scale values that represent the standard mounted in the exposure head, the amplifier output being fed to the balancing motors in the exposure head. These motors operate to adjust mechanically the positions of the photo-cells so that they provide the required relative photo-cell outputs. For sample measurement, a foot switch is depressed and one solenoid moves the internally mounted standard (17 of Fig. 3) out of the window in order to expose the test specimen. Another solenoid switches to the duplicate potentiometer circuit and switches amplifier signals to the motor-driven variable-contact potentiometer rheostats that move with indicators, thus showing the measured color values. This amplifier switching is shown in Fig. 5.

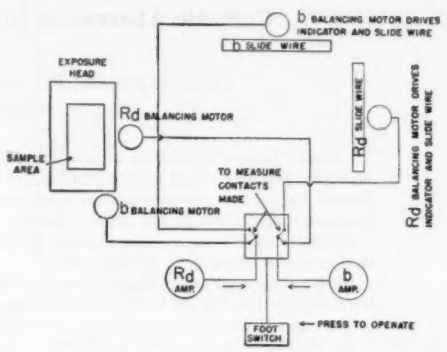

FIG. 5. Pictorial diagram of switching of amplifier output when changing from standard to sample measurement.

Instrument Calibration

A diagram showing the scales, based on a carefully spectrophotometered series of standard color samples, has been prepared. The intention was to use spectrophotometrically derived data for a number of standard samples in the cotton color range. Unfortunately, check measurements made on different spectrophotometers for a number of such standards, even though they were very carefully made, were so far apart in terms of the small-difference scales of this instrument that the scale for the diagram was prepared with reliance chiefly on a set of special measurements on five samples made for the purpose at the National Bureau of Standards. The data for these were reported at the last meeting of this society.[7] The other data were used as a check, a smooth line being drawn for both the R_d and b scales on the basis of general comparison to all the measurements available, leaning heavily on the special series of five made at the National Bureau of Standards. On the translucent screen the color areas occupied by each grade of cotton are indicated. In making measurements of cotton, the color of samples is referred more often to the color of the cotton grade standards than it is to the R_d and b scales of the instrument. The cotton scale-diagram is shown in Fig. 1.

As indicated before, the instrument has been in almost constant operation since its delivery in January —not by laboratory personnel, but by the classers themselves. In a surprisingly short time they have learned not only to use the instrument but to interpret the results. Thus already this new colorimeter has become the real aid to classification that it was intended to provide.

Comatic Aberration in Infra-Red Spectrometer Design

F. P. Elby
Physics Department, The Johns Hopkins University, Baltimore, Maryland
(Received March 1, 1950)

Comatic images formed by off-axis rays reflected from a good ellipsoidal mirror were studied experimentally. Horizontal and vertical knife edges were used to chop slices of these images, and the alternating current output of a photo-multiplier tube, proportional to the chopped radiation, was used to indicate the intensity distributions in the comatic images.

Calculations of intensity distributions in comatic images were made, and the experimental observations were predicted from them satisfactorily.

Infra-red detector sensitivity is inversely proportional to the square root of the detector area. Accordingly, the intensity distribution in the comatic image may be used to calculate optimum dimensions for both the exit slit and the detector in an infra-red spectrometer.

INTRODUCTION

In an infra-red spectrometer, the radiant power on the detector is proportional to the length of the exit slit. However, most spectrometers in current use in infra-red work use a mirror to focus the radiation emerging from the exit slit on the detector, and the off-axis rays from the ends of the slit are subject to comatic aberration. It is the purpose of this paper to discuss the extent to which coma is a limiting factor in the construction of a high resolving power infra-red spectrometer. Nielsen has also made calculations of coma.[1]

This investigation was divided into two principal phases. First, the intensity distribution of light in a comatic image was determined experimentally for a particular system, and second, the theoretical intensity distribution was calculated for any system. The two sets of results were then shown to be in agreement. Finally, a specific problem in spectrometer design was solved on the basis of this work, as an example of how this information can actually be used.

EXPERIMENTAL

The experimental phase of this problem was performed with the apparatus as indicated in Fig. 1. A Western Union zirconium point source unit, W, was arranged so that the point source, S, could be placed at the outer focus, F_0, of the ellipsoidal mirror, M, which had an unimprovable figure. S could be moved known amounts in two perpendicular directions in the plane perpendicular to the optic axis and containing F_0. The light from S was focused at the inner focus, F_i, if S was on the optic axis, or in the plane perpendicular to the optic axis and containing F_i if S was displaced from the optic axis.

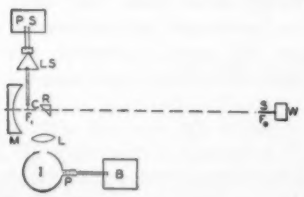

FIG. 1. Diagram of experimental apparatus.

A chopping device, C, consisting of a piece of safety razor blade, was placed at the location of the Gauss point of the comatic image in such a way that it chopped through the image in the plane perpendicular to the optic axis. The chopping was accomplished by mounting the razor blade on a rigid rod which was in turn mounted on the central portion of the cone of a loud speaker, LS. This latter was driven by a variable frequency power supply, PS. The chopped radiation was reflected from a piece of magnesia, R, which served as a good approximation to a Lambert surface. This reflected radiation was focused by a condensing lens, L, on the entrance window of an integrating sphere, I, and a Farrand photo-multiplier tube assembly, P, was attached to the exit window of this sphere. The photo-multiplier tube output was amplified, and this amplified output was put across a Ballantine voltmeter, B.

The voltmeter responded only to the a.c. component and therefore served to indicate the intensity of that portion of the image through which the razor blade was chopping, i.e., the chopped radiation.

It was desired to cut across the comatic image in two directions, along the axis of symmetry of the image and at right angles to it. Since the chopping assembly was free to move in a horizontal direction only, the former purpose was accomplished by displacing the source horizontally and the latter by displacing it vertically. This is illustrated in Fig. 2, the shaded area indicating the slice of the image chopped by the razor blade in an arbitrary position.

The readings were taken as follows: The source was displaced a known amount D_1 horizontally, hereinafter referred to as the X-direction. The Gauss point of the image was correspondingly displaced a distance d_1 along the X-axis, and the chopping assembly was positioned so that the Gauss point fell on the edge of the razor blade. After setting the chopping mechanism in operation, a reading was taken on the voltmeter. The chopping assembly was then moved a distance $0.1D_1$ into the image and another reading taken. This process was con-

[1] J. Rud Nielsen, J. Opt. Soc. Am. **39**, 59 (1949).

tinued across the image. The source was then moved to a new position D_2, placing the Gauss point of the image at d_2, and the entire process was repeated, taking readings at intervals of $0.1D_2$.

After several such sets of readings had been obtained, the source was returned to the optic axis and then displaced vertically, hereinafter referred to as the Y-direction. The identical procedure was carried out for these displacements, except for the fact that readings were taken at positions only $0.05D$ apart on each image, due to the lesser width of image available. The first reading was again taken at the Gauss point of the image.

The amplitude of vibration of the razor blade was 0.10 cm, and the focal distances of the mirror were 7.62 cm and 122 cm for the inner and outer foci respectively. Therefore, a d of 1 cm in the image plane corresponded to a 16 cm displacement D of the source in the outer focal plane. Results are shown in Table I.

COMPUTATIONS

A theoretical solution as a check on the experimental results and as a more flexible tool for further evaluations of coma follows.

Figure 3 is a diagram representing the comatic image, the area of which is $GABCG$. In the region $GADCG$, any point P is the intersection of two comatic circles, while in the circular area $DABCD$, a point P' can have only one comatic circle passing through it. All comatic circles are tangent to the two envelope lines of the image, which meet at a 60° angle at the Gauss point.

The distances $GD=DO=OB=OA=OC=\rho_0$, where ρ_0 is the radius of the largest allowed comatic circle. The zone h_1 on the mirror gives rise to the comatic circle of radius ρ_1, the zone h_2 gives rise to the comatic circle of radius ρ_2, and so on; the outermost zone on the mirror, h_0, gives rise to the largest comatic circle, the radius of which is ρ_0. The values of ρ are governed by the relation[2] $\rho=A\psi h^2$, where A is a constant, ψ is the angle between the optic axis and the line connecting the source and the center of the mirror, and h is the radial distance from the zone to the optic axis.

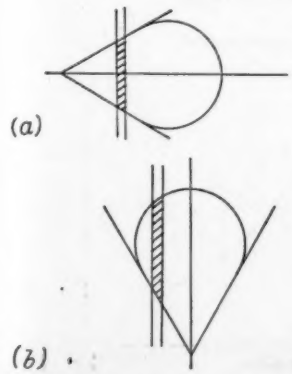

FIG. 2. (a) Horizontal slicing; (b) Vertical slicing.

[2] M. Born, *Optik* (Julius Springer Verlag, Berlin, 1933).

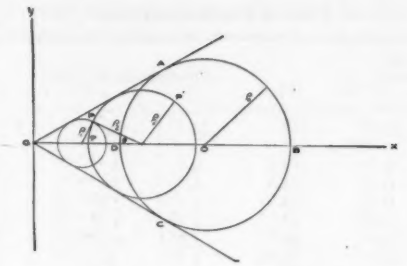

FIG. 3. The comatic image.

Now consider a zone on the mirror at a distance h from the optic axis and of thickness dh. Since the illumination of the mirror may be considered to be uniform over its entire area, the illumination of this zone will be proportional to its area, $2\pi hdh$. This light will be distributed in a comatic circle in the image, the radius of this circle being given by

$$\rho=A\psi h^2.$$

Differentiating, $d\rho=2A\psi hdh$. This indicates that the brightness of the comatic circle is proportional to $d\rho$.

Now take an infinitesimal area da crossed by a comatic circle. The illumination of da will be proportional to the brightness of the circle and also to the fraction of the area of the circle occupied by da. Therefore,

$$Ida\sim d\rho(da/2\pi\rho d\rho)=da/2\pi\rho,$$

where I is the brightness at da.

Letting $da=dxdy$, and introducing the proportionality constant B_0,

$$Idxdy=\frac{B_0}{2\pi}\frac{1}{\rho}dxdy.$$

Since two comatic circles may cross da,

$$Idxdy=\frac{B_0}{2\pi}\left(\frac{1}{\rho_1}+\frac{1}{\rho_2}\right)dxdy.$$

An additional factor is introduced by the fact that the center of the comatic circle corresponding to points of distance $h+dh$ from the axis of the mirror is shifted relative to the center of the comatic circle corresponding to points of distance h from the axis. Taking this into consideration, each comatic circle actually consists of two crescent-shaped zones, and the preceding expression becomes

$$Idxdy=\frac{B_0}{2\pi}\left[\frac{1}{\rho_1(2\cos\varphi+1)}+\frac{1}{\rho_2(2\cos\theta-1)}\right]dxdy.$$

Referring once again to Fig. 3, we obtain from purely geometrical considerations the relations

$$x=2\rho_1+\rho_1\cos\varphi=2\rho_2-\rho_2\cos\theta.$$

We also have the restraints, for the upper half of the

TABLE I. Experimental data.

Position of source (in cm)		Readings (in 10^{-3} volt)				
x	y	1	2	3	4	5
1.0	0	14	24	8	1.5	0
2.0	0	7	12.5	4	0	0
3.0	0	4.5	8	3	0	0
4.0	0	3.5	6	2	0	0
5.0	0	3	5	1.5	0	0
0	1.0	15	9	1.5	0	0
0	2.0	10	3.5	0.5	0	0
0	3.0	8	2	0	0	0
0	4.0	7	1.5	0	0	0
0	5.0	6	1	0	0	0

TABLE II. Flux distribution in the X-direction.

X/ρ_0	$L(°)$	$L'(°)$	I_x/B_0
0.1	120	0	0.58
0.2	120	0	0.58
0.3	120	0	0.58
0.4	120	0	0.58
0.5	120	0	0.58
0.6	120	0	0.58
0.7	120	0	0.58
0.8	120	0	0.58
0.9	120	0	0.58
1.0	120	0	0.58
1.1	120	25.84	0.44
1.2	120	36.87	0.39
1.3	120	45.58	0.35
1.4	120	53.13	0.32
1.5	120	60	0.29
1.6	113.58	60	0.265
1.7	107.46	60	0.245
1.8	101.54	60	0.225
1.9	95.74	60	0.21
2.0	90	60	0.19
2.1	84.26	60	0.175
2.2	78.46	60	0.16
2.3	72.54	60	0.145
2.4	66.42	60	0.135
2.5	60	60	0.12
2.6	53.13	60	0.105
2.7	45.58	60	0.087
2.8	36.87	60	0.070
2.9	25.84	60	0.048
3.0	0	60	0

image,

$$x \leqq 3\rho_0,$$
$$0 \leqq \varphi \leqq 120°,$$
$$\cos\varphi \geqq x/\rho_0 - 2,$$
$$0 \leqq \theta \leqq 60°,$$
$$\cos\theta \leqq 2 - x/\rho_0.$$

Therefore,

$$I dx dy = \frac{B_0}{2\pi}\left[\frac{2+\cos\varphi}{x(2\cos\varphi+1)} + \frac{2-\cos\theta}{x(2\cos\theta-1)}\right] dx dy.$$

To consider a slice of the image at any value of x and of width dx, we have only to perform the appropriate integration, with the integration limits as determined by the above restraints. Also, since the pattern is symmetric about the x-axis, the integration need be performed over the upper half of the image only and the result multiplied by 2. Accordingly,

$$I_x dx = 2\left(\frac{B_0}{2\pi}\right)\left[\int \frac{2+\cos\varphi}{x(2\cos\varphi+1)} dy + \int \frac{2-\cos\theta}{x(2\cos\theta-1)} dy\right] dx.$$

A change of variable is easily performed with the aid of the Jacobian, as follows:

$$I_x dx = \frac{B_0}{\pi}\left[\int_0^L \frac{2+\cos\varphi}{x(2\cos\varphi+1)} \cdot J\begin{vmatrix} x & y \\ x & \varphi \end{vmatrix} d\varphi + \int_{L'}^{60°} \frac{2-\cos\theta}{x(2\cos\theta-1)} \cdot J\begin{vmatrix} x & y \\ x & \theta \end{vmatrix} d\theta\right] dx,$$

$$I_x dx = \frac{B_0 dx}{\pi}\left[\int_0^L \frac{1}{2+\cos\varphi} d\varphi + \int_{L'}^{60°} \frac{1}{2-\cos\theta} d\theta\right],$$

$$I_x dx = \frac{B_0 dx}{\pi}\left\{\left[\frac{2}{\sqrt{3}} \arctan\left(\frac{1}{\sqrt{3}} \tan\frac{\varphi}{2}\right)\right]_0^L + \left[\frac{2}{\sqrt{3}} \arctan\left(\sqrt{3} \tan\frac{\theta}{2}\right)\right]_{L'}^{60°}\right\},$$

where L and L' are the upper limit of φ and the lower limit of θ respectively, as determined above.

The results of these calculations are tabulated in Table II and plotted in units of I_x/B_0 in Fig. 4.

We return now to the consideration of a slice of the image at any value y and of width dy. As before, we have

$$I dx dy = \frac{B_0}{2\pi}\left[\frac{1}{\rho_1(2\cos\varphi+1)} + \frac{1}{\rho_2(2\cos\theta-1)}\right] dx dy.$$

In addition, we have the relations

$$y = \rho_1 \sin\varphi = \rho_2 \sin\theta,$$

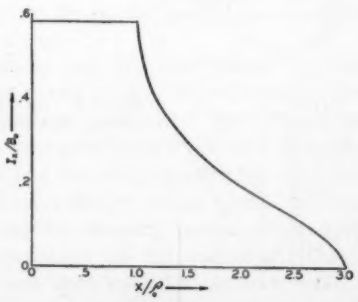

FIG. 4. Horizontal intensity distribution in the comatic image.

and the restraints, for either half of the image,

$$y \leqq \rho_0,$$
$$0 \leqq \varphi \leqq 120°,$$
$$\sin\varphi \geqq y/\rho_0,$$
$$0 \leqq \theta \leqq 60°,$$
$$\sin\theta \geqq y/\rho_0,$$

$$I dx dy = \frac{B_0}{2\pi}\left[\frac{\sin\varphi}{y(2\cos\varphi+1)} + \frac{\sin\theta}{y(2\cos\theta-1)}\right] dx dy,$$

$$I_y dy = \frac{B_0}{2\pi}\left[\int \frac{\sin\varphi}{y(2\cos\varphi+1)} dx + \int \frac{\sin\theta}{y(2\cos\theta-1)} dx\right] dy,$$

$$I_y dy = \frac{B_0 dy}{2\pi}\left[\int_{L_L}^{L_U} \frac{\sin\varphi}{y(2\cos\varphi+1)} \cdot J\begin{vmatrix} x & y \\ y & \varphi \end{vmatrix} d\varphi + \int_{L_L'}^{L_U'} \frac{\sin\theta}{y(2\cos\theta-1)} \cdot J\begin{vmatrix} x & y \\ y & \theta \end{vmatrix} d\theta\right],$$

$$I_y dy = \frac{B_0 dy}{2\pi}\left[\int_{L_L}^{L_U} \frac{d\varphi}{\sin\varphi} + \int_{L_L'}^{L_U'} \frac{d\theta}{\sin\theta}\right],$$

$$I_y dy = \frac{B_0 dy}{2\pi}\left\{\left[\ln\tan\frac{\varphi}{2}\right]_{L_L}^{L_U} + \left[\ln\tan\frac{\theta}{2}\right]_{L_L'}^{L_U'}\right\},$$

where L_U, L_L, L_U', and L_L' are the upper and lower limits of φ and the upper and lower limits of θ respectively, as determined above.

The results of these calculations are tabulated in Table III and plotted in units of $(I_y/(B_0/2\pi))$ in Fig. 5.

In the above work, only positive values of y have been considered, due to the symmetry of the image about the X-axis.

COMPARISON OF THEORY AND EXPERIMENT

In order to compare the theoretical results with the experimental data, the curves shown in Figs. 4 and 5

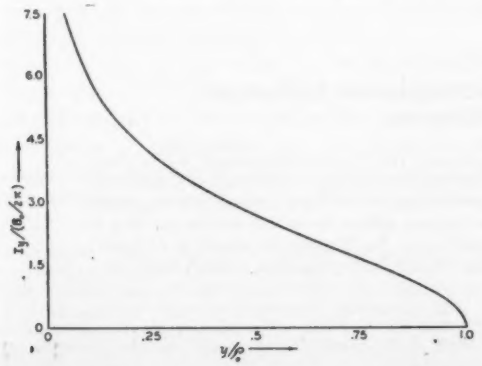

FIG. 5. Vertical intensity distribution in the comatic image.

TABLE III. Flux distribution in the Y-direction.

y/ρ_0	$L_L(°)$	$L_U(°)$	$L_L'(°)$	$L_U'(°)$	$I_y/\left(\frac{B_0}{2\pi}\right)$
0.01	0.057	120	0.057	60	15.22
0.05	2.82	120	2.82	60	7.40
0.10	5.74	120	5.74	60	5.98
0.15	8.64	120	8.64	60	5.16
0.20	11.54	120	11.54	60	4.58
0.25	14.48	120	14.48	60	4.12
0.30	17.46	120	17.46	60	3.74
0.35	20.49	120	20.49	60	3.42
0.40	23.58	120	23.58	60	3.13
0.45	26.74	120	26.74	60	2.87
0.50	30	120	30	60	2.63
0.55	33.37	120	33.37	60	2.41
0.60	36.87	120	36.87	60	2.19
0.65	40.54	120	40.54	60	1.99
0.70	44.43	120	44.43	60	1.79
0.75	48.59	120	48.59	60	1.59
0.80	53.13	120	53.13	60	1.38
0.85	58.21	120	58.21	60	1.17
0.90	64.16	115.84	60	60	0.93
0.95	71.80	108.20	60	60	0.65
0.98	78.53	101.47	60	60	0.40
1.00	90	90	60	60	0

were integrated graphically over the appropriate ranges of d for each position of the source, taking the amplitude of the chopper into consideration. An examination of the curve of Fig. 5 shows that although there is an infinity at $y=0$, it is possible to assign a fixed finite value to the curve in the range

$$0 \leqq y/\rho_0 \leqq 0.05.$$

This value is, to a close approximation, 16.8.

The quantity ρ_0 was obtained from the relation

$$\rho_0 = A\psi h_0^2.$$

The radius of the mirror, h_0, was 7.45 cm, the angle ψ was determined by the relation

$$\psi = d/F_i,$$

where F_i was 7.62 cm, and the constant A was determined empirically in the following manner.

The source was displaced a known distance from the optic axis, and photographs of the comatic image were taken by placing strips of double weight Kodabromide G-3 paper in the image plane. Since h_0 and ψ were known and ρ_0 could be measured on the photographs, the value of A was determined from the relation

$$A = \rho_0/\psi h_0^2.$$

Numerous photographs were taken at various displacements of the source, and A proved to have the value 0.206/cm.

Using this value of A, the value of ρ_0 could then be determined for any given displacement of the source.

Since both experimental and theoretical values are relative rather than absolute, an additional multiplying factor was applied to the theoretical values in order to compare them to the experimental data. This factor was

TABLE IV. Theoretical data (Cf. Table I).

Position of source (in cm)		Readings (arbitrary units)				
x	y	1	2	3	4	5
1.0	0	14.2	22.4	8.3	0.78	0
2.0	0	7.1	12.9	4.1	0.1	0
3.0	0	4.7	8.1	2.8	0	0
4.0	0	3.5	6.1	2.1	0	0
5.0	0	2.8	4.9	1.7	0	0
0	1.0	15.2	9.2	1.7	0	0
0	2.0	10.5	3.5	0.4	0	0
0	3.0	8.5	2.3	0.1	0	0
0	4.0	6.7	1.7	0.1	0	0
0	5.0	5.9	1.3	0	0	0

46 for values of I_x/B_0 and 2.5 for values of $I_y/(B_0/2\pi)$. These results are tabulated in Table IV, which is in very satisfactory agreement with Table I.

Example

It is now possible to consider actual problems of spectrometer design in the light of the above results. As a concrete example, suppose that it is desired to secure the maximum resolving power from a spectrometer, the exit slit of which is in the outer focal place of the mirror used in the above work and the detector of which is in the inner focal plane. Suppose the exit slit to have a width of 0.01 cm, and from the above data, determine (a) the optimum length of the exit slit; (b) the most satisfactory dimensions for a rectangular detector.

Let I be the intensity of radiation falling on the detector, and A be the area of the detector. The inherent detector sensitivity per watt of incident radiation is proportional to $1/A^{\frac{1}{2}}$. Therefore, the quantity $R=I/A^{\frac{1}{2}}$ will be proportional to the square of the resolving power.

It is quite obvious that R will be close to a maximum if the detector is in the shape of the image of the exit slit, ignoring aberrations. This approximation, of course, will be more accurate as the size of the exit slit is reduced. Since the reduction ratio of the mirror is 16:1, the first approximation for the optimum width of the detector will be considerably less than 0.01 cm. We shall therefore fix the width of the detector at the smallest value which can be constructed conveniently, 0.01 cm.

TABLE V. Comparison of slit lengths.

Slit length (cm)	I	A ($\times 10^{-3}$ cm^2)	R
1.0	9.77	0.0625	391
3.0	29.3	0.1875	677
5.0	48.9	0.3125	874
9.0	87.9	0.5625	1173
15.0	146	0.9375	1513

We now have to determine optimum lengths for the exit slit and the detector. We shall calculate R for various slit lengths, letting the detector length be $\frac{1}{16}$ of the slit length in each case. The value of I can be determined from Figs. 4 and 5 by graphical integration or numerical approximation, and the units remain arbitrary. This is done for various slit lengths in Table V.

It can be seen from Table V that an increase in slit length from 3 cm to 15 cm increases R by a factor of $15^{\frac{1}{2}}/\sqrt{3}=2.236$. Since the resolving power is proportional to the square root of R, the resolving power is increased by a factor of $2.236^{\frac{1}{2}}=1.50$. A 50 percent increase in resolving power would be a very poor return on the investment involved in lengthening the slit from 3 cm to 15 cm; on the other hand, a 3 cm slit has a 32 percent increase in resolving power over a 1 cm slit, and this lengthening is a comparatively cheap affair. Therefore, the slit length shall be fixed at 3 cm.

At small slit lengths, the optimum detector length will be $\frac{1}{16}$ of the slit length, so all necessary information has been obtained.

Similar calculations may be made for spheroidal or paraboloidal mirrors; the method is quite general.

In conclusion, I wish to thank John Strong for suggesting this problem and for advice.

Course at Cornell University in Techniques and Applications of the Electron Microscope

A summer laboratory course in "Techniques and Applications of the Electron Microscope" will be given from July 31 to August 12, 1950 by the Laboratory of Electron Microscopy in the Department of Engineering Physics, Cornell University, Ithaca, New York. The course is designed for those research workers, institutional and industrial, who have recently entered the field of electron microscopy or who are now planning to undertake research problems involving applications of this instrument. Further inquiries should be addressed to Professor Benjamin M. Siegel, Department of Engineering Physics, Rockefeller Hall, Cornell University, Ithaca, New York.

JOURNAL OF THE OPTICAL SOCIETY OF AMERICA VOLUME 40, NUMBER 7 JULY, 1950

The Carbon Arc as an Infra-Red Source*,†

C. S. RUPERT AND JOHN STRONG
Department of Physics, Johns Hopkins University, Baltimore, Maryland
(Received March 6, 1950)

The desirability of very high temperature sources for infra-red spectroscopy is pointed out. The crater radiation of the low intensity carbon arc is examined and recommended for practical use in this application. Details of arc mounting and use are given.

A MAJOR limitation on the performance of instruments in infra-red spectroscopy lies in inadequate monochromatic radiant power on the detector. Because of this, it is necessary to set the entrance and exit slits of the spectrometer wider than the limit determined by diffraction in the instrument, and a loss results in the attainable resolving power. A direct method of mitigating this limitation is by increasing the energy flux through spectrometers with higher temperature sources. Devotees of the Nernst glower have long sensed the advantages of a source of high temperature (around 2000°K) over the lower temperature Globar (around 1400°K), but the gain has not overbalanced the advantages of the ruggedness and long life of the Globar, with which much of the work in past years has been done.

This paper reports our examination of the use of the low intensity carbon arc, with a crater temperature of 3900°K, as a source of continuous radiation for infra-red spectroscopy.[1]

(1) The thermal radiation of a grey body is governed by the Planck law. For wave-lengths such that $\lambda T \gg 14{,}385$ micron degrees Planck's law becomes asymptotic to the Rayleigh-Jeans law, $E_\lambda \sim \lambda^{-4} T$. Thus, at these wave-lengths, the expected gain in signal-to-noise ratio by raising the source temperature is at least equal to the ratio of the higher to the lower temperature. For shorter wave-lengths the gain from a hotter source will be greater, and can be calculated from the ratio of the Planck functions for the two temperatures. These energy gains will permit narrowing of the slits and a corresponding increase in the resolving power at all wave-lengths, as long as resolving power is not otherwise limited by diffraction, aberration, etc.

As pointed out by one of us,[2] the wave number resolving power attained by an infra-red spectrometer whose performance is being limited solely by the radiant flux available is independent of wave-length in the Rayleigh-Jeans region (for a fixed dispersion and transmission efficiency). Now the actual Planck radiation is less than the predicted Rayleigh-Jeans radiation. For example, the Rayleigh-Jeans law for a given temperature predicts 28 times the Planck emission at the wave-length corresponding to the Planck maximum. This means that the wave number resolving power attainable at longer wave-lengths will be higher than that at shorter wave-lengths, if the dispersion and transmission remain the same. Therefore, a second desirable effect of increasing the source temperature is to reduce the great discrepancy between the Planck and the Rayleigh-Jeans law in the near infra-red, permitting the energy-limited resolving power in this part of the spectrum to approach more nearly that attainable in the Rayleigh-Jeans region. Thus there are strong reasons for using a source of the highest possible temperature, such as the positive crater of the carbon arc.

(2) The gain by use of a carbon arc over the conventional Globar was tested experimentally by taking sets of comparison spectra with all conditions the same except the source. The results are shown in Figs. 1–3 for three different spectral regions.

The spectra of Fig. 1 show the 2.8μ region of the atmospheric water spectrum with arc and Globar—the Globar operating at 1400°K. This comparison was made on a high dispersion prism-grating instrument using a liquid nitrogen-cooled lead telluride detector. Fig. 2 shows the comparison in the region of the atmospheric water spectrum around 6.6μ, and Fig. 3 shows the comparison in the region of the 10μ ammonia band. Figs. 2 and 3 were made on a different prism-grating spectrometer of moderate resolving power, using a Golay detector.

In the latter two figures the Globar operated at 1175°K. However, raising the temperature to 1400°K would have multiplied the Globar spectrum amplitude only by a factor of 1.5 in Fig. 2, and by a smaller factor in Fig. 3.

A summary of the experimental comparison of arc and Globar emission is given in Fig. 4 where the ratio of emissions is plotted as a function of wave-length.

The entrance and exit slits of the spectrometer may be narrowed by a factor equal to the square root of the gain in source brightness. Therefore, the greater emission of the arc permits a gain in resolving power by a factor of from 2 to 3 in the region 5–15μ where the monochromatic radiation power being received, and not diffraction or aberration, is limiting the resolving

* Preliminary report presented at the Buffalo meeting of the Optical Society of America, October, 1949.

† Supported in part by ONR Contract N5ori-166, Task Order V.

[1] A publication by other workers mentions simultaneous and independent use of the arc source for the lead sulfide spectral region. McMath, Mohler, Pierce, and Goldberg, Phys. Rev. **76**, 1533 (1949).

[2] J. Strong, J. Opt. Soc. Am. **39**, 320 (1949).

power. At shorter wave-lengths the resolving power gain will be much greater.

The peak in the experimental curve of Fig. 4, at 12.6μ, results from a deficiency in the emissivity of the Globar. This is caused by the presence of the characteristic residual-ray vibration of the SiC crystals of the Globar at this wave-length. The reflectivity of a single crystal of SiC becomes 97 percent at 12.6μ, and only the clay binder and the roughness of the Globar surface prevent its emissivity from falling even lower than Fig. 4 indicates.

(3) The carbon arc is a steady and reproducible source if properly used, and has been proposed as a radiation standard for the visible region.[3] When the arc is properly adjusted, changes in the arc current produce variations in the size but not the brightness of the crater in the visible region. Therefore, while the total radiation varies as the current varies, the brightness of the crater image focused on the spectrograph slit remains constant. To avoid variations it is only necessary to diaphragm off the light from the edge of the crater. It was presumed that the same precautions would lead to equivalent results in the infra-red spectrum.

Proper adjustment for this operation is easily obtained. The arc is likely to hiss and sputter when it is first struck and until the carbons come up to temperature, but after ten seconds or so the current can be adjusted by changing the gap length until it burns steadily and quietly without hissing. A current just below that at which hissing occurs then gives the desired performance.

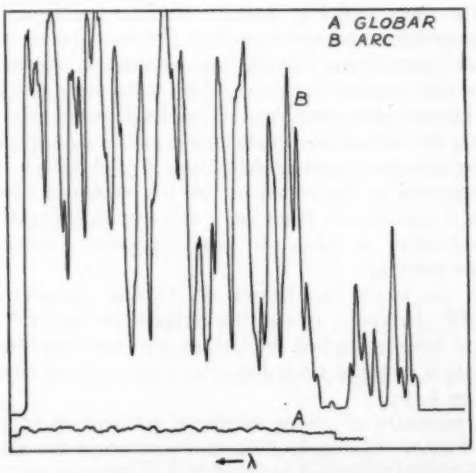

FIG. 1. Atmospheric water spectrum near 2.8μ with 1400°K. Globar and with carbon arc sources. The straight, horizontal sections of the record at the extreme right and left are the zero line with the radiation shut off. The amount of scattered light may be judged from the completely black water bands toward the right.

[3] H. G. Macpherson in *Temperature, Its Measurement and Control in Science and Industry* (Papers from a Symposium under the auspices of the American Institute of Physics) (Reinhold, New York, 1941), p. 1141.

The carbon arc operating off a 110 volt d.c. line with no regulation except a 1.8 ohm series resistance gave signals constant in time to 2 percent or better.

Calcium, strontium, and cerium cored positive carbons supplied by the National Carbon Company were tried in the region 6–12μ. They gave about the same signal as neutral-cored carbons which require less current and are more stable. Our particular apparatus uses neutral-cored projection carbons, a 12 mm diameter positive and an 8 mm negative. A current of 25 amperes with 65 volts drop across the arc gives a stable crater of about 5 mm diameter.

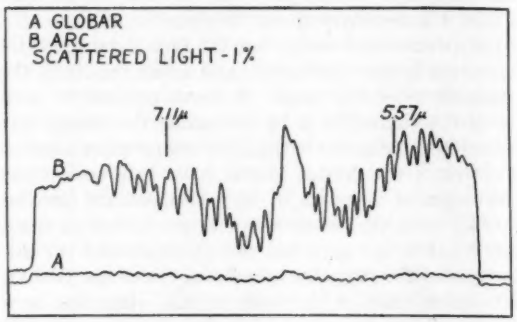

FIG. 2. Atmospheric water spectrum around 6.5μ with 1175°K. Globar and with carbon arc sources.

(4) The use of a high temperature source for long wave-lengths gives a greater amount of short wave-length radiation from which the long wave-length radiation is to be separated, so that scattered light in the spectrometer becomes relatively more important (roughly proportional to T^3).

The unwanted scattered light in the monochromatic radiations is determined by the quality of the polish on the optical surfaces which are exposed to the full arc radiations. On a small commercial monochromator with a single, well-polished, new prism of rock salt, the scattered light amounted to about 3 percent at 6μ, falling slowly to below 2 percent at 11μ. The grating instrument used in making Fig. 1, with the same monochromator in series, was relatively free from scattered light. It was less than 1 percent as determined by background at wave-lengths coincident with the most intense water lines. Scattered light in Fig. 2, using another and inferior monochromator with an NaCl prism in series with the grating spectrometer, was 1 percent.

However, when the NaCl prism of the latter instrument was replaced by a homemade KI prism for work at wave-lengths beyond 15μ, the scattered light became very serious, amounting to nearly 50 percent at 15μ. Considerable time was spent trying to secure a sufficiently good polish on this prism without success. The fine scratches left by the polishing scattered radiation to an objectionable extent even beyond the short wave-length cut-off of a silver sulfide filter.

This experience is similar to that of Smith[4] using his electrically heated carbon rod source at a temperature of 2075°K. He found that the scattered light from his KBr fore prisms was considerably greater than from NaCl.

It is necessary that the softer alkali halides be polished with very great care or by a new process in order to serve as preliminary dispersion when using an arc source. We have no doubt that some artisans can do this, but it is not easy. Here we have adopted the residual rays of MgO to eliminate unwanted higher orders for the region 13.5–25μ, as one of us has done in the past.[5] With five reflections off MgO surfaces the higher order contamination amounts to less than 1 percent even at the center of the grating blaze. Four reflections are sufficient to keep the contamination below this level when working slightly to one side of the blaze.

Enough visible light survives the five reflections to give a very faint image on the spectrometer entrance slit. In all work with the arc source we have minimized the effects of such stray radiation by constructing our radiation-chopping shutters of 1/16 inch plexiglass.

MgO is attacked by CO_2 in moist air, gathering a dull-looking coat of $MgCO_3$. This may be removed by immersing the crystals in cold HCl until all traces of effervescence cease, then rinsing and drying. It is convenient to construct crystal holders so that crystals may be removed and replaced easily and accurately without upsetting the alignment of the optical system.

(5) The arc should be operated in the laboratory in an enclosed, ventilated case to remove the waste gases, and radiation from it should be shielded from the room owing to its dangerously high ultraviolet content. The visible radiations are also intense enough to injure the eyes. In addition, the arc mounting and the arrangement by which arc radiations are made to fill the spectrometer slit and collimator must allow the fluctuating radiation from the edge of the crater to be diaphragmed out.

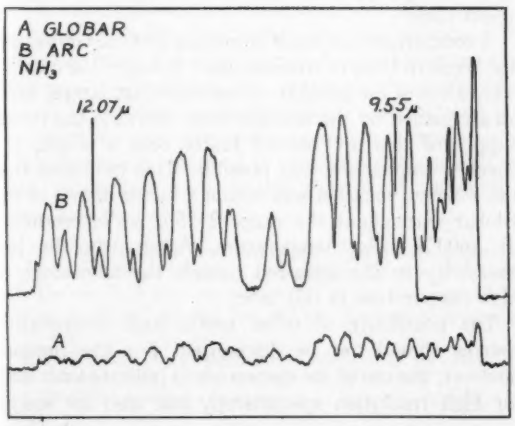

FIG. 3. Spectrum of NH_3 near 10μ with 1175°K. Globar and with carbon arc sources.

In the arrangement of Fig. 5 a Peerless low intensity motion picture projection arc has been modified for spectroscopic use. Originally, the positive and negative carbons were coaxial, with the negative carbon to the left. The negative carbon holder, together with the reflector and condensing lens, was removed and a new

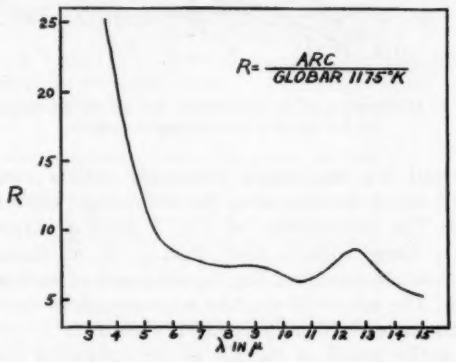

FIG. 4. The ratio R of signal obtained with a carbon arc source and with 1175°K. Globar under identical circumstances, plotted as a function of wave-length.

holder mounted on the arm A pivoted at O. A horizontal drive rod R sliding in guide G was attached to the nut that originally carried the negative carbon holder. As the positive carbon now moves to the right, R moves to the left, carrying I, whose angle can be adjusted to give the negative carbon proper advance. The drive is run in reverse to bring the carbons together, and the now unobstructed crater appears on the opposite end of the positive carbon from its former position. Radiation from the crater is focused by a spherical mirror M on the spectrometer slit S through a hole cut in the back of the case, the edges of the crater image being carefully kept off the slit. In operation the side of the arc housing, shown removed, is in place and the space between the mirror and case is enclosed by a tubular light shield. Ventilation is provided by the flue F. The obscuration due to the carbons is small and constant in amount.

This particular arrangement adapts an obsolescent arc, now available at low cost from theater supply houses, as an excellent spectroscopic source. A disadvantage is that after 2 inches of the 8-inch carbons are burned, the apparatus must be shut down briefly for resetting them (about every hour).

Naturally, any arc which permits a clear view into the positive crater and permits reasonably unobstructed focussing of the light with mirrors into a good quality image can be used for this work. If difficulties are encountered in securing a commercial machine of satisfactory dimensions for a particular spectroscopic set-up, it would not be very difficult to construct one. The only

[4] L. Smith, Rev. Sci. Inst. **13**, 54 (1942); Rev. Sci. Inst. **13**, 63 (1942).
[5] J. Strong, J. Frank. Inst. **232**, 7 (1941).

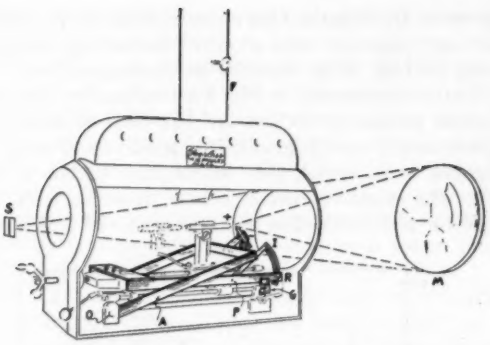

FIG. 5. Modification of an obsolescent motion picture projection arc for use as a spectrographic source.

essential is a mechanism, preferably with a variable speed motor, for advancing the two carbons uniformly.

(6) The arrangement of Fig. 5 gives a magnified crater image slightly more than 1 cm in diameter, which is adequate for filling the slit length of our instrument. The mirror *M* must be large enough so that the spectrometer collimator is filled. Failure to fill either the entire length of the slit or the collimator mirror cancels the advantages of using the high temperature source.

Meeting both these requirements with a smaller arc crater than ours and a mirror of reasonable diameter would constitute a problem. At the same time the circular shape of the crater means that most of the source area is not available for illuminating a long, narrow slit, the radiation falling to each side not being utilized. A similar problem was encountered by astronomers in getting the collected starlight in a circular star image through a spectrograph slit. Bowen[6] has solved this problem, and the same solution, with much less exacting requirements, applies here. An *image slicer* cuts up the circular crater image with an arrangement of small, plane mirrors and distributes the pieces of the image along the length of the slit.

The design of the image slicer for astronomical applications requires much more precision of construction than the simple one needed for the arc where only three or four slices are necessary.

(7) Several absorption bands complicate the spectrum with the carbon arc source in addition to the familiar atmospheric bands of H_2O and CO_2. A broad, shallow absorption extends from about 9.1μ to almost 11μ. This was originally assumed to be caused by ozone formed in the enclosed light path by the action of ultraviolet on atmospheric oxygen. However, the total absence of the strong O_3 band[7] at 4.7μ rules this out. The band has not so far been identified. It remains constant with time after the starting of the arc and is not influenced in intensity by removing our tubular light shield and allowing room air to diffuse in and out of the radiation path.

Two sharper absorptions occur at 3.42μ and 3.51μ.

The above bands are weak enough so that their only effect in most applications at low resolution is to put a few small *wrinkles* in the energy curve. It is possible that they can be eliminated by operating in an inert atmosphere. A slow, continuous flow of dry nitrogen maintained through an otherwise sealed system while in operation would provide a convenient means of realizing this, and we are now working on such a development.

CO_2 is undoubtedly present at a higher concentration than in the ordinary atmosphere but this is not readily apparent due to the strong absorption already shown by this gas in the air.

The most powerful emission in the visible and ultraviolet spectrum of the arc stream is caused by CN. The vibration frequency of this molecule in the ground electronic state is known from these spectra,[8] and corresponds to a wave-length of 4.84μ. No trace of such a band appears. This might be expected because of the high temperature of the molecule and the very short path length of the radiation through the arc stream.

(8) The low intensity carbon arc is probably the most convenient and most readily available source of high temperature radiation. The so-called high intensity carbon arc has not been investigated. Such an arc requires considerably higher current than the low intensity type, consumes electrodes much more rapidly, and lacks the self-regulating feature. On the other hand, it has been thoroughly developed for commercial use, and the very high color temperature (as much as 5800°K) is enough to arouse interest in view of the marked advantages of high temperature thermal radiation. The spectral characteristics are not known beyond about 1.2μ.[9]

A comparison was made between a 1400°K Globar and the Western Union zirconium oxide *Telcoarc*, the open air equivalent of the familiar concentrated arc lamps, using an arc loaned by the manufacturer. Because the power supply of this arc proved faulty only a single, unchecked comparison was possible. This indicated that the *Telcoarc* emission was within a factor of two of the Globar throughout the range 2–15μ, notwithstanding its 3600°K color temperature. Apparently the low emissivity in the infra-red cancels the advantage of high temperature in this case.

The possibility of other useful high temperature sources should not be discounted. For the present, however, the use of the carbon arc is indicated not only for high resolution spectroscopy but also for micro-

[6] I. S. Bowen, Astrophys. J. **88**, 113 (1938).

[7] Hettner, Pohlman, and Schumacher, Zeits. f. Physik **91**, 372 (1934).

[8] G. Herzberg, Molecular Spectra and Molecular Structure, Diatomic Molecules (Prentice-Hall, New York, 1939), p. 485.

[9] W. Finkelnberg, The High Current Carbon Arc (F.I.A.T. Final Report No. 1052-PB-81644, Department of Commerce, Washington, D. C., 1947); J. App. Phys. **20**, 468 (1949).

spectroscopy, high speed scanning of the spectrum, and any other application where the brightness of the source and not diffraction, aberration or some other factor sets the strategic limitation.

We wish to thank Mr. William Benesch for making possible the arc-Globar comparison of Fig. 1, and Dr. S. Silverman of the Johns Hopkins University Applied Physics Laboratory for his cooperation and assistance in the *Telcoarc*-Globar comparison. Acknowledgment is also due to Dave Broadhead for helpful advice.

JOURNAL OF THE OPTICAL SOCIETY OF AMERICA VOLUME 40, NUMBER 7 JULY, 1950

A Color Saturation Threshold Meter

HEINZ HABER AND HORST FLECK
USAF School of Aviation Medicine, Randolph Air Force Base, Texas

(Received December 15, 1949)

A color saturation threshold meter has been designed in which a gradually changeable mixture of white and colored light is produced. The variability of the mixture is produced by means of double refraction. A ray of white light is split into two beams; one traversing a color filter. The two rays are then reunited so that a homogeneous mixture of white and colored light is obtained. Polarization of the two rays involved permits a measurable change in the ratio of luminances of both lights between limits of zero and infinity. The instrument works satisfactorily in its present state. Yet, it could be rendered more useful by the following two devices which can easily be installed: (1) Instead of colored filters, interference filters producing an approach to spectrally homogeneous light can be installed. (2) Application of neutral density filters of proper dimensions would provide constancy of the mixture's luminance throughout the measuring range; a condition which is only approximated for a limited range in the present instrument.

IT is a well-known fact that the determination of the various thresholds of human sense organs provide almost the only means of gaining quantitative information as to their function. Insofar as color vision is concerned there are essentially two characteristic thresholds: (1) the wave-length discrimination threshold and (2) the color saturation (and desaturation) threshold. The former has been the subject of numerous determinations by various authors. However, there are very few determinations of saturation thresholds reported.[1–7] This may be partly attributed to the fact that instruments which can measure this latter threshold must be designed exclusively for this purpose. On the other hand, instruments for determination of the wave-length discrimination threshold are easily obtained by converting conventional spectroscopes or spectrographs in a comparatively simple manner.

An instrument designed to measure the threshold of color saturation and desaturation must meet the following requirements:

1. Two fields must be presented to the observer's eye, separated by a line of the utmost fineness, preferably by the edge of a prism.
2. The one field must be illuminated by light composed of a mixture of white light and colored light (preferably spectrally homogeneous). The ratio of luminance of the two component lights must be changeable between the limits $0 \leq [B_w/B_c] \leq \infty$. The combined luminance of the mixed light must be measurably changeable. The color of the chromatic component must be changeable.
3. The second half field, serving as a comparison field, must be illuminated by white light (illuminant A, C, or D). The luminance of this light must be measurably changeable.

Various suggestions and solutions concerning these requirements have been reported in the literature. Necessitated by the work on color vision conducted in this institute, a color saturation threshold meter has been designed and constructed. The performance of this instrument is satisfactory and a brief description of this instrument is presented. See Fig. 1.

Light is emitted by a light source S_1, traverses the lens L_1 and a daylight filter F_1 to form Part I of the light path. A Nicol prism N, mounted in a pitch circle is then traversed by the light which is thus rendered plane polarized. A lamp S_2 and a telescope T with a prism P_7 attached to it, permit readings of the pitch circle's position to 2 minutes of arc by means of a vernier. The light now enters a natural calcite crystal C_1. According to the laws of double refraction the incident light gives rise to an ordinary and an extraordinary beam forming two images I_1 and I_2 of the filament of S_1 in the image plane of the lens at F_c. The two images are not formed in exactly the same plane due to the difference of refractive indices for the ordinary and the extraordinary rays within the calcite crystal. This difference, however, is negligible. The lateral distance between the two images amounts to 6 mm. The rays forming the image I_1 propagate further

[1] S. V. Kravkov, Acta Ophthalm. Kobenhavn **17**, 89 (1939).
[2] H. Meister, Zeits. f. Sinnesphysiol. **65**, 217 (1934).
[3] J. G. Priest and F. L. Brickwedde, J. Opt. Soc. Am. **28**, 133 (1938).
[4] W. F. Grether, J. Exper. Psychol. **28**, 419 (1941).
[5] A. Chapanis, J. Exper. Psychol. **34**, 24 (1944).
[6] C. H. Graham and N. R. Bartlett, J. Exper. Psychol. **24**, 574 (1939).
[7] W. D. Wright, *Researches on Normal and Defective Color Vision* (C. V. Mosby Company, St. Louis, Missouri, 1947), p. 161.

unobstructed, while the rays of image I_2 traverse a color filter F_c which can be exchanged at will. The rays of the images then are united again by means of a second calcite crystal C_2 of similar dimensions as C_1. The reunited light falls upon a ground glass G_1 which serves as an illuminant for the one half of a Pulfrich photometer head consisting of conventional elements (Fresnel rhomboid prisms P_3 and P_4, a flat roof prism to produce the field division, circular diaphragm D_3 and Ocular O). The eye of the observer is located at E. The total amount of light entering the right-half field of the photometer head can be measurably controlled by means of a cats-eye diaphragm D_1 (J. G. Koehler, prior to 1800).[8]

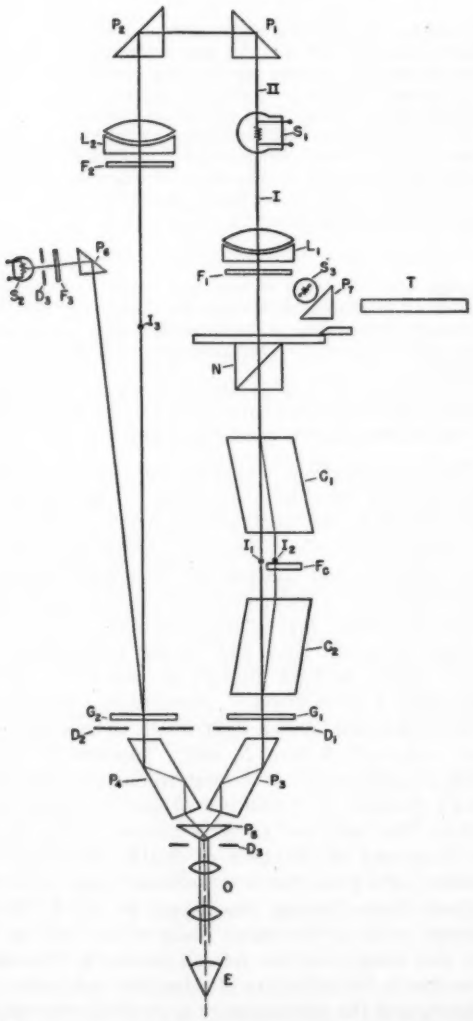

FIG. 1. Functional sketch of the color saturation threshold meter.

[8] C. F. K. Graff, *Grundriss der Astrophysik* (B. G. Teubner, Leipzig, Berlin, 1928), p. 221.

In accordance with the preceding description of the design, the effects of rotation of the Nicol prism N can be easily predicted. There will be a change in the luminance of the two images I_1 and I_2 which can be expressed by means of the laws of polarization associated with the phenomenon of double refraction. One has:

$$R=\cos^2\varphi/T_c\cdot\sin^2\varphi=(1/T_c)\cdot\cot^2\varphi, \qquad (1)$$

where R indicates the ratio of the white light and the colored light, T_c represents the transmittance of the various color filters used, and φ is the position angle of the Nicol which is read on the pitch circle after proper adjustment of the former. The total illuminance of the reunited rays behind the second calcite crystal C_2 illuminating the semicircle of the field of view varies as:

$$B=c\cdot[\cos^2\varphi+T_c\cdot\sin^2\varphi], \qquad (2)$$

where c is a constant characterizing the light source L_1 and the combined absorptive properties of the daylight filter F_1, the lenses and prisms transmitted. The conditions 1 and 2, as outlined in the introduction, are fulfilled.

Part *II* of the light path leads through two totally reflecting prisms P_1 and P_2 and traverses the daylight filter F_2. The lens L_2 forms an image of the filament at the point I_3 and is adjusted so that the diverging rays behind the image form a light patch on the ground glass G_2 about equal in size and luminance to that produced on the ground glass G_1. G_2 equally serves as an illuminant for the second half of the photometer head after having passed the cats-eye diaphragm D_2 controlling measurably the luminance of Part *II* of the field.

In contrast to the light path *II*, light of the polarizing side of the instrument must traverse a total length of more than 120 mm through natural $CaCO_3$ crystals. Due to minute impurities of the otherwise flawless crystals a slight yellowish tint of the emerging light is noticeable when closely opposed to the pure daylight in the field of view of the instrument. In order to render both half-fields undistinguishably equal, another light source S_2 has been attached to the instrument. Light from this source passes a slit D_3 (controlling the luminous flux of the ray) and an amber filter F_3. A prism P_6 throws the light upon the ground glass G_2. Manipulating the slit D_3 allows addition of proper amounts of yellowish light to the daylight emerging from the filter F_2 to match the crystal absorption. Condition 3 of the introduction is also fulfilled.

Two modifications in the design which would render the instrument useful for various other measurements may be discussed:

1. The color filters used do not transmit energy of a single wave-length, but a rather broad wave-length band. Thus, in the position of the Nicol characterized by $\varphi=90°$, the light produced does not exhibit a purity of 1. A set of interference filters with sufficiently small half-widths, however, could overcome this difficulty to a sufficient extent and render the instrument usable

for measurements of color desaturation thresholds starting with pure spectrum colors. At present, the instrument is used only for determinations of perception of colored light added to white light.

2. Equation (2) shows that the total luminance B of the light mixture is a function of the angle φ. It would be rendered constant by insertion of a neutral density filter at the image I_1 between the calcite crystals; the luminous transmittances of such filters, evaluated according to the sensitivity of the cones, must match the ones of the respective color filters F_c. This would multiply the term $\cos^2\varphi$ in (2) by T_c and yield $B=c\cdot T_c=$constant. A more powerful light source and procurement of neutral density filters of proper transmittance would achieve constancy of the light illuminating the test field for a considerable group of observers not having a protan deficiency. The instrument is used in the range between $\varphi=0°$ and $\varphi=25°$ exclusively making it permissable to disregard the variation of B within certain limits, since the function $\cos^2\varphi$ changes slowly in this range.

Photometric characteristics: S_1: Mazda Lamp 75 w, 10 v; S_2: Mazda Lamp 32 w, 16 v; luminance of the field of view with $\varphi=0°$: 8.64 millilamberts.

The light output of the polarizing side of the instrument has been measured by means of a filter photo-cell combination designed by Dresler,[9] adapted to the sensitivity of the cones. Three series of measurements were made through the range $\varphi=0°$ to $\varphi=90°$ in steps of $\Delta\varphi=5°$.

1. Total output without filter F_c; represented by $B=c\cdot[\cos^2\varphi+\sin^2\varphi]$.
2. Output with image I_2 blacked out; represented by $B=c\cdot\cos^2\varphi$.
3. Output with image I_1 blacked out; represented by $B=c\cdot\sin^2\varphi$.

The results are in agreement with the theoretical values well within the limits of the measuring errors. These amount to about 3 percent, almost entirely attributable to changes in the voltage of the city supply lines feeding the light source S_1. This is to be corrected by use of batteries.

The perception threshold of color added to white light usually is expressed in terms of luminance purity, p_B:

$$p_B=B_c/[B_w+B_c], \tag{3}$$

in which B_w and B_c are the luminances of the white and the colored light, respectively. From the design of the instrument the following expression for p_B holds:

$$p_B=T_c\cdot\sin^2\varphi/[\cos^2\varphi+T_c\cdot\sin^2\varphi]. \tag{4}$$

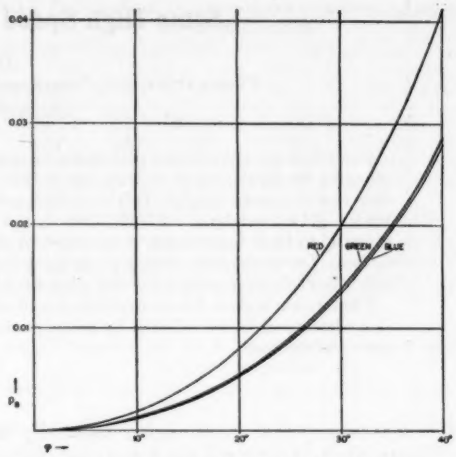

FIG. 2. The quantity $p_B=B_c/[B_w+B_c]$ (with B_w and B_c as the luminances of the white and the colored light, respectively) as a function of the angle indicating the position of the Nicol prism.

Figure 2 shows a graph giving p_B as a function of φ for three different color filters; the respective transmittances are: $T_{red}=0.061$, $T_{green}=0.042$, and $T_{blue}=0.041$.

We are indebted to Ingeborg Schmidt, Department of Ophthalmology of the School of Aviation Medicine, Randolph Air Force Base, Texas, for having collected the pertinent references and having carried out the measurements described.

[9] A. Dresler, Licht 3, 41 (1933).

Some High Speed Spectrograph Objectives

D. H. RANK
Physics Department, Pennsylvania State College, State College, Pennsylvania
(Received March 27, 1950)

Conditions are given for the performance requirements for a high speed spectrograph objective to be used primarily for the Raman effect in the region 4358 to 5000A. A formula is given for the construction of such an objective at a speed of $f/2.0$. This objective has a flat tangential field and gives extremely sharp definition. With slight retouching of the back of the second flint component perfection of definition can be achieved in lenses up to 12 in. focal length. A correction to the formula is given to render the field flat with all spherical surfaces. The unretouched system works perfectly satisfactorily up to an 8 in. focal length. The trignometrically calculated aberration curves are given for a lens of 10 in. focal length.

The formula is given for construction of a 10 in. focal length $f/3.5$ three element lens. The design consists of a telescope objective followed by an aplanatic element. Aberration and performance characteristics are given and discussed.

THE spectroscopy of weak light, especially the Raman effect, is rendered much more satisfactory if spectrographs of relatively good resolution at high photographic speed are available. For depolarization work it is frequently desirable to have a photographic speed of $f/2.0$ or greater. In many cases a dispersion of as low as 50A per mm at λ4600A is quite adequate for these spectra if the resolution of the camera is equal to or greater than the resolution of Type 1 photographic plates.

In this laboratory for the past few years we have been using two types of special high speed spectrograph objectives with very satisfactory results. These objectives are corrected for the region 4358 to 5000A. Spectrograph objectives ideally must fulfill a somewhat different set of conditions than those conditions usually set for high quality photographic objectives. The necessary conditions that this particular type of spectrograph objective should fulfill can be summarized as follows. 1. Extremely good definition over a field of about 5°. 2. Field should be flat, perpendicular to the optic axis, or only slightly tilted. It is in general only necessary to have the field flat for tangential monochromatic images. 3. The correction for spherical aberration and coma should approach "telescopic" perfection.

It can be seen that the above mentioned conditions are considerably easier to achieve than those corrections which are necessary for a high resolution photographic objective of the usual type. The correction for lateral chromatic aberration and astigmatism is of little or no consequence in these spectrograph objectives. (It is only necessary to produce monochromatic line images of a line object, i.e., line for line imagery rather than the usual photographic point for point imagery.) However, it is most desirable that no compromise can be tolerated with regard to soft definition, i.e., the spherical aberration and coma must be corrected as well as possible.

The general design and performance characteristics of two types of spectrograph objectives will be described in this paper. One of these objectives has a speed of $f/2.0$ and fulfills all three of the conditions mentioned above. The second type of lens which we shall call a "spectroaplanat" has a speed of $f/3.5$ and is of very simple design. This type of objective does not strictly fulfill condition 2 above but has proved to be very useful in practical performance.

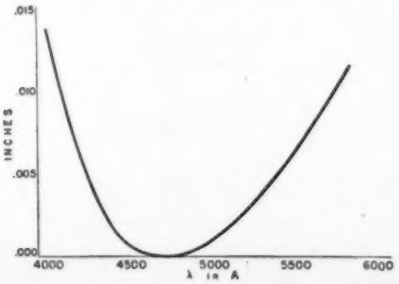

FIG. 1. Color curve of $f/2.0$ objective E.F.L. = 10.000 in.

F/2.0 OBJECTIVE

It is well known to optical engineers that in closely spaced multi-doublet systems minimum zonal spherical aberration is obtained when the powers of the doublets are approximately equal. The nearest approach to an analytic proof of this proposition that the author has knowledge of is a proof by Fulcher[1] which demonstrates the following. A compound telescope objective constructed of four thin minimum aberration lenses having the same index of refraction will have minimum spherical aberration if the powers of the thin lenses are equal.

Two closely spaced cemented achromatic doublets of equal power can be chosen so that strict correction of the rim zone for spherical aberration at $f/2.0$ is achieved. It is, of course, possible simultaneously to fulfill the optical sine condition. The field of such an objective can be rendered completely flat for tangential images by the use of a field flattener of suitable design, placed near the focal plane. Of course, it is necessary to include the field flattener in the computations for correction of spherical aberration (S.A.) and offense against the sine condition

[1] G. S. Fulcher, J. Opt. Soc. Am. 37, 49 (1947).

(O.S.C.) since the aberrations contributed by this lens are not negligible at $f/2.0$. The residual zonal spherical aberration in this system will just about equal the Rayleigh limit for zonal aberration for a 5 in. focal length.

In the particular lens which the author is describing, achromatization between 4047 and 5890A was used. The chromatic aberration curve is shown in Fig. 1 for a lens of 10 in. equivalent focal length. The variation of the spherical aberration with wave-length of the rim zone of this lens is shown in Fig. 2. Curve S.A. ordinates are given at left of figure in inches. In Fig. 2 Curve ΔE.F.L. shows the variation of the difference of the rim E.F.L. minus the paraxial E.F.L. as a function of wave-length. This curve is, of course, a measure of the completeness of fulfillment of the optical sine condition. Ordinates for curve labeled ΔE.F.L. are given to the right of the figure in inches.

The range of wave-lengths over which this lens is designed to be used is roughly from 4300 to 5000A. It can be seen from Fig. 1 that this region of wave-lengths is in the flat minimum of the chromatic aberration curve. From Fig. 2 it can be seen that correction for S.A. and O.S.C. are simultaneously achieved at approximately 4425A.

Table I gives the optical prescription for this $f/2.0$ lens for a 10 in. E.F.L. In Fig. 5 a drawing of the axial section of this lens is shown. Figure 3, curve marked T.F. shows the curvature of field obtained from ray tracing for the 0.7 zone for tangential monochromatic images. It can be seen that curvature of field (convex toward objective) has been over-corrected in this design. The curve in Fig. 3 marked S.A. shows the variation of S.A. with wave-length (off axis S.A.) as determined by ray tracing for the 0.7 zone. (Off axis S.A. difference of focus for intersection of upper and lower rim ray and principal and close principal ray). The angular distribution of wave-lengths assumed in these calculations is as follows. λ4680A is on the optical axis. The dispersing device a 15,000 lines per in. diffraction grating used in the second order at an angle of incidence of about 30°. λ4680 is approximately on the normal of the grating.

The choice of the 0.7 zone for the focus is dictated by experience. It can be seen from Fig. 4 that this choice is reasonable. Figure 4 shows axial S.A. for various zones for λ4861. The S.A. is plotted against $(h/h \text{ max.})^2$ which immediately shows that the mean focus is in the neighborhood of the 0.7 zone, since the abscissae are proportional to the intensity contributions from each zone. h and h max. are the respective heights of the zone in question and the rim zone.

If this type of lens is to be used with all spherical surfaces the prescription given in Table I should be changed to $R_7 = -1.266$. This change will render the field strictly flat and tilted from the perpendicular by 45 min. of arc. The red end, of course, comes to a focus slightly shorter than the violet due to increase of spherical aberration with increase of wave-length. With regard to off axis aberrations the ray tracing shows that at the edge of the field the coma patch reaches a maximum size of 0.0008 in. for a 10 in. E.F.L. lens.

This objective was designed as part of a large grating

TABLE I. Formula for $f/2.0$ spectrograph objectives. All dimensions are given in inches.

Lens	Glass	Nd	d	R_1	R_2	Axial air space
1	*BSC*-2	1.517	0.818	+8.639	−11.109	
	EDF-1	1.649	0.327	−11.109	−111.448	0.409
2	*BSC*-2	1.517	0.818	+6.410	−20.105	
	EDF-1	1.649	0.327	−20.105	+27.237	8.031
3	*BSC*-2	1.517	0.049	*−1.160	∞	
	E.F.L. = 10.000			B.F.L. = 0.050	For λ4358	

* $R_7 = -1.266$ will render the field flat with all spherical surfaces. The field will then be tilted towards the objective in the red end of the spectrum making an angle of 45 min. of arc inclined to the perpendicular to the optical axis.

TABLE II. Formula for $f/3.5$ "Spectroaplanat." All dimensions are given in inches.

Lens	Glass	Nd	d	R_1	R_2	Axial air space
1	*BSC*-2	1.517	0.496	+9.313	−6.335	
	EDF-1	1.649	0.244	−6.335	−20.751	0.585
2	*BSC*-2	1.517	0.603	+5.682	+8.811	
	E.F.L. = 10.000			B.F.L. = 8.782	For λ4358	

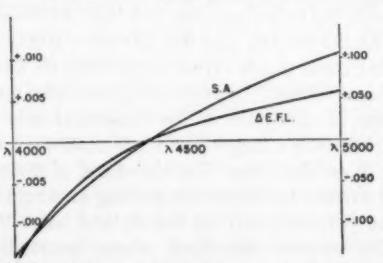

FIG. 2. Chromatic variation of axial aberrations of $f/2.0$ objective E.F.L. = 10.000 in. Curve marked S.A. refers to ordinates on left of figure and is for rim zone. Curve marked ΔE.F.L. represents difference in E.F.L. of rim and paraxial zones. Ordinates for this curve given on right of figure. All aberrations given in inches.

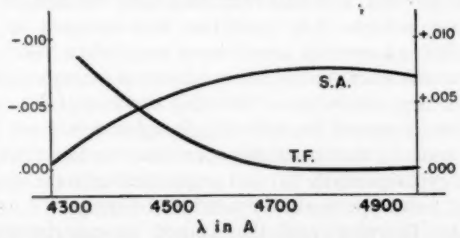

FIG. 3. T.F. field curvature determined trignometrically for 0.7 zone of 10.000 E.F.L. $f/2.0$ lens. Ordinates for this curve given at left of figure. S.A. off axis spherical aberration for 0.7 zone. Ordinates for this curve given at right of figure. Aberrations given in inches. The T.F. curve represents the relative departure of the focii for the various wave-lengths for the 0.7 zone from an arbitrarily chosen plane. The field angles for the various wave-lengths are dictated by the dispersing device i.e., grating which is described in detail in the text. λ4680 is on the optical axis of the lens.

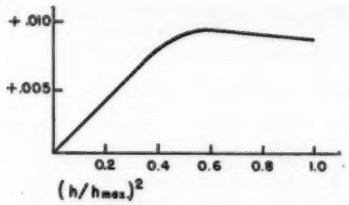

FIG. 4. Axial zonal spherical aberration for λ4861 for 10 in. E.F.L. $f/2.0$ lens. Aberrations in inches. Abscissae $(h/h \text{ max.})^2$

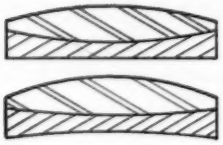

FIG. 5. Drawing of the axial section of the $f/2.0$ spectrograph objective described in Table I.

spectrograph being constructed for the Chemical Department, E. I. du Pont de Nemours & Co., Wilmington, Delaware, in cooperation with J. R. Downing. The lens was manufactured in a 12 in. focal length by Perkin and Elmer Corporation in accordance with the formula given in Table I.

It is well known that lenses of large aperture must be retouched after manufacture if conformance with design is required. In this case it was also proposed to remove the residual zonal spherical aberration in the retouching process. The 12 in. lens was retouched using the Foucault test. A cobalt blue glass filter was used in the testing process. S.A. correction was achieved in this fashion at somewhat longer wave-length than λ4425 and since this filter passes a broad band of wave-lengths a good compromise was achieved in removal of S.A. over the major part of the wave-length region of interest. The net result of the retouching operation was to render the field experimentally flat and perpendicular to the optical axis, a consequence anticipated in the design.

Dr. Downing and the author in experimentally focusing this camera were able to reach easily the limit of resolution set by grain size of Type 1 plates. Visual examination of images produced showed that the resolution of the camera greatly exceeded the limit set by the plates. (It should be noted that it is considerably more economical, if exposure time is the criterion of performance, to increase the focal length of the camera rather than to use fine grain plates to obtain more resolution.)

From the design data, and as a result of experience, it has been found that this design performs satisfactorily with spherical surfaces (no retouching) up to a focal length of 8 in. However, in this case it is necessary to give the plate the slight tilt required by the design.

F/3.5 SPECTROAPLANAT

This lens is of extremely simple design. It consists of a telescope objective followed by an aplanatic element.

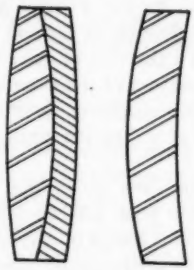

FIG. 6. Drawing of the axial section of the $f/3.5$ "spectroaplanat" described in Table II.

This type of construction allows complete correction for spherical aberration and the optical sine condition at the above mentioned speed with a three element lens, i.e., an achromatic cemented doublet followed by an aplanatic element. Since the aplanatic element is simple, the achromatization is not complete requiring the field to be tilted to focus the monochromatic tangential images. In addition, this lens suffers from the usual curvature of field which cannot be corrected very satisfactorily with a field flattener near the focal plane because of the very considerable tilt of the field.

The formula for the construction of this type of spectroaplanat is given in Table II. Figure 6 shows an axial section for this lens. In this laboratory we have been using this type of objective on a three-prism glass spectrograph with considerable satisfaction. The spectrograph consists of three 60° prisms of *DF*-2, $Nd = 1.617$ set for minimum deviation at about λ4650A. This wavelength is on the optical axis of the lens. The entrance pupil is 2.60 in. from the objective. Trignometrical ray tracing shows that the spherical aberration for the 0.7 zone yields the following data. S.A. for $\lambda 4358 = +0.0021$, in. for $\lambda 4650 = 0.000$, and for $\lambda 5000 = -0.0008$ in. The size of the coma patch varies from 0.0002 in. at λ4358 to 0.0015 in. at λ5000. The ray tracing data also shows that the radius of curvature of the tangential field is about 2.75 in., which is a larger curvature than one would like to have in an ideal case. The violet end of the spectrum is tilted toward the objective making an angle of 2° 57′ with the perpendicular to the optical axis. With the dispersing system described above decidedly satisfactory definition can be obtained with this objective from λ4358 to λ5000A on a flat plate.

The author is indebted to George Arnold for his assistance with much of the computation involved in the design of the $f/2.0$ objective.

JOURNAL OF THE OPTICAL SOCIETY OF AMERICA VOLUME 40, NUMBER 7 JULY, 1950

Propagation of Electromagnetic Waves through a Stratified Medium. I

BERNARD SALZBERG
Naval Research Laboratory, Washington, D. C.
(Received January 16, 1950)

A general analysis of the propagation of electromagnetic waves through a stratified medium, applicable to the entire class of problems of plane multilayer systems, is developed. The medium is assumed to be divided into m plane-parallel layers, the first and mth of which are semi-infinite. The electromagnetic properties of the m layers are unrestricted and dissimilar, and the thicknesses of the $(m-2)$ finite layers are also different in general. A steady-state monochromatic wave, generated in the mth layer, is assumed to be incident at any angle upon the $(m-1)$th layer. Formulas for the resulting reflection and transmission are derived. The methods which are employed in the paper facilitate application of these formulas, with a minimum of algebraic complications, to specific problems.

INTRODUCTION

DURING the past decade multilayer systems of films have been utilized to an increasing extent for such important technological purposes as the reduction of reflection from glass, and the development of new and improved optical filters. The precise measurement of thickness, by optical means, of semitransparent films on backing plates is also, for example, a problem in which multilayer systems are involved. The essential behavior and characteristics of all such multilayer systems can be analyzed in a comprehensive manner, as one generic problem, starting from Maxwell's equations. In fact, a general treatment of multilayer systems may be said to have been provided by Lord Rayleigh almost forty years ago,[1] in a paper entitled "On the propagation of waves through a stratified medium, with special reference to the question of reflection." In that paper the analysis is developed specifically in terms of the propagation of acoustic waves, but as the author remarks, extension to electromagnetic waves and generalization with respect to complex layer properties is straightforward, although perhaps not obvious. Rayleigh did not develop detailed formulas for reflection and transmission in the general case; he merely indicated how such formulas could be arrived at, and remarked that the algebra was rather involved, thereafter passing on to some special cases in which he was interested. In recent years several treatments of the electromagnetic situation have been presented,[2] from different points of view and with varying degrees of completeness. Generally speaking, however, in these papers physical content has been neglected in favor of mathematical treatment. Furthermore, while various detailed formulas for reflection and transmission have been derived, scant attention has been devoted to mitigating the algebraic complications which arise in applying these formulas to specific problems.

In the present paper, which takes its title from that of Rayleigh's, a general analysis of plane multilayer systems is provided. By taking advantage of the considerable effort devoted for the past few decades to solution of allied problems in other branches of physics, notably in electrical communications, it is possible to deal with the subject in a manner which does not suffer from the defects and gaps of the above-mentioned treatments. The general methods and results presented here have been found useful for some years in analysis and solution of a variety of optical and allied radio problems. For example, they have served as a basis for analysis of two-layer[3] and three-layer[4] low reflecting films on glass. The use of these general methods and results will be illustrated further in Part II by applying them to obtain detailed reflection and transmission characteristics of several specific multilayer systems.

ANALYSIS

The medium is assumed to be divided into m consecutively numbered plane-parallel layers of infinite area, the first and mth of which are semi-infinite in thickness. Each of the layers is uniform and isotropic, but the electromagnetic properties of the m layers are unrestricted and in general dissimilar, as are also the thicknesses of the $(m-2)$ finite layers. A steady-state monochromatic wave generated in the mth layer is assumed to be incident at any angle upon the $(m-1)$th layer. This wave is assumed to be linearly polarized, with either its electric or magnetic vector perpendicular to the plane of incidence (see Fig. 1). As is known, a solution of any more general situation can be obtained by superposing solutions of these two primitive cases.[5] Since the layers are dissimilar, a reflected wave is also present in the mth layer. Similarly, a transmitted wave and a reflected wave are present in each of the finite layers. In the final layer only a transmitted wave is present; because this layer extends to infinity, no reflection occurs. The amplitudes of the electric and magnetic vectors of these waves vary with time as $\exp(i\omega t)$, where $i=(-1)^{\frac{1}{2}}$, ω is the angular frequency of

[1] Lord Rayleigh, Proc. Roy. Soc. **A86**, 207 (1912). This paper also appears in Lord Rayleigh's *Scientific Papers* (Cambridge University Press, Cambridge, 1920), Vol. VI, p. 71.
[2] A. W. Crook, J. Opt. Soc. Am. **38**, 954 (1948).
[3] P. King and L. B. Lockhart, J. Opt. Soc. Am. **36**, 513 (1946).
[4] L. B. Lockhart and P. King, J. Opt. Soc. Am. **37**, 689 (1947).
[5] S. A. Schelkunoff, *Electromagnetic Waves* (D. Van Nostrand Company, Inc., New York, 1943). This text is recommended for any necessary collateral reading.

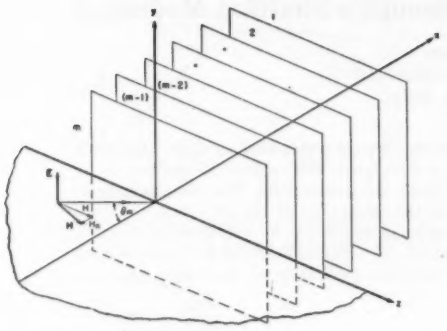

FIG. 1. The boundary planes of the m layers are parallel to the y–z plane. The normal to the incident plane wave, making an angle θ_m with the x-axis, is in the x–z plane, which is the plane of incidence. The situation depicted here corresponds to the case for which the electric vector is perpendicular to the plane of incidence and the magnetic vector has both normal and tangential components.

the source, and t is the time. The essential problem is to provide a quantitative description of the propagation of these waves in the layers of the stratified medium, and in particular to determine the reflection and transmission at the interface between mth and $(m-1)$th layers, and the transmission through the final interface. These quantities must be expressed in terms of the thicknesses and electromagnetic properties of the m layers and the state of polarization and angle of incidence of the wave which is incident upon the $(m-1)$th layer.

Electromagnetic Properties of the Layers

Each of the layers can be characterized electromagnetically by two complex parameters: (1) the propagation constant, P, which is proportional to the complex index of refraction, or to the square root of the product of complex dielectric constant and complex permeability, and (2) the characteristic admittance, A, for which there is no corresponding optical term, and which is equal to the square root of the ratio of complex dielectric constant to complex permeability. Explicit expressions for these parameters are:

$$P=(i\omega/c_0)[(\epsilon-i\epsilon')(\mu-i\mu')]^{\frac{1}{2}}$$
$$=[(\sigma+i\omega\epsilon\epsilon_0)(\rho+i\omega\mu\mu_0)]^{\frac{1}{2}} \quad (1)$$
$$A=A_0[(\epsilon-i\epsilon')/(\mu-i\mu')]^{\frac{1}{2}}$$
$$=[(\sigma+i\omega\epsilon\epsilon_0)/(\rho+i\omega\mu\mu_0)]^{\frac{1}{2}}.$$

In Eqs. (1), ϵ and ϵ' are the real and imaginary parts of the complex relative dielectric constant, μ and μ' are the real and imaginary parts of the complex relative permeability, ϵ_0 and μ_0 are the permittivity and permeability of free space, σ is the electric conductivity, and ρ is the magnetic conductivity, a term introduced by Heaviside many years ago[6] to make the curl relations more symmetrical. In recent years it has been necessary to make use of this once-fictitious term ρ, or the corresponding term μ', to account for energy loss of a magnetic type. The units used are those of the M.K.S. system, in which the velocity of wave propagation in free space is $c_0=(\epsilon_0\mu_0)^{-\frac{1}{2}}\cong 3\times 10^8$ meters/second, and the characteristic admittance of free space is $A_0=(\epsilon_0/\mu_0)^{\frac{1}{2}}\cong 2.65\times 10^{-3}$ ampere/volt. Since P and A are square roots of complex quantities, a choice of sign must be made for these parameters. The choice made here is that the real part of P, and therefore also the real part of A, is positive. Consequently $\exp(-Ps)$ is interpreted as the representation of a wave which decreases in amplitude along the positive s direction.

[6] O. Heaviside, *Electromagnetic Theory* (Electrician, London, 1894), Vol. I, Chapter II.

Waves in the Layers

The transmitted and reflected wave normals in each layer lie in the x–z plane, making angles θ and $-\theta$, respectively, with the x axis. The waves are propagated in accordance with the function $\exp(i\omega t-Ps)$, and the ratio of amplitudes of their magnetic to electric vectors is A, where P and A are given by Eqs. (1), and s is distance measured along the wave normals. In terms of components along x and z axes, these distances are $s=\pm x\cos\theta+z\sin\theta$, so that the corresponding propagation functions for transmitted and reflected waves are $\exp(i\omega t\mp px-qz)$, where $p=P\cos\theta$ and $q=P\sin\theta$. The factor $\exp(-qz)$ is, in general, complex; it therefore represents a combined amplitude and phase variation in the z direction. To satisfy the requirements of continuity at the layer boundary planes, the z-component, q, of the propagation constant must have the same value for waves in all layers. This observation can be used to derive, directly, expressions for the angle θ and for the x-component, p, of the propagation constant in each layer. If the subscripts k and m denote kth and mth layers, these expressions are

$$\sin\theta_k=(P_m/P_k)\sin\theta_m$$
$$p_k=P_k[1-(P_m/P_k)^2\sin^2\theta_m]^{\frac{1}{2}}. \quad (2)$$

The real part of p_k is taken positive; it gives an exponential attenuation, in the x direction, for waves in the kth layer. It will be observed, from the first of Eqs. (2), that θ_k is, in general, complex. This means that the waves are, in general, non-uniform, the equiamplitude and equiphase planes of the waves being non-coincident. These planes can be determined by equating to constants the real and imaginary parts of the propagation functions. If *Re* denotes *real part of* and *Im* denotes *imaginary part of*, the angles between x axis and the normals to equiamplitude and equiphase planes are given by $\tan\theta'=Re(q)/Re(p)$ and $\tan\theta''=Im(q)/Im(p)$, respectively. When θ_k is real, $\theta'=\theta''=\theta_k$. This means that the equiamplitude and equiphase planes coincide, forming a uniform plane wave whose normal makes an angle θ_k with the x axis. In the special case of perpendicular incidence, for which $\theta_m=0$, this is always true, regardless of the layer properties. On the other hand, when θ_m is not zero, θ_k may be complex even for non-

absorbing layers, and the waves will be non-uniform. This is what occurs, for example, when total reflection takes place at the boundary between two lossless materials; although incident and reflected waves are uniform, the transmitted wave in this case is non-uniform. Similar considerations indicate that when a uniform wave is transmitted at oblique incidence from a lossless layer to a lossy layer, a non-uniform wave is always set up in the lossy layer. It will now be apparent that the waves in the various layers—including the mth, which contains the source—need not be uniform in general. When the waves are non-uniform θ is complex, and the phrase "angle of incidence" must be discarded or replaced by more explicit information with respect to the angles between x axis and the normals to equiamplitude and equiphase planes.

The waves in each layer are propagated along the s direction with phase velocity

$$v=\omega[1/Im^2(p)+1/Im^2(q)]^{\frac{1}{2}},$$

the corresponding x- and z-components of the phase velocity being $v'=\omega/Im(p)$ and $v''=\omega/Im(q)$.

When the electric vector in the incident wave is perpendicular to the plane of incidence, as shown in Fig. 1, the electric vector, E, in each layer is tangential to the layer boundary planes; and the magnetic vector has two components, one of which, H, is tangential, and the other, H_n, normal to the layer boundary planes. The components H and H_n are given by $-(PH/A)=\partial E/\partial x$ and $-(H_n/E)=A\sin\theta$. When the magnetic vector in the incident wave is perpendicular to the plane of incidence, the magnetic vector in each layer is tangential to the layers; in this case the electric vector has a tangential component, E, and a normal component, E_n. The connections between the magnetic vector and the two components of the electric vector are given by $PAE=\partial H/\partial x$ and $(H/E_n)=A/\sin\theta$.

In both of the two primitive cases, all components of the electric and magnetic vectors in each layer can be regarded as consisting of a transmitted wave, propagated along the positive x axis, and a reflected wave, propagated in the opposite direction. In all layers, these waves have identical amplitude and phase variations along the z axis. Since only tangential components of the electric and magnetic vectors are directly involved in energy flow across the layer boundaries, no further explicit consideration need be given to the normal components. Wave equations for the tangential components, applicable to each layer, are

$$\begin{aligned} E&=E_t\exp(x_0-x)p+E_r\exp(x-x_0)p \\ H&=H_t\exp(x_0-x)p-H_r\exp(x-x_0)p. \end{aligned} \tag{3}$$

In Eqs. (3), E_t and E_r are the transmitted and reflected amplitudes of the tangential component, E, of the electric vector; and H_t and H_r are the corresponding amplitudes of the tangential component, H, of the magnetic vector. Each of these quantities contains the common factor $\exp(i\omega t)$, and the amplitudes on the right side of both expressions contain, also, the factor $\exp(-qz)$. For the case in which the magnetic vector is perpendicular to the plane of incidence, H is to be taken as negative. In each layer except the mth, the distance x is measured from an origin, x_0, which is assumed to be the intersection of the x axis with the left boundary plane of the layer. For the mth layer, the origin is the same as for the $(m-1)$th layer. The parameter p is given by the second of Eqs. (2). Corresponding electric and magnetic amplitudes are related by the appropriate directional characteristic admittances. For the case in which E is perpendicular to the plane of incidence, these relations are

$$(H_t/E_t)=(H_r/E_r)=A'=A\cos\theta. \tag{4E}$$

For the case in which H is perpendicular to the plane of incidence, the relations are

$$(H_t/E_t)=(H_r/E_r)=A'=A/\cos\theta. \tag{4H}$$

In Eqs. (4E) and (4H) the angle θ is given by the first of Eqs. (2).

The essential difference in results for the two primitive cases is contained in Eqs. (4E) and (4H). At normal incidence, for which $\theta=0$, the two cases become indistinguishable, as should be expected.

Equations (1) to (4H), and the statement that E and H are continuous at boundaries between adjoining layers, constitute the formal solution of Maxwell's equations for our stratified medium. This solution, in terms of transmitted and reflected waves in each layer, has a good deal of physical content. As it stands, however, it is not very useful for problems which call for a quantitative study of the reflection and transmission characteristics of multilayer systems. For such problems, the behavior of the waves in each layer is of no direct interest; it turns out, here, that the quantities of immediate concern are the ratios (H/E) at the two boundaries of each layer, and the relations between these ratios for the various layers.

Input and Terminating Admittances

The ratios (H/E) at the left and right boundary planes of each layer recur so often in problems of reflection and transmission that it is well, to avoid circumlocution, to have names for them. There are no optical designations for these quantities, but it happens that in the field of electrical communications names for similar quantities have been in use for many years. These designations, input admittance and terminating admittance, are so satisfactory and so suggestive physically, that we adopt them for our purposes.

The input admittance of a layer is defined as the ratio (H/E) at the left boundary of a layer; it is the admittance encountered by a wave incident upon the layer. For example, the input admittance of layer 1, in which there is no reflected wave, is $Y_1=(H/E)_1=A_1'$, from Eqs. (3) and Eq. (4E) or Eq. (4H); the input admittance of layer 1 is thus given in terms of the

electromagnetic properties of layers 1 and m, and the state of polarization and angle of incidence of the wave which is incident upon the $(m-1)$th layer. The terminating admittance of a layer is defined as the ratio (H/E) at the right boundary of a layer; by conditions of continuity, this ratio is equal to the input admittance of the adjoining layer, which may be regarded as terminating the layer to its left. Thus the input admittance Y_1 is also the terminating admittance for layer 2.

By eliminating the transmitted and reflected amplitudes in Eqs. (3), the values of E and H at the left boundary of any of the finite layers can be related to corresponding values at the right boundary. These relations are

$$\begin{aligned} E_1 &= E_2 \cosh pd + (H_2/A') \sinh pd \\ H_1 &= E_2 A' \sinh pd + H_2 \cosh pd. \end{aligned} \tag{5}$$

In Eqs. (5), E_1, H_1 and E_2, H_2 are the values of E and H at the left and right boundaries, respectively; A' is given by Eq. (4E) or Eq. (4H), depending upon which case is being investigated; and pd, which is the argument of the hyperbolic functions, is the product of layer thickness, d, and p, which is given by the second of Eqs. (2).

The conditions of continuity make it possible to express Eqs. (5) in a form which connects E and H at the left boundary of one layer, say the kth, with corresponding quantities for the adjoining layer on the right, which in this instance is the jth. These expressions are

$$\begin{aligned} (E_1)_k &= (E_1)_j \cosh(pd)_k + [(H_1)_j/A_k'] \sinh(pd)_k \\ (H_1)_k &= (E_1)_j A_k' \sinh(pd)_k + (H_1)_j \cosh(pd)_k. \end{aligned} \tag{6}$$

In Eqs. (6), the inner subscript 1 indicates that the quantity to which it is attached is evaluated at the left boundary of the jth or kth layers, identified by the subscripts j or k.

The input admittance, $Y_k = (H_1/E_1)_k$, of the kth layer is obtained by taking the ratio of the second to the first of Eqs. (6). Its value is

$$Y_k = A_k'[Y_j + A_k' \tanh(pd)_k]/[A_k' + Y_j \tanh(pd)_k]. \tag{7}$$

Equation (7) is a recurrence formula which relates the input admittance of a layer to its properties A' and pd, and to the input admittance of the preceding layer. It also represents a conformal transformation of the complex variable Y_j to the complex variable Y_k, in terms of the complex variables A_k' and $(pd)_k$. A graphical chart constructed in accordance with this conformal transformation can be used to effect a considerable reduction in the labor of computation which otherwise would be required in any given numerical case.[7]

[7] H. Cafferata, Marconi Rev. 6 (No. 64) 12 (1937); 6 (No. 67) 21 (1937). A limited quantity of charts of the type described in this reference is available. They may be obtained by requesting Charts H. O. Misc. 9999, 9999a, 9999b, and 9999b-1 from the Technical Information Division, Naval Research Laboratory, Washington 25, D. C.

By repeated use of Eq. (7) the input admittance of the $(m-1)$th layer can be expressed in terms of the input admittances of the preceding layers. In detail, this process of iteration goes as follows: To begin with, the input admittance of layer 1 is simply $Y_1 = A_1'$. The input admittance of layer 2 is then given by Eq. (7) if j is replaced by 1, and k is replaced by 2. Similarly, the input admittance of layer 3 is given by Eq. (7) if j is then replaced by 2, and k by 3. This process is repeated until j takes on the value $(m-2)$, and k assumes the value $(m-1)$, whereupon an explicit expression for Y_{m-1} is obtained. The value and characteristics of Y_{m-1} are decisive with respect to the magnitude and nature of the reflection at, and transmission through, the initial boundary plane. The method just outlined for obtaining this input admittance has the advantages of being systematic, and of concentrating attention on quantities of primary significance, with the result that algebraic complications are minimized, and physical clarity and insight are enhanced.

Reflection and Transmission Coefficients

The amplitude reflection coefficient is defined as the ratio of reflected to incident tangential electric or magnetic components in the mth layer, at the interface between mth and $(m-1)$th layers. A formula for this coefficient can be derived from Eqs. (3) and (4), and the conditions of continuity; it is

$$\begin{aligned} r = (E_r/E_i)_m &= (H_r/H_i)_m \\ &= (A_m' - Y_{m-1})/(A_m' + Y_{m-1}). \end{aligned} \tag{8}$$

The electric amplitude transmission coefficient is defined as the ratio of the tangential electric component in the $(m-1)$th layer, at the boundary between mth and $(m-1)$th layers, to the incident tangential electric component in the mth layer, at the same boundary. The magnetic amplitude transmission coefficient is defined as the ratio of corresponding magnetic components. Formulas for these coefficients can be obtained by use of Eqs. (3), (4), and (8), and the conditions of continuity; they are

$$\begin{aligned} t &= (E_1)_{m-1}/(E_i)_m = 1 + r = 2A_m'/(A_m' + Y_{m-1}) \\ t' &= (H_1)_{m-1}/(H_i)_m = 1 - r \\ &= 2Y_{m-1}/(A_m' + Y_{m-1}) = (Y_{m-1}/A_m')t. \end{aligned} \tag{9}$$

To illustrate the application of Eqs. (8) and (9), and the material which leads to these formulas, we digress to consider two elementary problems which are to be found in the literature. In the first of these, there are two adjoining semi-infinite non-absorbing dielectric layers. A steady-state monochromatic wave, generated in layer 2 and having either E or H normal to the plane of incidence, is incident at an angle θ_2 upon layer 1. Since the two layers are lossless dielectrics, ϵ' and μ' are zero for each, and $\mu_1 = \mu_2 = 1$. Denoting the indexes of refraction by $n_1 = \epsilon_1^{\frac{1}{2}}$ and $n_2 = \epsilon_2^{\frac{1}{2}}$, and substituting this information in Eqs. (1), we get for the two propagation

constants and the two characteristic admittances

$$\begin{aligned} P_1&=i\omega n_1/c_0 \quad P_2=i\omega n_2/c_0 \\ A_1&=A_0 n_1 \quad\quad A_2=A_0 n_2. \end{aligned} \tag{1.1}$$

From Eqs. (4E), (4H), (7), and (1.1) we get

$$\begin{aligned} A_1'&=Y_1=A_0 n_1[1-(n_2/n_1)^2\sin^2\theta_2]^{\frac{1}{2}} \\ A_2'&=A_0 n_2\cos\theta_2 \end{aligned} \tag{4E.1}$$

and

$$\begin{aligned} A_1'&=Y_1=A_0 n_1/[1-(n_2/n_1)^2\sin^2\theta_2]^{\frac{1}{2}} \\ A_2'&=A_0 n_2/\cos\theta_2. \end{aligned} \tag{4H.1}$$

Equations (4E.1) apply to the case for which E is normal to the plane of incidence, and Eqs. (4H.1) apply to the case for which H is normal to the plane of incidence. Corresponding formulas for the amplitude reflection and transmission coefficients are obtained by substituting Eqs. (4E.1) and (4H.1) in Eqs. (8) and (9). Letting $n=(n_2/n_1)$, these formulas are

$$r=[n\cos\theta_2-(1-n^2\sin^2\theta_2)^{\frac{1}{2}}]/[n\cos\theta_2+(1-n^2\sin^2\theta_2)^{\frac{1}{2}}] \tag{8E}$$

$$r=[n(1-n^2\sin^2\theta_2)^{\frac{1}{2}}-\cos\theta_2]/[n(1-n^2\sin^2\theta_2)^{\frac{1}{2}}+\cos\theta_2] \tag{8H}$$

$$t=1+r, \quad t'=1-r. \tag{9.1}$$

In Eqs. (9.1) the value of r is obtained from either Eq. (8E) or Eq. (8H), depending upon which case is being studied. When $\theta_2=0$, corresponding to normal incidence, Eqs. (8E) and (8H) become identical, and equal to $r=(n-1)/(n+1)$, a familiar result. The reader is reminded that the above expressions are complex amplitude ratios, and not the usual intensity or power ratios; for this reason they provide information with respect to relative phase, in addition to relative magnitudes. They can be used as they stand to yield well-known phenomena. For example, $r=0$ in Eq. (8H) when $n_1=n_2$, or when $\theta_2=\arctan(n_1/n_2)$; the first of these conditions is trivial, since it tells us that reflection vanishes when the two layers are identical, but the second gives us the well-known Brewster's angle, for which reflection vanishes at all wave-lengths. As another example, when $n_2>n_1$, and the angle of incidence is greater than the special value $\theta_2=\arcsin(n_1/n_2)$, the input admittance Y_1 given by Eq. (4E.1) or Eq. (4H.1) becomes imaginary, and the absolute values of r in Eqs. (8E) and (8H) become unity. This will be recognized as the phenomenon of total reflection. Although total reflection takes place, Eqs. (9.1) tell us that in layer 1 the components E and H are finite, but from Eqs. (4E.1) and (4H.1) we see that these components are in phase quadrature, and therefore no energy is actually transmitted across the interface during the steady-state. By means of Eqs. (2), we find that in layer 1 the equiamplitude planes are parallel to, and the equiphase planes perpendicular to, the interface.

In our second illustrative problem, there are two semi-infinite layers separated by a finite layer, each of these (dielectric) layers being non-absorbing; and their indexes of refraction obey the condition $n_3<n_2<n_1$. A steady-state monochromatic wave, with either E or H normal to the plane of incidence, is incident at an angle θ_3 upon finite layer 2. What are the conditions on the index of refraction, n_2, and the thickness, d_2, of layer 2 so that no reflection takes place? This is a problem which has been treated by means of conventional multiple-ray analysis, using the Fresnel formulas.[8] We deal with the problem much more concisely, as follows: Since the three layers are lossless dielectrics, ϵ' and μ' are zero for each of the layers, and $\mu_1=\mu_2=\mu_3=1$. Using these data in Eqs. (1), we get for the propagation constants and characteristic admittances

$$\begin{aligned} P_k&=i\omega n_k/c_0=i2\pi n_k/\lambda \\ A_k&=A_0 n_k, \quad k=1, 2, 3 \end{aligned} \tag{1.2}$$

in which λ is the free-space wave-length of the incident radiation. From Eqs. (2) and (4E), we get

$$p_2=i(2\pi n_2/\lambda)[1-(n_3/n_2)^2\sin^2\theta_3]^{\frac{1}{2}} \tag{2.2}$$

and

$$\begin{aligned} A_k'&=A_0 n_k[1-(n_3/n_k)^2\sin^2\theta_3]^{\frac{1}{2}}, \quad k=1, 2 \\ A_3'&=A_0 n_3\cos\theta_3. \end{aligned} \tag{4E.2}$$

From Eqs. (7) and (2.2), we find

$$\begin{aligned} Y_1&=A_1' \\ Y_2&=A_2'[A_1'+iA_2'\tan\psi]/[A_2'+iA_1'\tan\psi], \end{aligned} \tag{7.2}$$

in which $\psi=(2\pi n_2 d_2/\lambda)[1-(n_3/n_2)^2\sin^2\theta_3]^{\frac{1}{2}}$ is the optical thickness of layer 2. We observe that for oblique incidence, the optical thickness of layer 2 depends not only upon the physical thickness and index of refraction of layer 2, but on the given angle of incidence in layer 3, and on the given indexes of refraction of layers 1 and 3. Since $n_3<n_2$, this optical thickness is a real quantity for all values of θ_3.

Equation (8) tells us that reflection vanishes only if $Y_2=A_3'$. By inspecting the second of Eqs. (1.2) and (7.2), we see that this condition requires that Y_2 be real, and equal in magnitude to A_3'. For Y_2 to be real, however, $\tan\psi$ must be infinite; this tells us that the optical thickness must be equal to an odd number of quarter-wave-lengths. The physical thickness is thus given by $n_2 d_2=(n\lambda/4)[1-(n_3/n_2)^2\sin^2\theta_3]^{-\frac{1}{2}}$ where $n=1, 3, 5, \cdots$. When this condition is fulfilled we have, from Eq. (7.2), $Y_2=A_2'^2/A_1'$. Simple algebraic manipulation then yields, as the necessary explicit condition on n_2 for the case in which E is perpendicular to the plane of incidence,

$$(n_2^2/n_1 n_3)=[1-(n_3/n_1)^2\sin^2\theta_3]^{\frac{1}{2}}\cos\theta_3+(n_3/n_1)\sin^2\theta_3.$$

When H is perpendicular to the plane of incidence, the corresponding condition is obtained from the solution of the following quadratic equation in n_2^2:

$$n_2^4[1-(n_3/n_1)^2\sin^2\theta_3]^{\frac{1}{2}}\cos\theta_3-n_1 n_3 n_2^2+n_1 n_3^3\sin^2\theta_3=0.$$

[8] K. B. Blodgett, Phys. Rev. 57, 921 (1940).

For normal incidence these conditions simplify to

$n_2^2=n_1n_3$, and $d_2=(n\lambda/4n_2)$, where $n=1, 3, 5, \cdots$.

We observe, in passing, that (1) the input admittance of a non-absorbing layer, whose optical thickness is an integral number of half-wave-lengths, is equal to the admittance which terminates the layer, i.e., $Y_k=Y_j$. Also, (2) the input admittance of a non-absorbing layer, whose optical thickness is an odd number of quarter-wave-lengths, is obtained by reciprocating the terminating admittance with respect to the square of the characteristic admittance of the layer, i.e., $Y_k=A_k'^2/Y_j$. These observations follow immediately when Eq. (7) is applied to a non-absorbing layer, for which $\tanh pd=i\tan\psi$. From (2) we can derive the following useful theorem, almost by inspection: A non-absorbing multilayer system having any number of finite layers, the optical thickness of each of which is an odd number of quarter-wave-lengths, will have zero reflection for radiation at normal incidence when the indexes of refraction are related by

$$(n_m/n_1)=(n_{m-1}n_{m-3}\cdots n_3)^2/(n_{m-2}n_{m-4}\cdots n_2)^2, \quad m=4, 6, 8, \cdots \tag{10}$$
$$(n_m/n_1)=(n_{m-1}n_{m-3}\cdots n_2)^2/(n_{m-2}n_{m-4}\cdots n_1)^2, \quad m=3, 5, 7, \cdots.$$

In Eqs. (10) the number m is equal to the total number of layers, including the two semi-infinite layers which flank the finite layers, as shown in Fig. 1. If the optical thickness of any layer happens to be an integral number of half-wave-lengths, Eqs. (10) still apply; by virtue of observation (1) above, the presence of such a layer can be taken into account merely by not counting it as part of the number m.

For some problems it is desirable to have expressions available which relate E and H at the final interface, to E and H at the initial interface. Such expressions can be obtained from Eqs. (3) to Eqs. (9).

The over-all electric amplitude transmission coefficient is defined as the ratio of electric amplitude in layer 1, at the boundary between layers 1 and 2, to the incident electric amplitude in the mth layer, at the boundary between mth and $(m-1)$th layers. The over-all magnetic amplitude transmission coefficient is defined as the ratio of corresponding magnetic amplitudes. Formulas for these coefficients are given by the continued products:

$$t_{m,1}=(E_1)_1/(E_t)_m=t\prod_{k=m-1}^{k=2}[\cosh(pd)_k + (Y_j/A_k')\sinh(pd)_k]^{-1} \tag{11}$$

$$t_{m,1}'=(H_1)_1/(H_t)_m=(A_1'/A_m')t_{m,1}.$$

Reflection and transmission are commonly expressed in terms of reflectivity or transmissivity, these being defined as ratios of reflected to incident, and transmitted to incident, intensities or powers. It can be shown that the concept of incident and reflected power breaks down in the general case, where the medium in which the source is located is of an absorbing type.[9] This matter appears to have been overlooked,[10] or at least not well understood,[11] in analyses which purport to treat such general situations. Occasionally a practical problem is encountered, in which such a general situation must be considered, e.g., transmission from a source, located in the sea, to air or to a glass layer. Commonly, however, the source is located in air, and for problems in which this is so, the concept of incident and reflected power may be used with only small error. In such circumstances the reflectivity, R, and the transmissivity, T, can be expressed as

$$R=|r|^2, \quad T=1-R=|t|^2Re(Y_{m-1})/A_m'. \tag{12}$$

Similarly an over-all transmissivity can then be defined; it is

$$T_{m,1}=Re(E_1H_1^*)_1/Re(E_tH_t^*)_m = |t_{m,1}|^2Re(A_1')/A_m', \tag{13}$$

in which * indicates that the conjugate of the complex quantity with which it is associated is to be used.

In Part II the use of the methods and results described here will be illustrated further by applying them to the detailed solution of several problems of current interest.

[9] B. Salzberg, Am. J. Phys. **16**, 444 (1948).
[10] J. A. Stratton, *Electromagnetic Theory* (McGraw-Hill Book Company, Inc., New York, 1941), pp. 511–513.
[11] L. Pincherle, Phys. Rev. **72**, 232 (1947).

A Birefringent Frustrated Total Reflection Filter

B. H. BILLINGS
Research Laboratory, Baird Associates, Inc., Cambridge, Massachusetts
(Received January 18, 1950)

In the standard Turner Frustrated Total Reflection filter the pass bands occur in pairs which are oppositely polarized. The maximum theoretical transmission in any band is thus 50 percent. In this paper it is shown that if the high index layer of the filter is made of a birefringent material the oppositely polarized pass bands can be made to coincide so that the maximum theoretical transmission becomes 100 percent and the bands occur singly. Measurements are shown on a filter made with such a birefringent layer.

DURING the last few years an increasing amount of attention has been paid to the development of methods of isolating narrow spectral regions. A large part of this effort has been spent in the investigation of the possibilities of interference filters. At any given stage of development the complexity of these filters seems to vary inversely with the width of the pass band desired. For a band width of 15 mμ a simple Fabry-Perot interference filter[1] is perfectly satisfactory. With its three evaporated layers this filter certainly is the least complex of the interference family.

A pass band of 6 mμ requires a much more complex structure than that of the solid Fabry-Perot filter. These band widths were produced several years ago with a multilayer technique by Fogelsanger at Evaporated Metal Films. They have recently been described by Polster.[2] Here the two silver layers of the simple Fabry-Perot filter are each replaced by seven layers of dielectric. These narrow pass bands can also be achieved by the use of a mixture of dielectric layers and silver layers. This has been demonstrated by DuFour.[3]

Pass bands of 0.6 mμ or less require the still more complex structure of the polarization interference filter.[4–6] Although this filter pre-dates the Fabry-Perot and other interference filters by several years, it is so very difficult to manufacture that there are less than a dozen of these filters in existence. The Turner Frustrated Total Reflection filter[7–8] considerably reduces the complexity required for a given band width. With this filter good transmission can be achieved in the visible spectrum with band widths of only 1 mμ. The filter, however, is not much more complex than the simple Fabry-Perot filter and has only three interfering layers. In its basic form, the Frustrated Total Reflection filter has pass bands which occur in pairs and which are oppositely polarized. As a result, the theoretical maximum transmission of any one pass band is 50 percent. In this paper a method is described whereby the polarized double bands are replaced by a single isotropic band of twice the transmission.

THEORY OF THE BASIC FRUSTRATED TOTAL REFLECTION FILTER

The operation of the Frustrated Total Reflection filter is most easily understood by considering it as an analog to the solid Fabry-Perot filter. This filter consists of a layer of dielectric between two semitransparent layers of silver. Its operation may be explained by assuming that at the first silvered surface the light is partly reflected and partly transmitted. The transmitted part continues to the second silvered surface where it is again partly reflected and partly transmitted. The reflected light passes back to the first surface, part of this light is transmitted, and joins with the light that was previously reflected. If these two beams are out of phase the light will be transmitted through the filter. If they are in phase the light will be reflected. The pass band of the filter depends on the number of times the light can be reflected between the boundaries of the dielectric layer of the filter. The number of reflections will depend on the reflectivity of the silver layers. By summing the various transmitted amplitudes of the rays passing through the filter one obtains the formula:

$$\frac{I}{I_0}=\frac{t^2}{t^2+4r\sin^2[(\varphi-2\delta)/2]}, \tag{1}$$

where t is the transmission of the reflecting film, r its reflectivity, φ the phase shift through the dielectric layer is equal to $4\pi nd/\lambda$ and δ is the phase shift at the boundary of the dielectric layer. This equation ignores the absorption in the film and shows that the peak transmission is independent of the silver reflectivity. In the exact formula which considers the absorption of the metallic layers, the peak transmission is no longer independent of the band width and, as the reflectivity is increased and the band width decreased, the peak transmission is also decreased, so that for very narrow band widths the resulting filter is not particularly useful because of extremely low peak transmission.

The Frustrated Total Reflection filter uses the principle of the penetration into the second medium which occurs when light is incident on a surface beyond the angle of total internal reflection. When light is sent

[1] Walter Geffcken, German Patent No. 716153 (filed December 8, 1939).
[2] H. D. Polster, J. Opt. Soc. Am. **39**, 1054A (1949).
[3] C. DuFour, Le Vide **16**, 3 (1948).
[4] B. Lyot, Comptes Rendus **197**, 1593 (1933).
[5] J. Evans, Pubs. Astron. Soc. Pacific **52**, 305 (1940).
[6] B. Billings, J. Opt. Soc. Am. **37**, 738 (1947).
[7] P. Leurgans and A. F. Turner, J. Opt. Soc. Am. **37**, 983 (1947).
[8] B. Billings and M. A. Pittman, J. Opt. Soc. Am. **39**, 978 (1949).

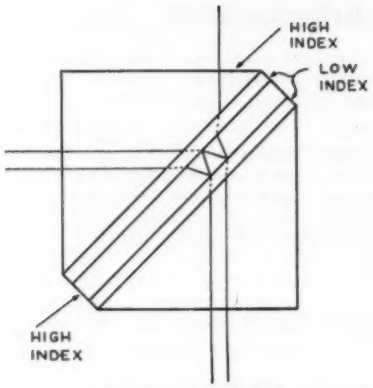

FIG. 1. Arrangement of the elements and path of the rays in the Turner Frustrated Total Reflection filter.

through the base of a right-angle prism, it is reflected at the hypotenuse. This reflection is 100 percent if the light strikes the hypotenuse of the prism at an angle of incidence greater than the critical angle. If now a convex lens is put in contact with the hypotenuse, the light at the point of contact will not be reflected but instead will be transmitted into the lens. When the light reflected from the prism hypotenuse is observed, a black spot is seen where this penetration takes place. The size of this black spot is found to be much larger than one would expect if the light went through only where actual optical contact was achieved. In other words, the light appears to penetrate into the air space between the lens and the prism, and where that air space is sufficiently thin it is able to reach the lens surface and be transmitted. Examination of Maxwell's equations at the prism hypotenuse shows that at angles bigger than the critical angle the light actually does penetrate into the low index medium. In this medium the amplitude drops off exponentially with the distance. If a high index surface is placed close enough to the hypotenuse so that the light amplitude has not dropped to zero, then a fraction of the light will be transmitted. No light will be lost in the low index layer. The surface of this low index layer thus constitutes a semitransparent reflector with no absorption loss.

The Frustrated Total Reflection filter consists of two such semitransparent reflectors. The prism hypotenuse is covered with a low index layer whose thickness is determined by the desired reflectivity. This is followed by a high index layer whose thickness determines the wave-length which will be transmitted. Another low index layer is then deposited so as to give another frustrated total reflection. Another prism is then laminated to the first prism with a material whose index is the same as the prism material. The resulting rhomb constitutes the interference filter.

This filter, unlike the regular solid Fabry-Perot filter, has no inherent limitations which make it unsatisfactory for wave-lengths in the ultraviolet or infra-red. The only requirements are that the materials of which the filter is made be transparent in the desired spectral region and that the indices have the proper relationship.

The wave-length of peak transmission is determined by the thickness of the high index layer and the band width by the thickness of the low index layer. Equation (1) gives a good approximation to the behavior of the filter at normal incidence. When the filter is tilted, the equivalent thickness of the high index layer changes and the peak transmission accordingly changes.

The change of peak transmission with angle of incidence is most easily derived by considering the behavior of the filter as arising from the interference of the light reflected from the boundary of the first low index layer with light reflected from the second low index layer.

In Fig. 1 is a sketch showing the path of the rays through the Frustrated Total Reflection filter. Since the same multiple reflections take place that occur in a solid Fabry-Perot filter, we can use the Fabry-Perot formula to describe the operation of this filter. The expressions for r, t, δ and φ are, however, quite different. By applying Maxwell's equations to reflection at a prism hypotenuse, they can be shown for the perpendicular component to be:

$$r_s=\frac{(\sinh^2 u)(n_1^2-n_2^2)^2}{D_s}, \tag{2}$$

$$t_s=\frac{4(n_1^2\sin^2\theta-n_2^2)n_1^2\cos^2\theta}{D_s}, \tag{3}$$

$$D_s=\sinh^2 u(n_1^2\cos^2\theta-n_1^2\sin^2\theta+n_2^2)^2 + (n_1^2\sin^2\theta-n_2^2)(2n_1\cos\theta)^2\cosh^2 u, \tag{4}$$

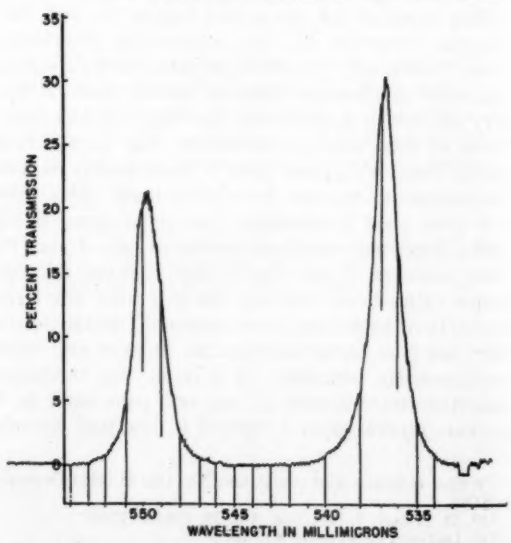

FIG. 2. Transmission as a function of wave-length of a simple Frustrated Total Reflection filter. The filter is made with 67.5° glass prisms. The low index layer has $n=1.38$ and an optical thickness of $\frac{3}{4}$ of a wave at 560 mμ. A high index layer has $n=2.38$ and an optical thickness of 6 waves at 600 mμ.

where

$$u=(2\pi d)/\lambda(n_1^2\sin^2\theta-n_2^2)^{\frac{1}{2}}. \quad (5)$$

n_1 is the low index, n_2 the high index, and θ the angle at which light is incident on the low index boundary. Similar expressions exist for the parallel component. For the various phase shifts

$$\tan\frac{\delta_s}{2}=\frac{(\sin^2\theta-(n_1/n_0)^2)^{\frac{1}{2}}}{\cos\theta}, \quad (6)$$

$$\tan\frac{\delta_p}{2}=\frac{(\sin^2\theta-(n_1/n_0)^2)^{\frac{1}{2}}}{(n_1/n_0)^2\cos\theta}, \quad (7)$$

$$\varphi=(4\pi nd/\lambda)\cos\theta, \quad (8)$$

where n_0 is the prism index. The subscript s refers to the perpendicular component and p to the parallel component. Note that there are now two values for the quantity δ, the phase shift at the boundary. This is because the light is incident at an oblique angle on the interfering surfaces. In Fig. 2 is shown the transmission curve of a typical Frustrated Total Reflection filter. This filter has the following characteristics:

$$\theta_0=67.5°$$
$$n_{\text{low}}=1.38$$
$$n_{\text{high}}=2.38$$
$$nd_{\text{low}}=3/4\lambda \text{ at } 560 \text{ m}\mu$$
$$nd_{\text{high}}=6\lambda \text{ at } 600 \text{ m}\mu.$$

The prism material had an index of 1.63.

One of the problems in making measurements on filters of this type is the high resolution required in the measuring instrument. To measure accurately the percent transmission of a filter whose band width is 1 mμ requires a spectrometer which can resolve at least 0.2 mμ, and for really accurate work even higher resolution is necessary. Most of the conventional recording spectrophotometers do not have this high resolution. A grating instrument has been assembled at Baird Associates, Inc. for the purpose of working at this high resolving power. The instrument uses a 15,000 line per inch grating and for these measurements was operated with a photo-multiplier tube as the receiver. The light falling on the entrance slit is interrupted by a mechanical chopper. The output of the photo-multiplier tube is fed through conventional a.c. electronics to a Leeds and Northrup recorder. With this instrument it is possible to achieve resolution of a fraction of an angstrom and thus make accurate and rapid transmission measurements of these narrow band filters. Complete description of the grating monochromator will appear in a forthcoming paper.

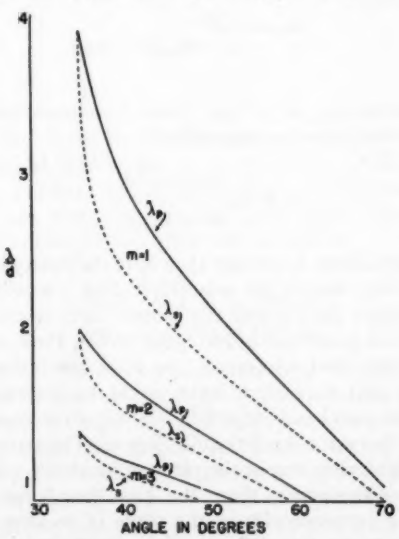

FIG. 3. Variation of wave-length of peak transmission with angle of incidence for a Frustrated Total Reflection filter. λ_s is the wave-length for light polarized perpendicular to the plane of incidence; λ_p for light polarized parallel to the plane of incidence. d is the thickness of the high index layer. The indices are the same as in Fig. 2.

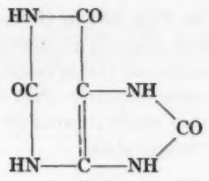

FIG. 4. Formula for uric acid.

The spacing of the pass bands is a function of the angle of the filter, of the indices of the high and low index layers, and of the order number. The equation for the wave-lengths of the peaks is:

$$\frac{4\pi nd\cos\theta}{\lambda}-2\delta=2m\pi \quad (9)$$

or

$$\lambda=\frac{2\pi nd\cos\theta}{m\pi+2\delta}, \quad (10)$$

where m is the order of the pass band. The band separation in cm^{-1} is expressed by the equation:

$$\Delta\nu=\frac{\delta_s-\delta_p}{2\pi nd\cos\theta}. \quad (11)$$

In Fig. 3 is a series of curves showing the way the wave-length of peak transmission changes as a function of the angle of incidence. In order to make the pass bands come together, it is apparent by inspection of Eq. (1) that the quantity $\varphi=2\delta$ must be made to be the same for each state of polarization. This can only be accomplished by making some layer of the filter birefringent. If the central layer is made birefringent the sum of the phase shift of traversal and the phase shift of reflection can be made equal for both states of polarization. The angular dependence of these phase shifts for birefringent layers becomes more complex

than that given in Eqs. (6) to (8) because the birefringence depends on angle. This dependence is a function of the orientation of the crystallographic axes of the layer. It is only recently that research at the Polaroid Corporation made it possible to prepare birefringent layers by evaporation.

EVAPORATED BIREFRINGENT LAYERS

Although the preparation of evaporated birefringent layers has not yet appeared in scientific literature, it is covered fairly well in a series of patents[9–12] owned by Polaroid Corporation. The substances which are strongly birefringent after evaporation are all, in general, organic. They are usually planar and have one or more benzene rings. Distributed around the rings are groups which will exert force between the molecule and a surface or between the molecules and each other. Layers of such molecules are symmetrical about an axis normal to the surface on which they are evaporated. The resulting medium is birefringent with its optic axis normal to the film. At a given angle the indices of such a film are:

$$\omega(\theta)=\omega$$

$$\epsilon'(\theta)=\frac{\omega\epsilon}{(\epsilon^2\cos^2\theta+\omega^2\sin^2\theta)^{\frac{1}{2}}}, \tag{12}$$

where ω is the ordinary index, ϵ the extraordinary index and θ is the angle between the wave front of the light and the optic axes. It is possible to achieve quite large values for the birefringence of these evaporated materials. A birefringence of 0.17 is obtainable with uric acid. This formula is given in Fig. 4.

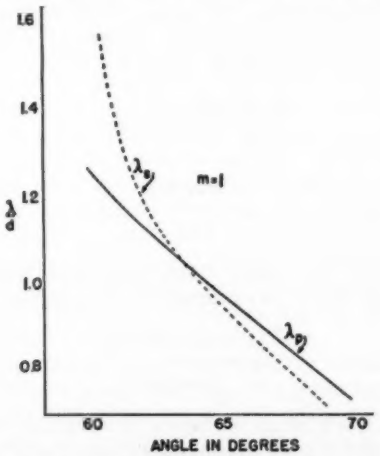

FIG. 5. Variation of wave-length of peak transmission with angle of incidence for a Frustrated Total Reflection filter. In this filter the central layer is birefringent with ω 1.72, ϵ 1.55, and the low index layer 1.38.

BIREFRINGENT LAYERS FOR THE FRUSTRATED TOTAL REFLECTION FILTER

For the Frustrated Total Reflection filter the birefringent layers must have certain, very specific characteristics in order to have a single pass band for both states of polarization. In case the central layer is birefringent both indices must be higher than the low index material. If one index is too low then for one state of polarization the filter transmits all wavelengths, whereas for the opposite state of polarization, the filter will have single narrow pass bands. If one of the lower index layers is made birefringent, both indices must be lower than the index of the high central layer, otherwise again a continuum will be passed for one state of polarization.

Consider now the case where the central layer is birefringent. Both indices must be high. It is apparent from Eq. (1) and Eqs. (6), (7), and (8) that a filter can be made which will have a single pass band at any desired wave-length. The two parameters which can be adjusted to achieve this result are the angle of the filter and the thickness of the central layer. For an anisotropic central layer Eq. (10) for the wave-length of peak transmission becomes:

$$\frac{4\pi\epsilon'(\theta)\omega d\cos\theta}{\omega\lambda}-2\delta_s(\theta)=2m\pi, \tag{13}$$

$$\frac{4\pi\omega d\cos\theta}{\lambda}-2\delta_p(\theta)=2m\pi. \tag{14}$$

By eliminating $\omega d/\lambda$ from these two equations one obtains the following expression:

$$\epsilon'(\theta)=\omega\frac{m\pi+2\delta_s(\theta)}{m\pi+2\delta_p(\theta)}. \tag{15}$$

As shown above, δ_s is larger than δ_p in the isotropic case. If this were true in the anisotropic case, ϵ would have to be bigger than ω and the central layer would thus need to be positively birefringent. When these experiments were first conceived, the false conclusion was reached that a positive layer would be necessary to bring the pass bands together. The intuitive reasoning behind this error seemed quite logical. The pass band of the light vibrating in the plane of incidence was at a shorter wave-length than the pass band for light vibrating perpendicular to the plane of incidence. To compensate for this difference it seemed obvious that the optical thickness of the filter for light vibrating in the plane of incidence should be greater than the optical thickness for the light vibrating perpendicular to the plane of incidence. Since these evaporated birefringent

[9] E. E. Barr and C. D. West, U. S. Patent No. 2,447,790 (filed April 11, 1945).
[10] E. R. Blout, U. S. Patent No. 2,447,792 (filed March 24, 1945).
[11] M. Hyman, Jr., U. S. Patent No. 2,447,805 (filed April 11, 1945).
[12] R. B. Woodward, U. S. Patent No. 2,447,831 (filed March 3, 1945).

layers are optically equivalent to a uniaxial crystal with its axes perpendicular to the plane of the layers, a positive crystal thus seemed necessary. Positive crystals or positive evaporated layers are relatively rare. This is because such materials are generally formed from rod like structures where the rods are arranged parallel to each other. Oil films or films of paraffin are positive but they cannot be made very thick as they tend to form aggregates which make the layers quite hazy.

An experiment was performed using a negatively birefringent material to see if perhaps the peak from one order could be made to coincide with the peak from the next higher order. When the experiment was carried out it was discovered, of course, that the bands of a single order could be brought together. The reason for this was that δ_s and δ_p, the two phase shifts, are quite strongly dependent on index and for a negatively birefringent layer, these phase shifts change in such a way that δ_p becomes larger than δ_s. Equation (16) can then be solved to find the value of θ at which the bands can be brought together in a given order. The birefringent layer must be negative. This is most fortunate as negative materials are easily prepared and a filter with a single pass band thus becomes a practical possibility.

When m is very large $\epsilon'(\theta)$ approaches ω. This is true only at normal incidence. Since the filter will only operate at angles larger than the critical angle, coincidence cannot be achieved at high orders. In Fig. 5 is shown a calculated curve for the first order showing the way in which the bands shift position with angle of incidence. The characteristics of this filter were:

$$\theta_0 = 67.5°$$
$$n_{\text{low}} = 1.38$$
$$\omega = 1.72$$
$$\epsilon = 1.55.$$

The coincidences for the different orders occur at angles and optical thicknesses shown in Table I. A filter was made up using magnesium fluoride for the low index layer and uric acid for the high index layer. The characteristics of this filter were as follows:

$$\theta_0 = 67°$$
$$(nd)_{\text{low}} = 3/4\lambda \text{ at } 520 \text{ m}\mu$$
$$(nd)_{\text{high}} = 9/4\lambda \text{ at } 600 \text{ m}\mu.$$

In Fig. 6 is shown the transmission of this filter when rotated through an angle of 10°. This is rotated so that the angle of incidence on the hypotenuse is smaller. In Fig. 7 the filter is tilted still farther so that the two bands coincide. In Fig. 8 the filter has been tilted so that the angle of incidence is still smaller and the bands have crossed over. The parallel band is now at a larger wave-length than the perpendicular band.

For very narrow transmission bands the tolerances in the thickness and uniformity of the evaporated layers are extremely small. The lower transmission of the birefringent filter shown in the figures is probably caused by roughness and non-uniformity in the organic film. To achieve high transmission it will be necessary to reduce this non-uniformity.

TABLE I. Values of $\omega d/\lambda$ and θ at which coincidence is achieved between bands of a given order. This is calculated for a filter with $n=1.38$ for the low index layer and with $\omega=1.72$ and $\epsilon=1.58$ for the high index layer.

$\omega d/\lambda$	θ	n
0.69	66.75°	0
1.68	64°	1
2.59	62°	2
3.47	60.75°	3

If the low index layer is made birefringent the crossover will depend only on the phase shift at reflection. In this case, all bands in all orders coincide at the same angle. This is quite different from the previous case in which coincidence was achieved at a different angle in each order. The wave-length of peak transmission is given simply by:

$$1/\lambda = \frac{m\pi + \delta(\theta)}{2\pi nd\cos\theta}, \tag{16}$$

where θ is that angle at which $\delta_s(\theta) = \delta_p(\theta) = \delta(\theta)$.

This case is somewhat more difficult to realize in practice because of the unavailability of birefringent substances in which both indices are low. A possible method of making such layers is the technique described by Wiener.[13] In this method birefringent layers are made by piling up alternate layers of high and low index material. The individual layer thicknesses are a small fraction of a wave-length in the region where the sandwich is to be birefringent.

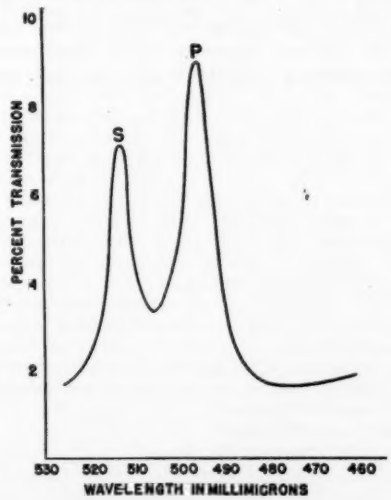

FIG. 6. Measured transmission of a birefringent Frustrated Total Reflection filter.

[13] O. Wiener, Sach. Akad. Leipzig Math. Phy. Kl. Berichte **53**, 54, (1901–1902).

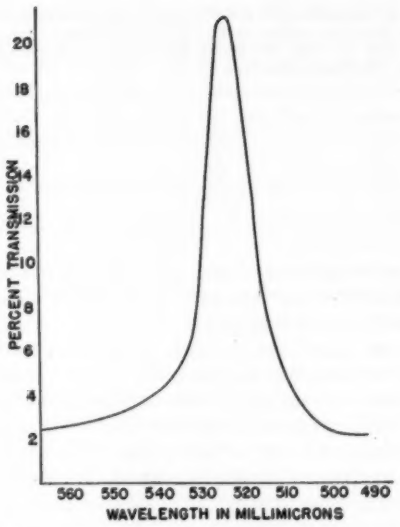

FIG. 7. Measured transmission of the filter shown in Fig. 6 tilted to the angle at which the pass bands coincide.

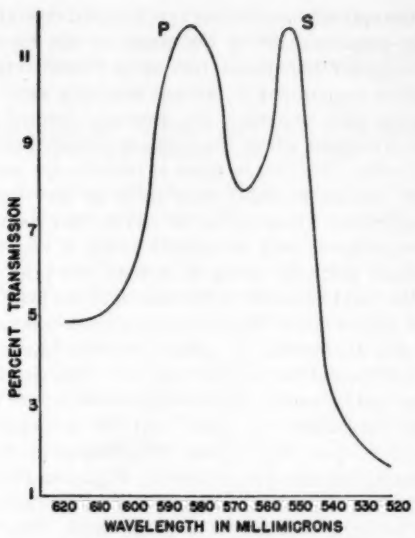

FIG. 8. Measured transmission of the birefringent filter of Figs. 6 and 7 tilted until the two bands have reversed their positions.

A treatment of this low index case will be given in a later paper.

CONCLUSION

Experimental measurements have been shown for the transmission of a birefringent Frustrated Total Reflection filter. It should be possible, using the technique demonstrated in this paper, to make filters of band widths of the order of 1 mμ and transmissions of perhaps 70 to 80 percent. There are many places where such filters could be most useful. The resolution is sufficiently high so that in many situations they become competition for an ordinary monochromator. Their main use, however, probably lies in image forming systems. There are occasions when it is desirable to take a photograph of a flame or of some luminous phenomenon in monochromatic light. A typical problem is the photography of solar prominences. If no occulting disk is used good measurements of the prominences require a band width of an angstrom or so. This is normally achieved with polarization filters which require many components. The Frustrated Total Reflection filter can be used as a fore filter for such a device. In this fashion it will save the use of a large part of the crystalline material used in the construction of polarization filters.

It is a pleasure to acknowledge the help of Edgar E. Barr, Grace E. Griffith, and Antonio F. Quesada in the preparation of this manuscript.

Book Reviews

Hyperfine Structure in Line Spectra and Nuclear Spin.
S. TOLANSKY. Pp. 120, Figs. 29, revised 1948. Price $1.50;

Mercury Arcs.
F. J. TEAGO AND J. F. GILL. Pp. 107, Figs. 50, revised 1949. Price $1.50;

Electron Diffraction.
R. BEECHING. Pp. 107, Figs. 43, second edition 1946. Price $1.25;

X-Ray Optics.
A. J. C. WILSON. Pp. 127, Figs. 33, new 1949. Price $1.50;

The Metre-Kilogram-Second System of Electrical Units.
R. K. SAS AND F. B. PIDDUCK. Pp. 60, Figs. 1, new 1947. Price $1.00.

These monographs are five of more than forty booklets on various physical subjects which are published by Methuen and Company, Ltd., London. The Methuen physics series is now available in the United States through John Wiley and Sons, Inc., New York.

Written by prominent scientists, the books serve to provide non-specialists with excellent surveys of selected fields of physics. The five monographs reviewed here are generally well documented with references to original articles.

Probably of major interest to Optical Society members will be Tolansky's book on hyperfine structure. Tolansky is an expert in the field of high resolution spectroscopy and this book is marked by his usual clarity of presentation and the detailed information. Certain of the tables containing data on nuclear moments are now out of date and the theory of the isotope displacement effect in the heavy elements is not as adequately presented as is the experimental or observational phase. Despite these minor objections, the book is heartily recommended to those interested in spectroscopic methods for studying nuclear moments.

Mercury Arcs will be important to those interested in high power (1 to 2500 kva) mercury arc rectifiers as regards construction details, operation and use, and theory—all from the standpoint of the electrical engineer. The application of McLeod and Pirani gauges to the measurement of pressure is also discussed.

Electron Diffraction is a review of investigations on the wave properties of electrons and on the effects of crystals in diffracting these electrons in both transmission and reflection. Applications of electron diffraction theory to studies of graphite, oils and greases, and metal oxides and surfaces are briefly discussed. Apparatus for and techniques of controlling electron beams are well presented topics. This book contains little mathematics and hence is suited to give a good general understanding of electron diffraction.

X-Ray Optics is concerned with the mathematical aspects of x-ray diffraction with considerable emphasis given to the reciprocal lattice method. The later chapters deal with such general problems as powder patterns of small crystals, the effects of crystal imperfections, and thermal agitation effects.

The Metre-Kilogram-Second System of Electrical Units is an interesting exposition of the M.K.S. dimensional system and contains a useful summary and explanation of the more important formulas. It suffers from a lack of table or tables comparing the magnitudes and relations between the different physical concepts in use today in the different systems. In fact, very little is mentioned of systems of units other than the M.K.S. Some of the statements are rather provocative, e.g., the radian per second is called a *pulse*, the term aperture has the form area/area rather than length/length as in optics. Also, the magnetic field intensity of the earth in England is given as 15 oersteds (horizontal component) and 35 oersteds (vertical component) in marked contrast with the values of 0.17 and 0.55, respectively, in America.

J. RAND MCNALLY, JR.
Carbide and Carbon Chemicals Division, Union Carbide and Carbon Corporation, Oak Ridge, Tennessee

Die Brechzahlen einiger Halogenidkristalle (The Refractive Indices of Halogen Salt Crystals).
H. HARTING. Sitzungsberichte der deutschen Akademie der Wissenschaften zu Berlin, Mathematisch-naturwissenschaftliche Klasse, No. 4, Akademie-Verlag, Berlin, 1948. Pp. 22.

The production of synthetic crystalline materials of optical quality and the increasing use of crystalline media for dispersion components of infra-red spectrometers has stimulated the use of crystals instead of optical glass for the construction of optical components when optical properties not possessed by the glasses are desirable. In view of this Dr. Harting has collected data relating to several of the more readily available crystals and reworked it in a form particularly useful to the lens designer or designer of optical instruments.

A modified Ketteler dispersion formula,

$$1/n^2 = x + y\lambda^2 + z\lambda^{-2} + u\lambda^{-4} + v\lambda^{-6},$$

was selected by Harting to interpolate values of the index of refraction at uniform intervals. This 5 constant formula was selected partly because its linear form simplifies the derivation of the constants and because it seemed sufficiently accurate for the purpose at hand. Nevertheless in some instances two sets of constants were used, one applicable to the greater part of the spectrum and the second set used to give a better fit in the short wave-length region.

Values of the index of refraction are given for the following materials: NaF, LiF, CaF_2, NaCl, KCl, KBr, and KI. The wave-length intervals are 10 between 1120 and 398 and 2 for the shorter wave-lengths. In most instances the shortest wave-length tabulated is 238 but for CaF_2, KBr, and KI the tabulation stops with values for 248.

In addition to these tables of indices at uniform intervals, for each material data are given, including values of the Abbe number (ν) and partial dispersions exactly paralleling the data that is given for optical glass in Schott's catalog. Comparisons are also presented of the values of the index of refraction obtained by different observers for the same crystals. The tabulated values of the index of refraction are given in all cases to 5 decimal places and the differences between the measured values and the values computed from the dispersion formulas seldom exceed 5 in the fifth place and show a reasonably random distribution of signs.

IRVINE C. GARDNER
National Bureau of Standards, Washington, D. C.

International Optical News

The International Commission of Optics

THE International Commission of Optics is one of the commissions affiliated with the International Union of Pure and Applied Physics, and as such comes within the general framework which is headed by the International Council of Scientific Unions. The U.S. participation in I.C.O. affairs is managed by the U.S. National Committee of the International Commission of Optics, which committee is appointed by the Board of Directors of the Optical Society of America. The present U.S.N.C.-I.C.O. consists of Irvine C. Gardner, Max Herzberger, Herbert E. Ives, Francis A. Jenkins, Deane B. Judd, Rudolf Kingslake, George Wald, Mary E. Warga, and Stanley S. Ballard, *Chairman*. The first formal meeting of the I.C.O. was its constitutional assembly which was held in Delft, Holland in July, 1948. United States delegates were F. A. Jenkins, D. B. Judd, and S. S. Ballard. The next regular meeting of the Commission was the London meeting of July 17 to 21, 1950, which will be reported upon in these columns later.

The formally stated objectives of the I.C.O. are as follows: to contribute on an international basis to the progress of theoretical and instrumental optics, the applications of optics, and the measurement and correction of the defects of the optical system of the eye. In particular the I.C.O. proposes to define programs of work, to assist in the carrying out of certain researches, to facilitate the rapid exchange of information, to promote international agreement on nomenclature, units, symbols, specifications, methods of control and similar subjects. The informal working understanding arrived at in Delft is that the activities of the I.C.O. are expected to be along the following lines: to gather and distribute information regarding optical work going on in the various countries, and the availability of optical materials and parts; to work toward a unified set of terms, symbols, and definitions in optics; to prepare summaries and bibliographies covering work and workers in the several fields of optics; to prepare suggestions or recommendations on standards in optics for submission to regularly constituted standardizing bodies; and to sponsor congresses at which sets of invited papers on some restricted field or fields of optics are given. The I.C.O. shall not act as a vehicle for publishing original research papers—full use should be made of existing scientific journals.

The General Secretary of the I.C.O., P. Fleury of the Institut d'Optique in Paris, publishes documents from time to time and sends these to the chairmen of the various national committees for dissemination among interested persons. These are usually in the form of mimeographed leaflets, and only a few copies are received. Their proper distribution in a country as large as the U.S. hence raises serious practical problems. After consultation with the several persons concerned, it was decided to list the titles or brief descriptions of these documents in the pages of this Journal from time to time. All who are interested in receiving copies of any of these, on a loan or a retention basis, are invited to address suitable requests to the undersigned.

The various I.C.O. documents are identified by the numbers and titles as listed below. Some of them are information circulars which are chiefly of administrative interest regarding I.C.O. affairs. Others are lists of optical publications, still others are review articles on technical subjects, while a few are similar to the contributed papers found in regular scientific journals. An attempt is made in the following listing to indicate the classification of the contents of these leaflets, with a statement, where needed, as to the language in which each is written. The authorship is noted in appropriate cases.

STANLEY S. BALLARD
Chairman, U.S.N.C.-I.C.O.
Tufts College
Medford 55, Massachusetts

48–1 Information circular. Questionnaires on thin films and microscope optics. In French.
48–2 List of Dutch optical publications, 1939 and 1940.
48–3 List of Swedish optical publications, 1939 to 1946.
48–4 Preview of the Delft meeting. List of recent optical publications from Belgium, France, and Great Britain. Chiefly in French.
48–5 List of Dutch optical publications, 1941 to 1943.
48–6 List of Swiss optical publications, 1939 to 1943.
48–7 List of Italian optical publications, 1947.
48–8 Report on the combined influence of diffraction and various aberrations on image formation, by J. Korringa, B. Nijboer, and A. Maréchal of the Dutch and French National Committees. In English and French.
48–9 Report on the calculation of the photographic triplet, by F. Temmerman. In French.
48–10 Report on electron optics, by the Dutch National Committee. In English.
48–11 Subjective properties of vision, by A. Arnulf. In French.
48–12 Report on the classification of optical subjects, by F. Donker Duyvis and P. M. van Alphen. In English.
48–13 Report on multipole radiation in atomic spectra, by A. Rubinowicz. In English.
48–14 Determination of the photographic properties of emulsions of interest to optical workers, by E. H. Selwyn. In English.
48–15 Critical report on the general laws of diffraction, by G. Toraldo di Francia. In French.
48–16 Geometry and geometrical optics of the eye (preliminary report), by the Optical Subcommittee of the British National Committee for Physics.
48–17 Notes on drawings and notation of tolerances on optical designs and specifications, by the British Optical Subcommittee.
48–18 Standardization of the drawings of optical parts, by the Italian National Committee. In French.
48–19 The manufacturing of diffraction gratings, by E. Inglestam. In English.
48–20 Reflecting and nonreflecting films, by A. Vasicek. In French.
48–21 Report on precision measurements, by B. Jurek. In French.
48–22 Preliminary report on the conventions and notations of geometrical optics. In French.
48–23 Minutes of the Delft meeting of the International Commission of Optics, July 12 to 17, 1948. In French.
48–24 List of British optical publications, July 1939 to January 1946.
48–25 List of Italian optical publications, 1947 and 1948.
48–26 List of Dutch optical publications, 1940 to 1943 (Supplementary).
48–27 Information circular. Optical publications from Belgium, France, Great Britain, and Italy. Chiefly in French.
49–1 Information circular. News from the National Committees. Optical publications from Belgium, France, Great Britain, and Italy. In French and English.
49–2 List of subjects assigned to the various National Committees for study, 1948 to 1950.
49–3 List of Dutch optical publications, 1939 to 1942 (Supplementary).
49–4 List of Czechoslovakian optical publications, 1940 to 1949.
49–5 Bibliography of publications from France, Great Britain, and Italy.
49–6 Information circular. List of the reports to be presented and the names of speakers at the 1950 meeting of the I.C.O. Information on the London Conference on Optical Instruments.

ICO–2 Booklet published by the I.C.O. in September, 1949. Lists the officers, the functions, and the statutes of the Commission, the members of the various National Committees, and the subjects studied in 1948 to 1950; gives the complete minutes of the 1948 Delft meeting. In English and French.

Announcements

Spectrophotometry (200 to 1000 Millimicrons).

KASSON S. GIBSON. Circular 484, National Bureau of Standards. Obtainable from Superintendent of Documents, U. S. Government Printing Office, Washington 25, D. C. Pp. 48. Price 25 cents.

The National Bureau of Standards has applied the spectrophotometer to its color research, development, and testing, and to various other work, for nearly 40 years. It pioneered in the development of the photoelectric spectrophotometer and in its application to the colorimetry of diffusing materials. With the advent of commercial photoelectric spectrophotometers, the Bureau began preparing and issuing spectrophotometric standards of various kinds, and hundreds of these are now in use, affording checks on the reliability of the various instrumental scales. Circular 484 has been issued to make available to users of spectrophotometers the experience, techniques, and data that have resulted from the Bureau's work in this field. Various instruments and methods are described, with emphasis on the basic principles, and various possible errors and the means used to eliminate them are considered in some detail. The various types of spectrophotometric standards are also described.

Old-timers in the Optical Society of America may recall the report of the Opt. Soc. Am. Progress Committee on Spectrophotometry[1] which proved to have considerable usefulness in this field. Circular 484 has been prepared with somewhat similar purpose and scope but with considerably changed emphasis because of the advances in spectrophotometry that have taken place during the past 25 years. Among the items of interest may be noted (1) a table of wave-lengths for sources of special utility in the calibration of spectrophotometers in the ultraviolet, visible, and near infra-red regions, (2) the spectral transmittance of typical glass, dyed gelatine, and interference filters from 200 to 1200 mμ, (3) curves showing the effect of change of temperature on the spectral transmittance of various types of glasses, (4) a consideration of the errors possible when strongly fluorescent samples are being measured spectrophotometrically, and (5) several pages devoted to the General Electric recording and Beckman quartz (non-recording) spectrophotometers, particularly with respect to the Bureau's experience with these instruments. In addition a bibliography of 127 references is given, including special reference to 19 other publications on spectrophotometry or related subjects that treat the matter historically, are of résumé nature, or give extensive bibliographies, so that those who wish may pursue the subject to any desired extent.

[1] J. Opt. Soc. Am. **10**, 169 (1925).

Colorimetry.

DEANE B. JUDD. Circular 478, National Bureau of Standards. Obtainable from Superintendent of Documents, U. S. Government Printing Office, Washington 25, D. C. Pp. 58. Price 30 cents.

The National Bureau of Standards has contributed importantly during the past 30 years to the science of color measurement. It has carried out studies of the fundamental method of colorimetry based upon the spectrophotometer, has developed a number of colorimeters and methods for special purposes, and has applied all of these methods to a considerable volume of testing for private and government agencies. Accounts of these activities are scattered through several score scientific and technical publications. Circular 478 brings together a summary of these results in concise form, and shows how the various methods of setting up color standards, and establishing and administering color standards, supplement each other.

The tristimulus method of colorimetry is carried from basic consideration of metameric pairs and the influence of macular and lens pigment on such color matches, through Grassman's laws, to the I.C.I. standard observer and coordinate system for colorimetry. Three methods of deriving the tristimulus values of a color from spectrophotometric data are described. Tables of the numerical data required for each (the summation method, the selected-ordinate method, and the semigraphical method) are given, and their use is shown by examples. Colorimetry by such reduction of spectrophotometric data has almost wholly supplanted the use of absolute visual colorimeters such as tristimulus colorimeters, colorimeters measuring dominant wave-length and purity directly, and the Guild vector method of colorimetry. However, extensive use is made of working standards of color calibrated by means of the spectrophotometer. This use had led to development of techniques that may be classed under small-difference colorimetry. The unknown specimen is compared either visually or photoelectrically to a calibrated working standard of color, and from the measured difference and the known tristimulus values for the standard, the color of the unknown is evaluated. A treatment is given of rotary mixture by Maxwell disks, of the Martens photometer, of the subtractive differential colorimeter, and of the photoelectric tristimulus colorimeter used for this purpose. Expression of the color difference between specimen and standard in terms approximately in accord with the perceptibility of the difference has led to the use of various transformations of the I.C.I. colorimetric coordinate system (Judd, Breckenridge-Schaub, Scofield-Hunter-Judd) and to the "NBS unit of color difference." Approximate indices of hue, lightness, and saturation are described together with the expression of differences in these parameters in NBS units. Indices of whiteness and yellowness are also given.

Material standards of color are also used extensively for color control by direct visual comparison. Sets of material color standards give substantially complete coverage of commercially available colors. Those covering this range in a systematic way are the Lovibond, the Ostwald, and the Munsell color systems. Because of the good correlation of Munsell hue, value, and chroma of the color with the hue, lightness, and saturation of the color perception itself, for usual observing conditions, a fairly detailed account of the Munsell system is given. This includes the ideal system of Munsell renotations, the use of the Munsell Book of Color to evaluate colors by tri-dimensional visual interpolation, and the use of the Munsell scales for expression of color tolerances.

Although color is tri-dimensional in nature, a number of color-grading problems have been solved to a satisfactory approximation by the use of one-dimensional scales. Those discussed in detail are color temperature, Lovibond grading of vegetable oils, Union-colorimeter grading of lubricating oils, Saybolt-chromometer grading of refined petroleum, and the U. S. color standards for rosin. The circular also gives summaries of general methods of color specification formally adopted by TAPPI, ASTM, and ASA, and in Federal Specifications; and there is a bibliography of 144 titles.

Letters to the Editor

A Diffraction Grating Interferometer*

R. KRAUSHAAR
Department of Physics, New York University, New York, New York
April 17, 1950

THE work of Ladenburg, Van Voorhis, Winkler, and others on interferometric studies of aerodynamic flow has caused a great deal of interest in interferometers of the Mach-Zender type, i.e., that variety of the Michelson interferometer in which the optical beam traverses the phenomena under observation once. The beam splitting and recombination for this type of instrument is accomplished by reflection and transmission in semisilvered mirrors and requires, therefore, parallel-surfaced homogeneous optical flats which necessarily limit the size of the field of view. A compact new kind of interferometer has been developed by the writer at this laboratory, which can produce much larger fields at very low cost, and involves only reflections of light beams in the essential portions of the apparatus. This instrument is an outgrowth of a modified Ronchi-schlieren apparatus.

The usual Ronchi-schlieren uses a slit source of light and a coarse grating of approximately 100 lines per inch in place of the ordinary schlieren knife-edge, with the important condition that the grating apertures be smaller than or equal to the width of the grating opacity, i.e., the grating space minus the grating aperture width. If the grating is in the plane of the image of the slit, a schlieren field is observed. But if the grating is displaced from the image plane of the slit, the slit image acts as a new source throwing a shadow of the grating lines on the observed field. The number of lines in the field is directly related to the distance of the grating from the image of the slit. However, because of the slit source, the intensity of the field is not as great as might be desired. It was found that by substituting for the slit source a grating having the same constant as the first, the intensity was increased without a loss of definition in the pattern. An analysis of the Ronchi-schlieren system indicates that if a local inhomogeneity in the optical path refracts the pencil of rays through it, it will produce a corresponding perturbation of the shadow pattern in such a manner that the displacement of a grating line shadow is proportional to the gradient of the logarithm of the refractive index averaged through the inhomogeneity. In addition, this analysis shows that the sensitivity increases with an increase in the grating constant. However, the use of gratings of somewhat more than 100 lines per inch was found to produce extraneous images associated with the diffraction pattern of the gratings. This led to difficulties in the interpretation of the schlieren field. To circumvent this, it was suggested that employing gratings with a much larger number of lines per inch might displace the higher order diffraction images from the mirror aperture leaving the central image alone to act as a Ronchi-schlieren.

To test this hypothesis, a pair of commercial replica transmission gratings (2000 lines/inch) were obtained. It was found that these gratings did not obey the important first condition for Ronchi-schlieren, the aperture to opacity ratio being approximately 4:1. Furthermore, and of utmost importance and good fortune, as it turned out, their grating constants were half as large as was originally thought to be desirable; consequently, the diffraction images of the field, i.e., the images of the schlieren mirror, overlapped considerably. However, during the experimentation with these gratings, it was observed that instead of a Ronchi-schlieren pattern, interference fringes could be seen almost covering each of the overlapping images of the field of view (Fig. 1). It was soon found, however, that under optimum conditions, these fringes consisted actually of two sets in each field image, slightly overlapping at the center of the field, with one set being the complement in intensity of the other. By introducing several standard thermal gradients in the atmosphere in one-half of the light beam, typical interference shifts were observed (Fig. 2), and moreover, corresponding shifts appeared in each set of fringes. Because of the necessary presence of the two sets of fringes, the useful field is limited in our apparatus to approximately one-third the area of the 18-in. diameter schlieren mirrors used, or only 99 square inches.

The operation of the system may be illustrated with the aid of Fig. 3, where for convenience reflection gratings are used, as in later forms of the apparatus. If a monochromatic beam of light from a source S is reflected from a diffraction grating G', a series of diffracted beams are formed obeying the grating equation $n\lambda = d \sin\theta_n$; where n is the diffraction order, λ the wave-length, d the grating constant, and θ_n the angle between the zeroth and the nth order beam. These diffracted beams are coherent (i.e., they are produced by the same source) and if they are recombined, it is possible to produce interference between them. Two of the

FIG. 1. Interference fringes produced by the diffraction grating interferometer. Note the two slightly overlapping sets in the circular image of the field of view. The slight deviations from straight fringes are due to thermal gradients in the otherwise quiescent atmosphere, unavoidable in the present apparatus. There are about five and one-third fringes to the inch in each set. A 6100A filter was used in this photograph.

FIG. 2. A standard fringe pattern. A photograph of isothermal contours in the atmosphere surrounding a heated cylinder (approximately 100°C) with walls one-quarter inch thick, one-half inch long, and an inside diameter of four inches. The interferometer was adjusted so that one fringe covered the entire field when no thermal gradients were present in the atmosphere.

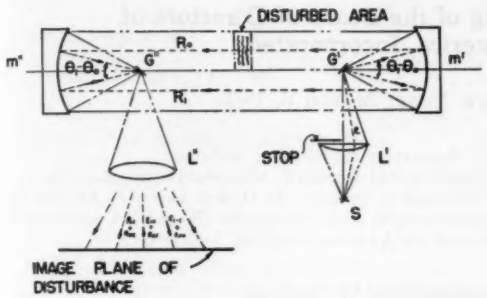

FIG. 3. Schematic diagram of diffraction grating interferometer. S, source; R, center ray of beam; L', condensing lens; G', first reflection grating; R_1, first-order ray of R produced by G'; R_0, zeroth-order ray of R produced by G'; $\theta_1-\theta_0$, angle between R_1 and R_0; M', first parabolic mirror; M'', second parabolic mirror; G'', second grating; L'', focusing lens; $R_{10}+R_{01}$, combined zeroth-order ray of R_1 and first-order ray of R_0.

beams, say the nth and the $n+1$st, are collimated by a mirror M'; they are then refocused by a similar mirror M'', so that the axes of the converging beams are inclined at an angle equal to the original diffraction angle, $\theta_{n+1}-\theta_n$, between them. If now a diffraction grating G'' having the same constant d as the original grating is introduced at or near the conjunction of the converging beams, each beam will in turn be split into a series of diffracted beams. These two series will combine in such a way that the mth order of one series will interfere with the $m+1$st order of the other, because the grating constant is such that images of the mirrors overlap in the way described previously. Each such combination produces an interferometric pattern covering, with optimum apertures, about one-third the area of the mirrors.

It will be noted that the gratings need not be at the focus of the mirrors, the only requirement being that the image of the first grating be in close proximity to the second. Also, diverging beams are not necessary; a parallel beam of light through the gratings will still permit operation as an interferometer. The light source may be very broad, as in the Michelson or Mach-Zender interferometer.

* This work was performed under the auspices of Project Squid, New York University, with the support of the ONR and the Air Research and Development Command, under Contract N6ori-11, Task Order 2.

Calibration of Infra-Red Spectrometers

P. TORKINGTON
British Rayon Research Association, Urmston, Lancashire, England
April 12, 1950

SOME while ago, an improved method of calibrating infra-red prism spectrometers was described.[1] It is convenient to summarize it here. All except about fifteen of the one hundred and fifty or so points available for calibration from the ammonia, carbon dioxide, and water bands[2] are discarded and these are used to determine the constants in an empirical equation (resembling in form the refractive index equation):

$$T_i+T_0=A\nu_i^2+B(\nu_r^2-\nu_i^2)^{-1}.$$

T_i is the spectrometer screw-turn value for a frequency ν_i cm^{-1}, ν_r is a restrahlen frequency of the prism material, for which A and B are constants, and T_0 is very nearly constant. The plot of T_i against $(\nu_r^2-\nu_i^2)^{-1}$ is said to be sufficiently linear in the 3 to 15μ region to extrapolate to obtain an approximate value for the constant A (from T_i for the sodium D line and the intercept), which can then be used to calculate a final B value from the two CO_2 readings at 2367 and 720.7 cm^{-1}. Finally A is adjusted till the plot of T_0 against wave-length is smooth.*

This method was attempted in the laboratory here with a Grubb Parsons S3 Spectrometer (serial number 23, rocksalt prism). It was found that the plot of T_i against $(\nu_r^2-\nu_i^2)^{-1}$ was far from linear when drawn on a scale sufficiently large to give a reasonable reading for the calculation of A. The following data illustrate:

ν(cm^{-1})	$B(\times10^{-6})$
828.2	0.0815
892.4	0.0813
948.8	0.0810
1012.6	0.0812
1104.1	0.0816
1177.9	0.0820
1474	0.0840
1637	0.0848
1830	0.0855
2351	0.0870

The B values were obtained by plotting (T_i-T_j) against $[(\nu_r^2-\nu_i^2)^{-1}-(\nu_r^2-\nu_j^2)^{-1}]$ and reading at $T_i=T_j$, using $\nu_r=184$ cm^{-1}. The deviation from linearity is therefore quite definite; there is an inflection in the region of 850 cm^{-1} which appears to correspond to the maximum found in the T_0 curve.[1] Although the equation in McKinney and Friedel's paper[1] was checked against all of Randall, Kao, and Oetjen's points,[2] it is suggested here that this would probably be regarded as necessary in the calibration of each new instrument. The procedure seems rather lengthy.

The method adopted by the author is to use all of the ammonia, carbon dioxide and water bands, drawing a smooth best curve as usual. The frequencies are then read from the curve at regular screw-turn intervals, giving a calibration table. Then the differences $\Delta\nu$ in this table are adjusted where necessary to give a smooth relationship. By plotting $\Delta\nu$ against T and reading from the curve obtained, the differences can be determined more accurately than the absolute frequency at any point can be read. Over the region 2.5 to 5μ, it was decided, since B was changing more rapidly here, that the empirical equation was definitely untrustworthy. Accurate calibration with rock salt is not to be sought over this region. Nine points may be obtained from 0.5 and 1.0 mm layers of methylene chloride, using the data of Corin and Sutherland.[3] These are fairly well distributed. Cyclohexane also has some useful overtones and combinations. There are a number of available compounds, such as chloroform and various hydrocarbons, for the region 2900 to 3150 cm^{-1}.

The spectrometer was used with a pen recorder. The region from 3 to 15μ is covered by about eighteen whole screw turns, and these can be read within 0.01 by means of a vernier. A separate pen gives a calibration mark every 0.1 revolution. The differences $\Delta\nu$ for $\Delta T=0.1$ vary from over 250 cm^{-1} at 2.7μ to less than 2 cm^{-1} at 15μ. The motor driving the screw can be run at various speeds and the recorder fitted with different gears. At one revolution per minute the spread on the chart with an average gear in the recorder is 1.35 cm per 0.1 revolution. At this (lowest convenient) speed the screw-turn value can be read to within 0.01 definitely, and to within 0.005 in favorable cases. At higher speeds, displacement of the spectrum is found to occur; corrections of the order $\Delta T=0.02$ become necessary. Errors can also be introduced through the recorder and marker pens becoming relatively shifted. If a spectrum is being repeated, the absorption maxima may be read from the vernier while running; this would eliminate this last error, but the procedure is obviously inconvenient.

[1] D. S. McKinney and R. A. Friedel, J. Opt. Soc. Am. **38**, 222 (1948).
[2] Oetjen, Kao, and Randall, Rev. Sci. Inst. **13**, 515 (1942).
* It is not pointed out in McKinney and Friedel's paper (see reference 1) that the S shape of the T_0 curve is probably due to neglect of terms higher than ν^3 in the expansion of the unknown ultraviolet term.
[3] C. Corin and G. B. B. M. Sutherland, Proc. Roy. Soc. (London) **A165**, 43 (1938). The Hilger Instrument used was calibrated from the dispersion curve of rocksalt.

Minutes of the Thirty-Fifth Meeting of the Board of Directors of the Optical Society of America, Incorporated

HOTEL STATLER, NEW YORK, NEW YORK, MARCH 8, 1950

IN addition to the transaction of routine business, the following items of general interest to members of the Society were considered.

Announcements by Secretary

Under authority conferred by a previous Board, the President and Secretary had appointed George R. Moffitt and A. G. Shenstone as proxies for the Optical Society of America at the annual meeting of the American Institute of Physics, Inc., on February 25, 1950.

Results of letter ballots:

1. Approval of the appointment of the following Program Committee for the winter meeting to be held in New York City on March 9, 10, and 11, 1950:

H. R. J. Grosch, *Chairman*

W. F. C. Ferguson — J. R. Nielsen
R. Clark Jones — Daniel Smith
John E. Tyler

2. Approval of appointment of the following committees:

Frederic Ives Medal Committee

Wallace R. Brode, *Chairman*

G. R. Harrison — George A. Nahstoll
Raymond T. Birge — E. P. Tyndall

Adolph Lomb Medal Committee

H. Keffer Hartline, *Chairman*

James G. Baker — R. A. Sawyer
Deane B. Judd — Harvey E. White

3. Approval of the appointment of the following as Auditors, and alternates, for the accounts of the Optical Society of America, Inc.

E. H. Greppin — L. T. Steadman
H. F. Bennett, *Alternate* — H. R. Condit, *Alternate*

4. Approval of the appointment of Duncan E. Macdonald to succeed Brian O'Brien as O.S.A. representative on A.S.A. Sectional Committee Z38 (Photography).

5. Approval of the following resolution:

Resolved, that Duncan E. Macdonald be appointed for a term of two years to represent the Optical Society of America on the Cinematographic and Photographic Standards Correlating Committee of the American Standards Association.

Announcement by President

Appointment of F. S. Harris, Jr. to represent the Optical Society of America at the Centennial of the Founding of the University of Utah, on February 27 and 28, 1950.

Appointment

Paul R. Gleason was appointed to succeed A. G. Worthing (deceased) as a member of the Sponsor's Administrative Committee for A.S.A. Sectional Committee Z58 (Optics).

Future Meetings of the Society

The annual meeting of the Optical Society will be held at the Hotel Statler, Cleveland, Ohio, on October 26, 27, and 28, 1950, and a winter meeting will be held at the Wardman Park Hotel, Washington, D. C., on March 1, 2, and 3, 1951. The annual meeting in 1951 will be held in Chicago, Illinois, in conjunction with meetings of all the founder societies of the American Institute of Physics, and has been tentatively scheduled for the week of October 22, 1951.

Membership

The Secretary reported a net gain in membership of one hundred and two members between January 1, 1949, and January 1, 1950. On recommendation of the Committee on Transfer, forty-three associate members were approved for transfer to regular membership. The names of those accepting transfer will appear in the annual report of the Secretary for 1950.

ARTHUR C. HARDY, *Secretary*

Annual Report of the Editor of Publications

STATEMENT OF OPERATIONS OF THE JOURNAL OF THE OPTICAL SOCIETY OF AMERICA FOR THE YEAR ENDING DECEMBER 31, 1949

Income		
Non-member subscriptions	$13,282.17	
Net income from page charge	3,243.09	
Net income from back numbers	4,100.21	
Total Income Exclusive of Member Subscriptions		$20,625.47
Expense		
Printing and mailing	$22,251.89	
Engraving	3,857.87	
Editorial mechanics:		
Salaries	$2,115.07	
Office expense	505.70	

		2,620.77
Subscription expense:		
Salaries	$2,386.57	
Office expense	541.30	
		2,927.87
Editorial offices, Cambridge and Washington:		
Salaries	$1,250.00	
Office expense	105.80	
		1,355.80
Total Cost of Editing and Publishing Journal		$33,014.20
Net Cost of Operating Journal and Furnishing it to Members		$12,388.73

(Signed) GEORGE R. HARRISON, *Editor*

Annual Report of the Secretary of the Optical Society of America, Inc., for the Calendar Year 1949

MEMBERSHIP RECORD

JANUARY 1, 1949 TO JANUARY 1, 1950

	Honorary	Regular Emeritus	Associate Emeritus	Regular Life Payment	Associate Life Payment	Regular Annual Payment	Associate Individual Annual Payment	Associate Corporation	Student	Total
Membership as of record in the books of the Secretary 1/1/49	3	25	1	11	1	609	1088	32	28	1798
Gains during 1949										
By election as of 1/1/49							127	1	53	181
By election as of 1/1/50							31		1	32
By reinstatement		3				4	10		3	20
By transfer to Associate Membership							15			15
Total gains	(0)	(3)	(0)	(0)	(0)	(4)	(183)	(1)	(57)	(248)
Losses during 1949										
By death		2		1		5	7			15
By resignation						17	35	4	1	57
By transfer to Associate Membership									15	15
By separation for non-payment of dues						2	30			32
By failure to renew student membership									27	27
Total losses	(0)	(2)	(0)	(1)	(0)	(24)	(72)	(4)	(43)	(146)
Total membership	3	26	1	10	1	589	1199	29'	42	1900

NEW MEMBERS

Elected during 1949 as of January 1, 1949

Acquista, Nicolo (3000 A)
Albright, Charles L. (2931 A)
Allbright, Burnard D. (3114 S)
Allen, Ralph G. (3069 A)
Arnold, George W., Jr. (2971 A)
Back, F. G. (2949 A)
Baker, Howard D. (3044 A)
Ball, Joseph J. (3001 A)
Banet, Leo (2947 A)
Bednarz, Felix (3040 A)
Beiswanger, John P. G. (2972 A)
Bell, G. C., Jr. (3052 S)
Bergere, Leonard M. (3002 A)
Bergman, Lester V. (3096 A)
Bixler, Milo E. (2936 A)
Blackmer, L. L. (2973 A)
Blaisdell, B. E. (2929 A)
Brady, Lynn J. (3003 A)
Breitman, Seymour (2974 A)
Brundage, William E. (3024 A)
Bube, Richard H. (3027 A)

Budde, E. F. (3078 A)
Burke, Bernard F. (3050 S)
Burton, Charles J. (3042 A)
Campbell, Charles J. (3133 S)
Canina, Vittorio Garino (3041 A)
Carman, P. D. (2965 A)
Champeny, J. C. (3048 S)
Clark, John W. (3109 A)
Cohen, Irving E. (3103 S)
Craig, William M. (3082 A)
Crouch, C. L. (3049 A)
Culver, William H. (3004 S)
Dalrymple, George F. (3083 S)
Davidson, H. R. (2946 A)
Davis, William Chester (3032 S)
DeBell, Arthur G. (2961 A)
Doane, Edwin A. (2959 A)
Dress, Kenneth S. (2932 A)
Drumheller, Carl E. (3066 A)
Duboc, Charles A. (3072 A)
Dwyer, Robert J. (2975 A)
Ednalite Optical Co., Inc. (3106 AC)
Erikson, G. L. (3051 A)
Estes, William B. (2976 A)
Finkelstein, Nisson A. (2968 S)
Fipphen, John S. (3077 A)
Fleischman, William E. (3065 S)
Forman, Nyna L. (3053 A)
Foster, Charles, Jr. (3081 A)
Foster, Irving G. (3055 A)
Franck, Kurt (2944 A)
Frels, Robert H. (2977 S)
Fridge, D. L. (2978 A)
Fuehring, Christina (2979 A)
Fuhr, Allen B. (2980 A)
Gallipeau, Robert B. (2981 S)
Gentry, Robert (3043 A)
Gilstein, J. Burrill (3056 A)
Goetz, William E. (3005 S)
Gordon, Arnold H. (2923 A)
Griffin, Paul M. (2963 A)
Grojean, Richard E. (3035 S)
Haber, Heinz (3104 A)
Haines, Jesse H. (3021 A)
Hamman, Robert L. (3038 S)
Harding, H. G. W. (2926 A)
Hariharan, P. (3085 A)
Harjes, Frederick W. (2982 A)
Harrold, James H. (3086 A)
Hatch, Edwin F. (2983 A)
Hayward, Robert M. (3110 A)
Hill, Otto Herman (2984 A)
Hole, Winston L. (2985 A)
Howald, T. S. (3006 A)
Hutchinson, Nancy (3030 S)
Jean, J. N. (3007 S)
Johnson, Elgeon L. (3068 S)
Kasha, Michael (3008 A)
Keehner, John B. (3045 A)
Kehres, Paul W. (2986 A)
Keller, John S. (3080 A)
Kerr, H. S. (3059 S)
Kloepfer, Barbara R. (3028 A)
Kunz, Joseph (3070 S)
Lamb, Mary A. (3009 A)
Lambert, William E. (3010 S)
Lapp, Philip A. (3075 S)
LeRoy, V. M. (2987 A)
Lerse, John J. (3039 A)
Lipinski, Albert J. (2950 S)
Lock, Charles (3098 A)
Lyon, Lloyd F. (3119 A)
MacNeille, Stephen M. (2970 A)
Mager, Louis (3124 S)
Marcus, Bernard (2939 A)
Marshall, E. E. B. (3060 A)
Matz, Charles H. (2955 A)
Mayo, Eleanor G. (3087 A)
McCutchen, Roberta L. (2988 A)
McGann, James C. (3084 S)
McKinley, Robert W. (2930 A)
McPherson, Paul M. (3088 A)
McWilliam, Leslie Henry (2989 A)
Mersereau, E. P. (2927 A)
Mikkelsen, Louis (2943 S)
Miller, Wendell E. (3061 A)
Mitchell, Walter E., Jr. (3036 S)
Mooney, C. Frank (3071 A)
Mortimer, Forrest S. (3012 A)
Nadir, Mark T. (3025 A)
Newell, Raymond F., Jr. (2962 S)
Nielsen, Waldo J. (3090 A)
Olsen, Robert M. (3046 S)
Osgood, G. Robert, Jr. (3022 A)
Parker, Donald J. (2990 S)
Patten, Robert R. (3034 S)
Perry, Edward C., Jr. (3073 A)
Porter, Galen (2948 A)
Raitiere, Louis (2951 A)
Reese, Warren B. (2925 S)
Richardson, K. T. (2991 A)
Rippel, Charles W., Jr. (3026 S)
Rudatis, Domenico (3013 A)
Ruhloff, Robert A. (3076 A)
Roberts, Richard G. (2960 A)
Robinson, True W. (2992 A)
Rood, Joseph L. (2934 A)
Rosenberger, Harold E. (2993 A)
Sacher, David (2940 A)
Sanders, William G. (2964 A)
Sandford, Wayne H., Jr. (3097 S)
Schauer, Charles H. (2942 A)
Schlauch, John E. (2969 S)
Schulte, Daniel (3067 S)
Schulz, L. G. (2928 A)
Schwartz, Samuel (3113 A)
Schwarz, George (3058 A)
Scott, Ralph H. (3014 A)
Seass, Stewart (2935 A)
Shaftan, Kenneth (2994A)
Shean, J. W. (2995 A)
Siegmund, Walter (3015 S)
Sinsheimer, Robert L. (2945 A)
Smith, Erwin Stuart (2996 S)
Smith, F. Dow (3016 S)
Smith, Richard E. (3095 A)
Sorem, Allan L. (3127 A)
Speck, Robert S. (3031 S)
Spengeman, W. F. (2941 A)
Sprentall, H. Robert (2952 A)
Stateler, Jack G. (3023 S)
Stimson, Allen (3063 A)
Stukenbroeker, George L. (2956 A)
Terrio, F. J. (3102 A)
Thiers, Ralph E. (3029 A)
Thorburn, Eugene K. (3017 S)
Torley, Robert E. (3018 A)
Townsend, Charles V. R. (2958 S)
Travis, James R. (3033 S)
Ullom, James R. (3062 S)
Vaux, George (2933 A)
Waidelich, John A., Jr. (2954 S)
Walker, M. J. (3064 A)
Watson, John T. (2938 A)
Webb, Carl E. (2967 A)
Webster, R. R. (3074 A)
Weiler, Harold F. (3092 A)
West, Robert B. (2997 A)
Westermann, Fred E. (2998 A)
Wheeler, Burton W., Jr. (2953 A)
Wheeler, Gilbert V. (2937 A)
Wieder, Harold (3019 S)
Williams, F. D. (3054 S)
Williamson, D. E. (2999 A)
Woodruff, Robert W. (3020 S)
Woods, Calvin Robert (3037 S)
Yonts, Oliver C. (2966 A)
Young, Tkeodore R. (2957 S)
Zeeb, Lawrence E. (2924 S)
Zimmerman, Carlton F. (3079 A)

Elected during 1949 as of January 1, 1950

Barbera, Robert A. (3122 A)
Bozman, William R. (3121 A)
Brooke, Richard Thomas (3125 A)
Carter, Jefferson A. (3100 A)
Cox, Maurice E. (3093 A)
Dalton, Charles C. (3112 A)
Dorman, William H. (3108 A)
Earls, Lester T. (3128 A)
Edgerton, Richard O. (3101 A)
Erlandson, Paul M. (3115 A)
Fuhrmeister, John C. (3111 A)
Greenhouse, Harold M. (3134 S)
Grinoch, Paul (3099 A)
Harvey, Marion M. (3120 A)
Jurmain, Jacob H. (3116 A)
King, Robert B. (3135 A)
MacKay, Ernest (3123 A)
Martin, Robert H. (3129 A)
McIntosh, R. (3011 A)
Menzies, A. C. (3117 A)
Meservey, A. B. (3047 A)
Nagel, Max R. (3089 A)
Robinson, David Z. (3118 A)
Rothrock, Robert W. (3130 A)
Saunders, James B. (3094 A)
Senko, Julia (3107 A)
Smith, Clara D. (3057 A)
Smith, Richard P. (3091 A)
Smith, Richard S. (3132 A)
Swede, Hillard B. (3131 A)
Szegho, C. S. (3126 A)
Williamson, Harold G. (3105 A)

Student Members

Transferred to Associate Membership as of January 1, 1950

Finkelstein, Nisson A. (2968 A)
Frels, Robert H. (2977 A)
Gallipeau, Robert B. (2981 A)
Haskell, Stanley W. (2629 A)
Jordan, Joseph, Jr. (2594 A)
Jean, J. N. (3007 A)
Keuper, Jerome P. (2601 A)
Reese, Warren B. (2925 A)
Sanford, Cecil E. (2866 A)
Schottmiller, Gerard (2841 A)
Smith, Erwin Stuart (2996 A)
Townsend, Charles V. R. (2958 A)
Waidelich, John A., Jr. (2954 A)
Young, Theodore R. (2957 A)
Zeeb, Lawrence E. (2924 A)

Losses by Death

Albright, Charles L. (2931 A)
Cooley, J. P. (795 AA)
Ellis, J. H. (494 R)
Henderson, George H. (814 AA)
Humphreys, William J. (505 R)
Luneberg, Rudolf K. (2145 A)
Martling, M. G. (1214 A)
Merritt, Ernest (275 RE)
Millar, Preston S. (443 R)
Nixon, Ivan L. (1397 A)
Nutting, Perley G. (20 RL)
Pfund, A. H. (83 R)
Silberstein, Ludwik (170 RE)
Stewart, Thomas S. (289 A)
Worthing, A. G. (261 R)

Arthur C. Hardy, *Secretary*

Annual Report of the Treasurer of the Optical Society of America

Cash Transactions January 1, 1949 to December 31, 1949

Receipts		
Dues	$ 6,048.93	
Dues in advance	9,023.75	
Income from unallocated securities	1,797.61	
Income from Ives Medal Fund	12.50	
Income from Adolph Lomb Fund	50.00	
Sale of Securities	1,000.00	
Total Receipts		$17,932.79
Disbursements		
Journal Publication Expense	10,267.89	
Journal Editorial Expense	1,350.00	
President's Expense	6.50	
Secretary's Expense	1,911.76	
Secretary's Travel Expense	175.46	
Secretary Local Sections Expense	498.23	
Treasurer's Expense	538.99	
Meetings & Programs	292.08	
Ives Medal	20.83	
Investments	103.56	
Contributions to the support of other organizations		
American Institute of Physics	1,905.83	
Inter-Society Color Council	35.00	
U.S.N.C. of I.C.I.	200.00	
U.S.N.C. of I.C.O.	160.00	
Contingency Account		
Engraving of Gavel	4.50	
Total Disbursements		$17,470.63
Excess of Receipts over Expenditures		$ 462.16

Balances December 31, 1948		
Unallocated cash	$ 4,659.53	
Ives Medal Fund	141.43	
Adolph Lomb Fund	256.66	
Total		$ 5,057.62
Balance December 31, 1949		$ 5,519.78

Ives Medal Fund

Income		
Principal	$ 500.00	
Interest balance, January 1, 1949	141.43	
Interest accrued during 1949	12.50	
Total		$ 653.93
Disbursements		
Medal for George R. Harrison	$ 20.83	20.83
Balance December 31, 1949		$ 633.10

Note: The principal sum of $500.00 is invested in Series G War Bonds. They are included in the bonds reported in the accompanying Investment Statement.

Adolph Lomb Fund

Income		
Principal	$ 2,000.00	
Interest balance January 1, 1949	256.66	
Interest accrued during 1949	50.00	
Total		$ 2,306.66
Disbursements		
None		0.00
Balance December 31, 1949		$ 2,306.66

Note: The principal sum of $2,000 is invested in Series G War Bonds. They are included in the bonds reported in the accompanying Investment Statement.

Investments

Investment portfolio with market value of securities as of December 31, 1949.

		Book Value	Market Value	Annual Income
8M	U. S. Treasury Bonds 2¼%	$ 8,083.70	$ 8,300	$ 180.00
11.6M	U. S. War Savings Bonds Series "G" 2½%	11,600.00	11,600*	290.00
5M	Atch. Top. & Santa Fe 4% Gen. Mtg. 1995	5,000.00	6,450	200.00
2M	American Tel. & Tel. Co. Conv. Deb. 2¾% 1957	2,114.00	2,180	55.00
3M	Consolidated Cigar Corp. S. F. Deb. 3¼%	3,137.25	3,060	97.50
15 Shares	El Paso Natural Gas Co. Cum. Pfd. $4.10	1,636.50	1,470	61.50
30 Shares	20th Century Fox Film Corp. Pr. Pref. $4.50	3,077.80	3,090	135.00
20 Shares	Philip Morris & Co., Ltd. Cum. Pfd. 4%	2,173.70	2,100	80.00
75 Shares	Indianapolis Power & Light Co. Common	2,543.81	2,100	112.50
52½ Shares	National Lead Co. Common	1,605.79	1,942	65.50
53 Shares	Eastman Kodak Company Common	1,741.06	2,438	90.00
65 Shares	General Electric Co. Common	2,544.23	2,730	130.00
35 Shares	Kennecott Copper Corp. Capital	1,729.53	1,750	140.00
43 Shares	Standard Oil Co. of N. J. Capital	2,272.10	2,839	84.00
		$49,259.47	$52,049	$1,721.00
	Average yield			3.49%

* Maturity value.

The undersigned, having been duly appointed to audit the books of the Treasurer of the Optical Society of America, Inc. from January 1, 1949 to December 31, 1949, hereby certify that the Treasurer's report of receipts and disbursements is correct as shown by records, vouchers, bank statement, etc., and that his accounts check accurately with vouchers and bank statements.

(Signed) L. T. STEADMAN, H. F. BENNETT, *Auditors*